Power-Aware Spatial Multiplexing with Unilateral Antenna Cooperation

vorgelegt von
Diplom-Ingenieur
Martin Schubert
aus Haltern in Westfalen

Von der Fakultät IV - Elektrotechnik und Informatik
der Technischen Universität Berlin
zur Erlangung des akademischen Grades
Doktor der Ingenieurswissenschaften
- Dr.-Ing. -

genehmigte Dissertation

1. Berichter: Prof. Dr.-Ing. Dr. rer. nat. Holger Boche
2. Berichter: Prof. Dr. techn. Helmut Bölcskei (ETH Zürich)

Tag der wissenschaftlichen Aussprache: 11. Dezember 2002

Berlin 2003
D 83

Zusammenfassung

In der Arbeit wird eine leistungsoptimierte Lösung für das Problem des räumlichen Multiplexings von unabhängigen Datenströmen in einem Mehrantennen-System vorgestellt, unter der Annahme, daß entweder die Sendeantennen oder die Empfangsantennen nicht kooperieren und die Gesamtleistung beschränkt ist.

Kooperation wird durch lineare räumliche Filterung (Beamforming) erzielt, die gemeinsam mit den Sendeleistungen optimiert wird. Grundlage der Optimierung ist Kanalkenntnis an der kooperierenden Seite, welche als bekannt vorausgesetzt wird. Das Optimierungsziel ist die Gewährleistung individueller Signal-zu-Interferenz-plus-Rausch-Verhältnisse (signal-to-interference-plus-noise ratio, SINR) bei gleichzeitiger Minimierung der Gesamtleistung. Dieses Problem tritt z.B. in einem zellularen Mobilfunksystem auf, wo eine Basisstation über ein Antennenarray gleichzeitig mit mehreren unabhängigen Mobilstationen kommuniziert, welche jeweils mit einer Einzelantenne ausgerüstet sind. Die Signalübertragung erfolgt im Downlink über kooperierende Sendeantennen und im Uplink über kooperierende Empfangsantennen.

Ein erster Schritt zur Lösung dieses Optimierungsproblems ist die Annahme unveränderlicher Beamformer. Dies ermöglicht eine Charakterisierung des globalen Optimums. Es zeigt sich, daß eine fundamentale Dualität zwischen räumlichem Multiplexing in Abwärts- und Aufwärtsverbindung besteht. In beiden Kanälen können die gleichen SINR-Werte erreicht werden, wobei jeweils die gleiche Beschränkung der Gesamtleistung zugrundegelegt wird. Eine Lösung für das Downlink-Problem, welches eine komplizierte analytische Struktur aufweist, kann demnach durch Lösen des „glatteren“ Uplink-Problems gefunden werden.

Ein zweiter wichtiger Schritt zur Lösung der allgemeinen Aufgabenstellung ist die Untersuchung von Mehrnutzer-Beamforming unter Vernachlässigung des Rauschens, wie von Gerlach and Paulraj [10] vorgeschlagen. Dies führt zur Minimierung eines nicht-differenzierbaren ℓ_∞ Funktionals. Ein wichtiger Schritt zur Lösung dieser Aufgabenstellung ist die Formulierung eines äquivalenten Eigenwert-Optimierungsproblems und der Beweis, daß jedes lokale Optimum auch ein globales Optimum ist. Weiterhin wird ein interessanter Zusammenhang zwischen dem optimalen ℓ_∞ Problem und einem in [10] vorgeschlagenen ℓ_1-Ansatz aufgezeigt. Die analytischen Ergebnisse dieser Untersuchungen führen schließlich zu einer iterativen Lösung mit streng monotonem Konvergenzverhalten. Das globale Optimum wird bereits nach einigen wenigen Iterationsschritten erreicht.

Aufbauend auf den Erkenntnissen aus der Betrachtung des rauschfreien Falls, wird eine Lösung des allgemeinen Problems hergeleitet. Der neue Algorithmus hat dieselben exzellenten Konvergenzeigenschaften wie die oben beschriebene Lösung und minimiert zudem die Gesamtleistung unter Berücksichtigung des Empfangsrauschens. Mittels individueller Zielvorgaben lassen sich so beliebige SINR-Werte erreichen, solange das Problem lösbar ist. Notwendige und hinreichende Bedingungen für die Lösbarkeit werden angegeben. Eine geschlossene Lösung für den 2-Nutzer-Fall wird hergeleitet.

Schließlich wird gezeigt, wie die gefundene Lösung auf das Problem der Raten-Kontrolle im Gauß'schen Broadcast-Kanal mit vektorwertigem Eingang und skalarem Ausgang angewendet werden kann. Mit dem obigen Dualitätsresultat folgt, daß es eine Übereinstimmung erzielbarer Kapazitäten in Broadcast und Multiple-Access-Kanal gibt, solange eine Kombination aus linearer Filterung und Decision-Feedback-Entzerrung bzw. -Vorverzerrung betrachtet wird. Dies zeigt, daß die bekannte Kapazitätsregion des Multiple-Access-Kanals eine direkte Entsprechung im Broadcast Channel hat, einschließlich der maximalen Summenkapazität. Die Dreiecks-Struktur des Kanals, hervorgerufen durch die Decision-Feedback-Strategie, ermöglicht eine auf Rücksubstitution basierende Lösung, welche eine effiziente Steuerung individueller Datenraten erlaubt. Auch für diese Aufgabenstellung wird eine geschlossene Lösung für den 2-Nutzer-Fall hergeleitet.

Abstract

This thesis offers a power aware solution to the problem of spatial multiplexing of independent data streams in a multi-antenna system, assuming that either the transmit antennas or the receive antennas are not allowed to cooperate and a sum power constraint is imposed.

Cooperation is achieved by using spatial linear filters (beamformers), which are optimized jointly with the power allocation. To this end, the spatial channel characteristics must be known at the cooperating side. The design goal is to achieve individual signal-to-interference-plus-noise ratios (SINR) with minimal power consumption. This problem occurs, e.g., in a cellular wireless communication system, where a multi-antenna base station communicates simultaneously with several decentralized mobile terminals, each equipped with a single antenna. Downlink and uplink correspond to cooperating transmit and receive antennas, respectively.

As a first approach to this optimization problem, the beamformers are assumed to be fixed. This allows for a characterization of the global optimum, which will prove useful for the following analysis. It turns out that there is a fundamental duality between uplink and downlink spatial multiplexing. In particular, the same SINR values can be achieved in both channels under the same power constraint. Hence, a solution of the downlink problem, which has a complicated analytical structure, can be found by solving the "smoother" uplink problem instead.

A second important step towards a general solution is the investigation of joint beamforming in the absence of noise, as proposed by Gerlach and Paulraj [10]. This problem consists of minimizing a non-differentiable ℓ_∞ objective function. A key step in finding a global solution is to formulate an equivalent eigenvalue optimization problem and to show that each local minimum is a global minimum. Also, there is an interesting relation between optimal ℓ_∞ optimization and the alternative ℓ_1 objective proposed by [10]. The analytical results of this study lead to the development of globally convergent algorithms with strictly monotone iteration sequences. Typically, only a few iteration steps are required.

The insight gained from studying interference balancing in the absence of noise is used to derive a power aware strategy for SINR balancing with minimal power consumption. This new algorithm has the same excellent convergence behavior as the one derived for the noiseless case. By choosing individual target thresholds, arbitrary SINR levels can be achieved as long as the problem is feasible. Necessary

and sufficient conditions for feasibility are provided and a closed form solution is derived for the 2-user case.

Finally, it is shown how the solution can be applied to the problem of controlling rate tuples in a Gaussian broadcast channel with vector inputs and independent scalar outputs. By exploiting the above duality result, it is shown that there is a one-to-one correspondence between capacities achievable in broadcast and multiple access channel, as long as a combination of linear filtering and decision feedback equalization is considered. Hence, the well known multiple access capacity region has a direct counterpart in the broadcast channel, including the point of maximum throughput. Exploiting the triangular channel structure imposed by decision feedback equalization, a rate balancing technique based on back-substitution is derived. This approach allows to control individual rate tuples with minimal power consumption and high computational efficiency. A closed form solution is given for the 2-user case.

Contents

1. Introduction

The spatial structure of the wireless propagation channel can be exploited by using multiple transmit and receive antennas. By adding the spatial dimension to the classical system resources bandwidth and power, significant gains in spectral efficiency can be achieved. This has been demonstrated by evaluating the information-theoretical capacities [11, 12]. The potential gains depend on the spatio-temporal characteristics of the propagation channel, the degree of cooperation among the antennas, as well as the channel information available at transmitter and/or receiver. For an overview, see e.g. [13].

The general problem of spatial multiplexing consists in finding a transmit covariance matrix and a detector, which are jointly optimal with respect to a chosen design goal. If both transmit and receive antennas cooperate, then the throughput maximizing strategy is known to be the water-filling solution based on the singular-value decomposition of the channel matrix [11, 14].

In many wireless systems, however, maximizing the throughput is not the primary design goal. Additional system constraints should be considered, like bandwidth-limited channel feedback or the limited ability to resolve fast fading. So it may be necessary to trade off spectral efficiency against diversity by sending multiple replicas of the same signal in order to make reception more reliable. For multi-antenna systems, this leads to the concept of *space-time coding* [15–17].

Another important constraint is the degree of antenna cooperation. Cooperation may be impractical, e.g., for antennas belonging to different decentralized users. In this case the waterfilling power allocation is generally not optimal. A new strategy is required, which jointly optimizes the power allocation and the spatial transmission strategy. In general, this leads to the relatively new field of multiuser MIMO (multiple input, multiple output) transmission, for which only partial results have appeared so far. The challenging goal is to adaptively allocate individual data rates in a multiuser environment. These rates should be achieved with minimal transmission power.

1.1. Problem Statement

This thesis deals with a special case of multi-antenna transmission. Unilateral antenna cooperation is considered, which means that cooperation is allowed at either transmitter or receiver. In the following, these scenarios are referred to as *downlink* and *uplink*, respectively. This is in analogy to a cellular wireless communication system with a multi-antenna base station and several single-antenna mobile terminals. Due to the different geographical positions of the mobiles, mutual co-operation is often impractical. Note, that studying this special scenario is a first step towards the general case, where also the mobiles are allowed to employ multiple antennas.

The spatial structure of the multiuser channel has to be known at the base station in order to facilitate meaningful antenna cooperation. The benefit of cooperation is to enable spatially directed transmission between the base station and the K decentralized mobile terminals. Thereby, mutual interference is reduced and the overall system performance is enhanced. Such spatial multiplexing provides additional degrees of freedom through which communication can take place.

Spatial multiplexing always goes hand in hand with power control, which has to ensure reliable communication by counterbalancing the joint effects of signal propagation and residual interference. Hence, a reasonable design goal is to achieve a certain link quality for each channel with minimal transmission power. If this problem is infeasible, the requirements must be relaxed by the resource management, e.g., by switching off one or more channels. Such a power aware transmission scheme exploits the available system resources in an optimal way.

A reasonable and often used model is the transmission of Gaussian distributed signals. Then, the performance measure for each of the K channels is the signal-to-interference ratio (SINR). Considering individual target thresholds $\gamma_1, \ldots, \gamma_K > 0$, the design goal can be formulated as

$$\mathrm{SINR}_i \geq \gamma_i, \qquad 1 \leq i \leq K \ . \tag{1.1}$$

It is desirable to achieve these targets with minimum total transmission power. This is a joint optimization problem, since all users are typically coupled by the corporate effects of channel propagation, power adjustment, and spatial filtering. One difficulty in understanding such systems stems from the intertwining of the effects of all of the interferers in the system.

1.2. Related Works

- In the context of a **synchronous CDMA** system with random spreading sequences, a similar multi-user problem was studied by Tse and Hanly [18]. The temporally spread system considered in this work is the direct equivalent to the spatially spread system considered here. Tse and Hanly carried out an asymptotical analysis, which shows the limiting effect of mutual interference for several linear receiver types. They provided an upper bound on the achievable system performance depending on the number of antennas M and the number of users K. However, this provides no complete answer to the question how SINR requirements $\gamma_1 \dots \gamma_K$ can be controlled under a sum power constraint.

- In the context of **classical beamforming** (for an overview see e.g., [19–23] and the references therein), the problem of jointly separating several signal sources in space was addressed. For this purpose, a fixed power allocation is mostly assumed. The interaction of several users in a power controlled network with limited transmission power, however, is less well understood.

- **Power control** strategies for achieving the design goal (1.1) were already studied [24–28] (assuming fixed beamforming, i.e., each transmitter-receiver pair has a fixed link gain). An overview is given, e.g. in [29]. This is a special case of the above problem formulation. The general case that is studied here, however, is more complicated in that the optimal transmission power can only be found when knowing the optimal spatial pre-processor. The pre-processor, in turn, depends on the co-channel interference and therefore on the transmission powers. Thus, both quantities must be optimized jointly.

- In the context of the **Gaussian Broadcast Channel** (GBC), a similar problem was recently studied in [30–34], where strategies for obtaining the sum capacity and an achievable region were investigated. Most of these results are based on an information theoretical duality between the BC and the Gaussian Multiple Access Channel (GMAC), which allows to transfer the well known principle of decision feedback multiuser equalization (see e.g. [35]) to the GBC. Yet, an efficient and general strategy for achieving arbitrary target rates within the resulting achievable region is not known.

- Another line of work is the development of **downlink beamforming** techniques [10, 36–43], where a joint optimization of beamforming and power allocation is studied. Three different approaches are known:
  - In [10, 43] the problem of interference balancing was studied in the absence of noise. This provides an upper bound on the jointly achievable SINR margin. This approach will be discussed in detail in Chapter 3.
  - Another approach is to minimize the total transmission power while fulfilling SINR requirements (1.1). This was first proposed in [36] and later in [37–40]. The disadvantage of this strategy is that it neglects the important aspect of feasibility. Algorithms designed under the assumption that a solution exists may yield unpredictable results in case that the problem is infeasible.
  - A conceptually different approach to the above power minimization problem appeared in [41, 42], where it was proposed to embed the beamforming

problem in a semidefinite optimization program. Thus, recently developed semidefinite programming techniques can be applied to solve the problem and infeasible scenarios can be handled. However, the optimization is performed over matrices with more degrees of freedom than the original beamforming vectors. Hence, the solution comes at the cost of relatively high computational complexity.

1.3. Outline

Chapter 2. In order to keep this thesis self-contained, some basic concepts of narrowband space processing are reviewed and discussed in Section 2.1.

In Section 2.2, the two seemingly different beamforming concepts of power minimization [36–42] and interference balancing [10, 28, 43] are analyzed and compared. It turns out that both techniques are equivalent, as long as the problem is feasible, i.e., certain SINR thresholds $\gamma_1 \dots \gamma_K$ can be achieved. The problem of feasibility is studied in Section 2.3, where necessary and sufficient conditions are given.

An interesting duality between uplink and downlink channels was observed throughout the last decade in seemingly different contexts, e.g. [27, 33, 39]. In Section 2.4 it is tried to generalize these results and to provide necessary and sufficient conditions under which duality holds true.

Chapter 3. In this chapter, the problem of interference balancing by jointly adjusting beamformers and transmission powers is studied in the absence of noise.

As a starting point serves the work of Gerlach and Paulraj [10] who have analyzed this problem and proposed to replace the highly non-smooth ℓ_∞-norm objective function of the original problem by a smoother ℓ_1-norm objective. This leads to an algorithm which was conjectured to solve the original ℓ_∞ problem [10]. Another algorithm based on eigenvalue optimization was proposed by Montalbano and Slock [43]. The global convergence of neither of these algorithms could be proven so far.

In this chapter, both problems are analyzed and a convergence analysis is carried out. As will turn out, the eigenvalue strategy is globally convergent, whereas the ℓ_1-based strategy only approximates the optimum. These results provide useful insight into the analytical structure of the general problem addressed later in Chapter 4, where SINR levels are balanced under the assumption of noise.

Chapter 4. In this chapter the general problem of controlling SINR levels under a sum power constraint is addressed. Exploiting the duality result, a solution for the complicated downlink problem is found by solving the "smoother" uplink problem instead. This yields a global optimizer for both uplink and downlink.

A key problem that has to be solved in this context, is to expand the interference balancing technique derived in Chapter 3, such that receiver noise is taken into account.

Chapter 5. In this chapter, a multiuser Gaussian channel with coding for known interference is considered. For this special scenario, controlling user capacities is equivalent to controlling SINR levels. Hence, the solution found in Chapter 4 immediately carries over to the rate balancing problem. The solution can even be simplified by exploiting the triangular structure of the channel that is imposed by the successive coding strategy. It turns out, that for this special case no iterative optimization is required. The problem can be solved efficiently by an algorithm based on back-substitution.

Chapter 6. An overall assessment is given and open problems for future research are pointed out.

A summary of the notation and symbols used in this work is given in the appendix on page 81.

2. Duality Between Downlink and Uplink Multiplexing

In this chapter we focus on finding the optimal power allocation that ensures SINR target thresholds $\gamma_1 \ldots \gamma_K$ under a sum power constraint. To this end, it is assumed that all beamformers are kept fixed, which has the advantage that the power allocation can be studied isolated from the effect of spatial processing. Hence the results can also be seen in the light of classical power control and resource management (see [29] and the references therein). The insight gained from this approach will prove useful for the following chapters, where the mutual interaction between beamforming and power allocation will be studied.

2.1. Narrowband Signal Model

We start with a brief introduction in the signal model and some basic concepts of spatial signal processing.

2.1.1. Propagation Channel

The wireless propagation channel between transmitter and receiver is characterized by multipath propagation, which spreads the transmitted signal in three dimensions: time, frequency and space. In the following, some fundamental properties of wireless signal propagation are discussed and the vector channel model used in this thesis is introduced. Note, that this is a special case of the general MIMO channel (see e.g. [44] for an overview).

Time dispersion is caused by reflections around transmitter and/or receiver, which cause many delayed replicas of the signal. The channel bandwidth can be defined as the reciprocal maximum excess delay. If the channel bandwidth is smaller than the signal bandwidth, then the signal is distorted and the channel is called "frequency selective". If the signal is narrowband with respect to the channel bandwidth, the channel is called "frequency flat". This means that the channel impulse response has a multipath delay spread which is much smaller than the reciprocal bandwidth of the transmitted signal.

In the following we assume a frequency flat channel. However, most concepts proposed here immediately carry over to frequency selective channels, e.g. when assuming independent spatial processing for each channel tap. In principle, each frequency selective channel can be turned into a flat channel by temporal equalization.

Frequency dispersion is caused when scattered signals experience a Doppler shift due to motion. The Doppler increases with the velocity of the transmitter and/or the receiver. Doppler shifts can even occur when both transmitter and receiver are static, caused by moving objects in the surrounding. The superposition of the scattered signals fades in time, due to different angular frequencies caused by the Doppler shifts.

Space dispersion is caused by multipath reflections with different propagation angles as seen from the array (cf. Fig 2.1). This causes coherence loss in the spatial domain, depending on the angle spread as well as the distance between the antenna elements.

In the following it is assumed that the signal is narrowband with respect to the array aperture, i.e., the propagation time of the signal across the array is much less than the reciprocal bandwidth of the transmitted signal. No restriction is made, however, concerning the angle spread or the geometry of the array.

In this thesis, the channel between the i^{th} mobile and the base station antenna array is modeled as the superposition of Q scattered multipath replicas (see Fig. 2.1). The multipath channel is characterized by Doppler shifts $\hat{\omega}_{iq}$, $1 \leq q \leq Q$, complex path attenuations β_{iq}, and propagation angles θ_{iq}. The path attenuation β_{iq} models the joint effects of path attenuation and phase shifts. The angle θ_{iq} is typically measured with respect to array broadside. From the narrowband assumption follows that the time delays at the M base station antennas can be modeled as phase shifts collected in an *array response vector* $\boldsymbol{a}(\theta) \in \mathbb{C}^M$. The phase shifts are measured with respect to an arbitrary reference point, which is commonly chosen to be the first antenna element. Assuming a carrier frequency ω_c, the time-varying channel of the i^{th} mobile is characterized by a vector function

$$\boldsymbol{h}_i(t) = \sum_{q=1}^{Q} \beta_{iq}\, \boldsymbol{a}(\theta_{iq})\, \mathrm{e}^{j(\omega_c + \hat{\omega}_{iq})t} , \quad 1 \leq i \leq K . \tag{2.1}$$

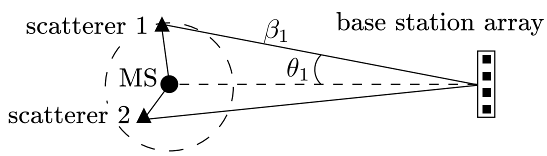

Figure 2.1.: Schematic illustration of multipath propagation

The spatial covariance matrices are given by

$$\boldsymbol{R}_i = \mathcal{E}\{\boldsymbol{h}_i(t)\boldsymbol{h}_i^H(t)\} , \qquad 1 \leq i \leq K , \tag{2.2}$$

where the operator $\mathcal{E}\{\cdot\}$ denotes the ensemble average over the time-fluctuating fading channel. The variation of $\boldsymbol{h}_i(t)$ in time and space is illustrated in Fig. 2.2.

Based on the knowledge of the spatial correlation properties (2.2) at the base station, all K communication links can be jointly optimized. While the representation (2.2) is a statistical measure for the propagation channel, it is general enough to incorporate also the case of perfect channel information. Coherent spatial processing is possible if $\text{rank}\{\boldsymbol{R}_i\} = 1$. This is fulfilled, e.g., when the channel does not change within the observation window, in which case perfect channel information is available. In general, however, the channel may be rapidly time-variant and the total number of transmission paths per user easily exceeds the number of antenna elements. Then, $\boldsymbol{R}_i$ will have full rank.

Note, that most techniques derived in this thesis are general enough to hold for channels of arbitrary rank, except for the results in Chapter 5. Here, a block fading channel model is assumed. The channel gains are approximated as piecewise constant over many symbol intervals, which is fulfilled if the Doppler spread is much less than the bandwidth of the transmitted signal. This model reflects the need for perfect channel information, which is required for the techniques described in Chapter 5.

2.1.2. Cooperating Transmit Antennas (Downlink)

Consider a signal vector $\boldsymbol{s} \stackrel{\text{def}}{=} [S_1, \ldots, S_K]^T$ to be transmitted from the base station to the K mobiles. The components of $\boldsymbol{s}$ can be modeled as wide-sense stationary stochastic processes which are mutually and temporally uncorrelated, with zero mean. The variances $\mathcal{E}\{|S_i|^2\}$, $1 \leq i \leq K$ are stacked in a vector $\boldsymbol{p} = [p_1 \ldots p_K]^T$. A sum power constraint

$$\|\boldsymbol{p}\|_1 \leq P_{\max} \tag{2.3}$$

is imposed. A matrix $\boldsymbol{U} \in \mathbb{C}^{M \times K}$ is used to map the signal vector $\boldsymbol{s}$ on the M transmit antennas. The i^{th} data stream is spread over the antenna array by the i^{th} column of $\boldsymbol{U}$, which is denoted by $\boldsymbol{u}_i \in \mathbb{C}^M$ and constrained to fulfill

$$\|\boldsymbol{u}_i\|_2 = 1, \quad 1 \leq i \leq K . \tag{2.4}$$

The base station antennas are uncoordinated if the operator $\boldsymbol{U} = [\boldsymbol{u}_1, \ldots, \boldsymbol{u}_K]$ has a diagonal structure. This, is the case, e.g., for the Bell Laboratory Layered Space-Time (BLAST) architecture [45], which assumes that no channel information is available at the transmitter. Large performance gains are possible, however, by allowing the antennas to cooperate.

Cooperation requires that channel information is available prior to transmission. Then, the vectors $\boldsymbol{u}_i$ can be interpreted as beamformers which can be adjusted so as

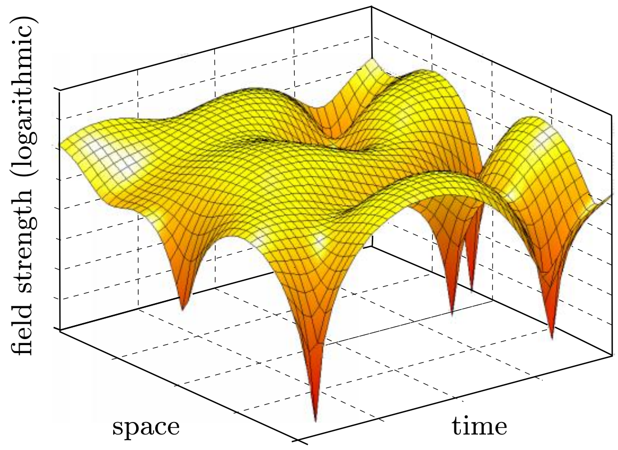

Figure 2.2.: Space-time fading caused by angle/frequency dispersion

to focus energy in space. This approach has a positive impact on the SINR measured at the antenna output of the i^{th} mobile:

$$\mathrm{SINR}_i^{\mathrm{DL}}(\boldsymbol{U}, \boldsymbol{p}) = \frac{p_i \boldsymbol{u}_i^H \boldsymbol{R}_i \boldsymbol{u}_i}{\sum_{\substack{k=1 \\ k \neq i}}^{K} p_k \boldsymbol{u}_k^H \boldsymbol{R}_i \boldsymbol{u}_k + \sigma_i^2} \,, \quad 1 \leq i \leq K \,, \tag{2.5}$$

where σ_i^2 is the variance of the additive white Gaussian noise. The stochastic noise processes are assumed to be mutually uncorrelated, i.e., the vector

$$\boldsymbol{\sigma} = [\sigma_1^2, \ldots, \sigma_K^2]^T \tag{2.6}$$

satisfies $\mathcal{E}\{\boldsymbol{\sigma}\boldsymbol{\sigma}^H\} = \boldsymbol{I}$.

In order to illustrate the impact of antenna cooperation on the SINR, think of a single user channel $\boldsymbol{h}_1 = \beta \boldsymbol{a}(\theta_1)$, as illustrated in Fig. 2.3, for which maximum ratio combining $\boldsymbol{u}_1 = \boldsymbol{h}_1 / \|\boldsymbol{h}_1\|_2$ is the optimal transmit strategy. It can easily be verified that $\mathrm{SINR}_1 = p_1 \beta^2 \|\boldsymbol{a}(\theta_1)\|^2 / \sigma_1^2$, which is an improvement by a factor $\|\boldsymbol{a}(\theta_1)\|^2 = M$ as compared to single antenna transmission. The SINR linearly increases with the number of antenna elements. Note, that the same does not necessarily hold for a multi-user channel, which is limited by the effects of mutual interference, as will be shown in the remainder of this chapter.

2.1.3. Cooperating Receive Antennas (Uplink)

Now, assume an uplink scenario, with M cooperating receive antennas at the base station. The K non-cooperating mobiles are equipped with single antennas. Independent data streams with powers $q_1 \ldots q_K$ are multiplexed from the mobiles to the

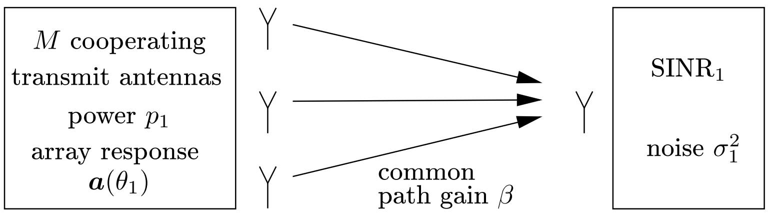

Figure 2.3.: SNR improvement by coordinated multi-antenna transmission for a single user scenario

base station. As in the downlink, the transmission powers are stacked in a vector $\boldsymbol{q} = [q_1, \ldots, q_K]^T$. The same beamforming matrix $\boldsymbol{U} = [\boldsymbol{u}_1 \ldots \boldsymbol{u}_K]$ that has been used for downlink transmission is now used for reception and can be interpreted as a linear multiuser receiver. The uplink SINR is given by

$$\mathrm{SINR}_i^{\mathrm{UL}}(\boldsymbol{u}_i, \boldsymbol{q}) = \frac{q_i \boldsymbol{u}_i^H \boldsymbol{R}_i \boldsymbol{u}_i}{\boldsymbol{u}_i^H \left(\sum\limits_{\substack{k=1 \\ k \neq i}}^{K} q_k \boldsymbol{R}_k + \sigma_i^2 \boldsymbol{I} \right) \boldsymbol{u}_i} , \quad 1 \leq i \leq K . \tag{2.7}$$

Observe, that the uplink SINR levels (2.7) are coupled by the transmission powers $\boldsymbol{q}$, but not by the beamformers $\boldsymbol{U}$. This special structure makes the uplink SINR more tractable than the downlink SINR expressions (2.5), which are intertwined in a complicated way. This is the reason why most studies in the literature so far have focused on uplink processing. One key result of this chapter will be to show that albeit their seemingly different structure, there exists a fundamental duality between multiuser processing in uplink and downlink, thus both links can be optimized jointly.

Again, a first motivating example is provided by the single user scenario depicted in Fig. 2.3. By reversing the role of transmitter and receiver, the problem immediately carries over to the uplink. It can easily be verified that the same gain M is achievable for both links. Does this observation also hold true for a multiuser scenario? This problem will be studied in the remainder of this chapter. To this end, we assume that the uplink transmission powers are constrained in the same way as the downlink powers, i.e.,

$$\|\boldsymbol{q}\|_1 \leq P_{\max} . \tag{2.8}$$

2.1.4. Crosstalk

The SINR values in uplink and downlink are mutually coupled by cross-talk, which can be collected in a $K \times K$ matrix

$$[\boldsymbol{\Psi}(\boldsymbol{U})]_{ik} = \begin{cases} \boldsymbol{u}_k^H \boldsymbol{R}_i \boldsymbol{u}_k , & k \neq i \\ 0 , & k = i \end{cases} . \tag{2.9}$$

In general, this matrix is non-negative and asymmetric.

If the spatial covariance matrices are full rank, then $\boldsymbol{u}_k^H \boldsymbol{R}_i \boldsymbol{u}_k > 0$ always holds. Then, it is impossible to completely cancel out the interference by using a zero-forcing strategy. This situation occurs, e.g., when $\boldsymbol{R}_i$ is obtained by averaging over the time-fluctuating fading channel and the channel has several spatially resolved propagation paths, as discussed in Section 2.1.1. Then, the matrix $\boldsymbol{\Psi}$ is strictly positive and all users are coupled by interference.

Another, more extreme assumption is perfect channel information. If, in addition, $K \leq M$, then all covariance matrices have rank one and interference can be canceled out completely. This results in $\boldsymbol{\Psi} = \boldsymbol{0}$, thus the users are no longer coupled by interference.

However, complete interference cancellation is not necessarily optimal when a power constraint is imposed. In the uplink, linear zeroforcing mostly comes at the cost of noise enhancement, whereas in the downlink a power enhancement is caused. Hence, zeroforcing only performs well in the high SNR regime. whereas the aim of this thesis is to find a power aware transmission strategy that shows good performance over the whole SNR range. Therefore, the design objective can be seen as to find the optimal tradeoff between residual interference and signal-to-noise ratio (SNR).

Now, let's make the notion of "cross-talk coupling" more precise:

Coupled users. A set of users is called *coupled* by cross-talk if an increase in one user's transmission power has direct or indirect impact on the interference experienced by the other users. This is obviously fulfilled if the link gains between all users are positive. If, however, there is no direct connection between two users A and B, they may still be connected via a third party C. Suppose that A causes interference to C. Then C has to increase its power level to maintain the same SINR. This in turn may increase the interference level at user B.

An appropriate mathematical model is provided by the theory of directed graphs (see e.g. [46]). Suppose that each user is represented by a node. The nodes are connected by directed edges which are given by the positive entries of the link gain matrix $\boldsymbol{\Psi}$. If $\boldsymbol{\Psi}_{ij} > 0$ then there is a connection from node i to node j. A system of nodes is called *strongly connected* if for each pair of nodes (N_i, N_j) there is a sequence of directed edges leading from N_i to N_j. In the following, a set of users will be called *coupled* by cross-talk if and only if its directed graph is strongly connected. An example scenario is illustrated in Fig. 2.4.

Uncoupled users. A user is defined to be uncoupled in terms of cross-talk if he does not belong to a set of coupled users. There are two possible scenarios for which this is fulfilled:

1. the user receives no crosstalk from other users,
2. the user causes no cross-talk to other users.

$$\boldsymbol{\Psi} = \begin{array}{cc} \text{base station beamformers} & \\ \begin{bmatrix} 0 & \boldsymbol{\Psi}_{12} & \boldsymbol{\Psi}_{13} & \boldsymbol{\Psi}_{14} \\ 0 & 0 & \boldsymbol{\Psi}_{23} & \boldsymbol{\Psi}_{24} \\ 0 & 0 & 0 & \boldsymbol{\Psi}_{34} \\ \boldsymbol{\Psi}_{41} & 0 & 0 & 0 \end{bmatrix} & \text{mobiles} \end{array} \quad \Rightarrow$$

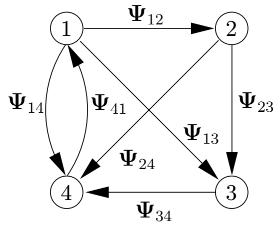

Figure 2.4.: All users are coupled by cross-talk. The directed graph is strongly connected

In both cases the transmission power of the user can be increased without the penalty of increasing its own interference level by the control mechanism of the multiuser power control. Then, arbitrary levels $\mathrm{SINR}_i \geq \gamma_i$ can be achieved (provided that the transmission power is unconstrained). An example scenario is illustrated in Fig. 2.5.

$$\boldsymbol{\Psi} = \begin{array}{cc} \text{base station beamformers} & \\ \begin{bmatrix} 0 & \boldsymbol{\Psi}_{12} & \boldsymbol{\Psi}_{13} & \boldsymbol{\Psi}_{14} \\ 0 & 0 & \boldsymbol{\Psi}_{23} & \boldsymbol{\Psi}_{24} \\ 0 & 0 & 0 & \boldsymbol{\Psi}_{34} \\ 0 & 0 & 0 & 0 \end{bmatrix} & \text{mobiles} \end{array} \quad \Rightarrow$$

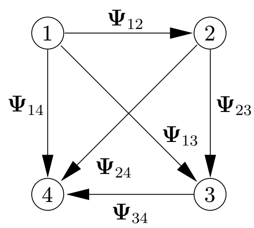

Figure 2.5.: All users are uncoupled. Such a matrix structure is imposed, e.g., by coding for known interference (see Chapter 5 for a detailed study of this scenario)

Note, that even when the users are completely uncoupled in terms of interference, i.e., $\boldsymbol{\Psi} = \mathbf{0}$, their SINR levels are still connected via the sum power constraint. The absence of interference does not imply independent AWGN channels, as it is the case for independent power constraints. That is, increasing one users power immediately forces one or more other users to decrease their power in order for the sum power constraint to be fulfilled. This aspect will be considered in the next section.

2.2. Uplink Power Allocation under a Sum Power Constraint

Let's begin studying the multiuser uplink scenario for a fixed beamforming matrix $\tilde{\boldsymbol{U}} = [\tilde{\boldsymbol{u}}_1, \ldots, \tilde{\boldsymbol{u}}_K]$. The goal is to find the power allocation that jointly achieves $\mathrm{SINR}_i^{\mathrm{UL}} \geq \gamma_i$, $1 \leq i \leq K$ under a sum power constraint (2.8). This goal may be infeasible, thus one important aspect of the problem is to find necessary and sufficient conditions for feasibility.

2.2.1. Maximizing the Balanced SINR Margin

The SINR requirements are fulfilled if and only if $\min_{1\le i\le K} \mathrm{SINR}_i^{\mathrm{UL}}/\gamma_i \ge 1$. A straightforward strategy to achieve this design goal is to solve the following optimization problem:

$$C^{\mathrm{UL}}(\tilde{\boldsymbol{U}}, P_{\max}) = \max_{\boldsymbol{q}} \min_{1\le i\le K} \frac{\mathrm{SINR}_i^{\mathrm{UL}}(\tilde{\boldsymbol{u}}_i, \boldsymbol{q})}{\gamma_i} , \qquad (2.10)$$
$$\text{subject to} \quad \|\boldsymbol{q}\|_1 \le P_{\max} \text{ and } \boldsymbol{q} \in \mathbb{R}_+^K .$$

Observe that $\mathrm{SINR}_i^{\mathrm{UL}} \ge \gamma_i$ is feasible for $i = 1, \ldots, K$ if and only if $C^{\mathrm{UL}}(\tilde{\boldsymbol{U}}, P_{\max}) \ge 1$. The function C^{UL} is characterized by the following two lemmas:

Lemma 1. *Let $\tilde{\boldsymbol{q}}$ be a global maximizer of the optimization problem (2.10), then*

$$C^{\mathrm{UL}}(\tilde{\boldsymbol{U}}, P_{\max}) = \frac{\mathrm{SINR}_i^{\mathrm{UL}}(\tilde{\boldsymbol{u}}_i, \tilde{\boldsymbol{q}})}{\gamma_i} , \quad 1 \le i \le K , \qquad (2.11)$$
$$P_{\max} = \|\tilde{\boldsymbol{q}}\|_1 . \qquad (2.12)$$

Proof. Assume that there exists an index i_0 such that $\mathrm{SINR}_{i_0}^{\mathrm{UL}}/\gamma_{i_0} > \min_{1\le k\le K} \mathrm{SINR}_k^{\mathrm{UL}}/\gamma_k$. From (2.7) it can be observed that each $\mathrm{SINR}_i^{\mathrm{UL}}$ is strictly monotonically increasing in q_i and monotonically decreasing in q_k for $k \ne i$. Thus, q_{i_0} can be reduced without decreasing the minimum level. This leads to a new power vector $\hat{\boldsymbol{q}}$ with $\|\hat{\boldsymbol{q}}\|_1 < P_{\max}$. This power saving can be redistributed among all users by using a scaled power vector $\alpha\hat{\boldsymbol{q}}$, where the scalar $\alpha > 1$ is chosen such that $\|\alpha\hat{\boldsymbol{q}}\|_1 = P_{\max}$. It can be verified that $\mathrm{SINR}_i^{\mathrm{UL}}(\alpha\hat{\boldsymbol{q}}) > \mathrm{SINR}_i^{\mathrm{UL}}(\hat{\boldsymbol{q}})$ for all $i = 1, \ldots, K$. Thus, it would be possible to obtain a point with the cost function larger than the global maximum, which is a contradiction. ∎

Lemma 2. *The function $C^{\mathrm{UL}}(\tilde{\boldsymbol{U}}, P_{\max})$ is strictly monotonically increasing in $P_{\max}$.*

Proof. This follows from $\mathrm{SINR}_i^{\mathrm{UL}}(\tilde{\boldsymbol{u}}_i, \alpha\boldsymbol{q}) > \mathrm{SINR}_i^{\mathrm{UL}}(\tilde{\boldsymbol{u}}_i, \boldsymbol{q})$, with $1 \le i \le K$ and $\alpha > 1$. ∎

The monotony result stated in Lemma 2 is illustrated in Fig. 2.6. It can be observed that there is a one-to-one relationship between each balanced SINR margin and a total transmission power. Each point is characterized by the set of equations (2.11) and (2.12), which can be rewritten using matrix notation. To this end we define

$$\boldsymbol{D} = \mathrm{diag}\left\{ \frac{\gamma_1}{\boldsymbol{u}_1^H \boldsymbol{R}_1 \boldsymbol{u}_1}, \ldots, \frac{\gamma_K}{\boldsymbol{u}_K^H \boldsymbol{R}_K \boldsymbol{u}_K} \right\} , \qquad (2.13)$$

$$\boldsymbol{\Lambda}(\boldsymbol{U}, P_{\max}) = \begin{bmatrix} \boldsymbol{D}\boldsymbol{\Psi}^T(\boldsymbol{U}) & \boldsymbol{D}\boldsymbol{\sigma} \\ \frac{1}{P_{\max}} \mathbf{1}_K^T \boldsymbol{D}\boldsymbol{\Psi}^T(\boldsymbol{U}) & \frac{1}{P_{\max}} \mathbf{1}_K^T \boldsymbol{D}\boldsymbol{\sigma} \end{bmatrix} . \qquad (2.14)$$

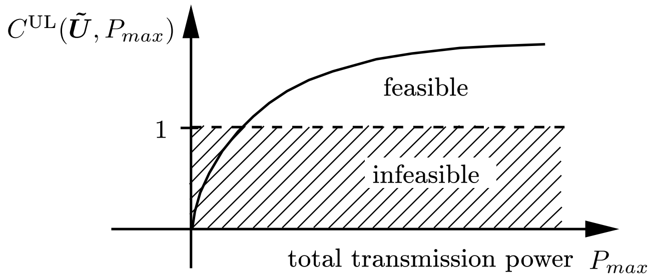

Figure 2.6.: Balanced SINR margin $C^{\mathrm{UL}}(\tilde{\boldsymbol{U}}, P_{\max})$ vs. total transmission power $P_{\max}$

It can be verified that (2.11) and (2.12) together form an eigensystem

$$\boldsymbol{\Lambda}(\tilde{\boldsymbol{U}}, P_{\max}) \begin{bmatrix} \tilde{\boldsymbol{q}} \\ 1 \end{bmatrix} = \frac{1}{C^{\mathrm{UL}}(\tilde{\boldsymbol{U}}, P_{\max})} \begin{bmatrix} \tilde{\boldsymbol{q}} \\ 1 \end{bmatrix} . \tag{2.15}$$

The balanced level $C^{\mathrm{UL}}(\tilde{\boldsymbol{U}}, P_{\max})$ is a reciprocal eigenvalue of the non-negative extended coupling matrix $\boldsymbol{\Lambda}$. However, not all eigenvalues represent physically meaningful balanced levels. In particular, $\boldsymbol{q} \in \mathbb{R}_+^K$ and $C^{\mathrm{UL}}(\tilde{\boldsymbol{U}}, P_{\max}) \in \mathbb{R}_+$ must be fulfilled.

Lemma 3. *For any non-negative real matrix $\boldsymbol{B}_{K\times K} \geq 0$ with spectral radius $\rho(\boldsymbol{B})$, there exists a vector $\boldsymbol{q} \geq 0$ and $\lambda_{\max}^{(B)} = \rho(\boldsymbol{B})$ such that $\boldsymbol{B}\boldsymbol{q} = \lambda_{\max}^{(B)}\boldsymbol{q}$.*

Proof. See e.g. [46, p. 670]. ∎

It was shown by Yang and Xu [28] that if the non-negative matrix has the special structure (2.14), then the non-negative eigenvector associated with the maximal eigenvalue, denoted by $\lambda_{\max}(\boldsymbol{\Lambda})$, is strictly positive and the solution is unique. The uniqueness of $\lambda_{\max}(\boldsymbol{\Lambda})$ also follows immediately from Lemma 2, which rules out the existence of two different balanced levels with the same sum power. For each eigenvalue the power constraint $\|\tilde{\boldsymbol{q}}\|_1 = P_{\max}$ can be ensured by scaling the eigenvector such that the last component equals one. If there are two eigenvalues with strictly positive eigenvectors, then we know from Lemma 2 that they must have the same value. Hence, the solution of the SINR balancing problem (2.10) is given by

$$C^{\mathrm{UL}}\big(\tilde{\boldsymbol{U}}, P_{\max}\big) = \frac{1}{\lambda_{\max}\big(\boldsymbol{\Lambda}(\tilde{\boldsymbol{U}}, P_{\max})\big)} . \tag{2.16}$$

2.2.2. Minimizing the Sum Power

In the previous section it was shown how to take full advantage of the available total transmission power $P_{\max}$ in a fair (balanced) fashion. From a network operator's perspective, however, it is desirable to multiplex as many channels as possible under the given SINR constraints (1.1). Thus, another optimization strategy is to minimize the total transmission power while maintaining $\mathrm{SINR}_i^{\mathrm{UL}} \geq \gamma_i$ for $i = 1, \ldots, K$. Mathematically, this can be expressed as

$$\min_{\boldsymbol{q}>0} \|\boldsymbol{q}\|_1 \quad \text{subject to} \quad \mathrm{SINR}_i^{\mathrm{UL}}(\tilde{\boldsymbol{u}}_i, \boldsymbol{q}) \geq \gamma_i \ , \quad 1 \leq i \leq K \ . \tag{2.17}$$

If problem (2.17) is feasible, then it leads to a balanced solution with active constraints. This is a direct consequence of Lemma 2. Thus, (2.17) can be seen as a special case of the balancing problem (2.10), where $P_{\max}$ is chosen such that the balanced optimum equals one (cf. Fig. 2.6 on p. 14). In this case, the global optimum is characterized by the set of equations (2.11) with $C^{\mathrm{UL}}\big(\tilde{\boldsymbol{U}}, P_{\max}\big) = 1$. This can be rewritten as

$$\big(\boldsymbol{I} - \boldsymbol{D}\boldsymbol{\Psi}^T(\tilde{\boldsymbol{U}})\big)\ \tilde{\boldsymbol{q}} = \boldsymbol{D}\boldsymbol{\sigma} \ . \tag{2.18}$$

where $\tilde{\boldsymbol{q}}$ is the optimizer of (2.17).

Note, that $C^{\mathrm{UL}}\big(\tilde{\boldsymbol{U}}, P_{\max}\big) = 1$ is not always feasible. This can be best illustrated by considering a 2-user scenario with fixed link gains $\alpha_{ik} \stackrel{\mathrm{def}}{=} \tilde{\boldsymbol{u}}_i^H \boldsymbol{R}_k \tilde{\boldsymbol{u}}_i$, $i,k \in [1,2]$. With (2.7) the constraints $\mathrm{SINR}_i^{\mathrm{UL}} \geq \gamma_i$ can be expressed as

$$q_2 \geq \frac{\gamma_2\alpha_{12}}{\alpha_{22}} q_1 + \frac{\gamma_2\sigma_2^2}{\alpha_{22}} \ , \tag{2.19}$$

$$q_2 \leq \frac{\alpha_{11}}{\gamma_1\alpha_{21}} q_1 - \frac{\sigma_1^2}{\alpha_{21}} \ . \tag{2.20}$$

These inequalities describe half spaces, as illustrated in Fig. 2.7. If these half spaces intersect in the positive quadrant, both targets γ_1 and γ_2 can be supported and the solution is feasible. The power minimum is characterized by the intersection point. It can be easily verified that a feasible solution exists if and only if the slope of (2.20) is larger than the one of (2.19). This leads to the following necessary and sufficient condition for feasibility:

$$\alpha_{12}\alpha_{21}\gamma_1\gamma_2 < \alpha_{11}\alpha_{22} \ . \tag{2.21}$$

In the next section, necessary and sufficient conditions for an arbitrary number of users are derived.

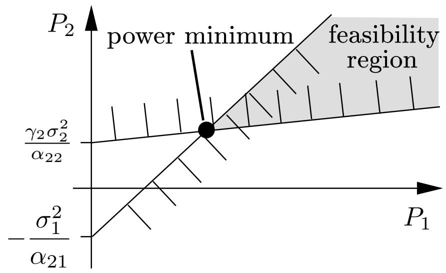

Figure 2.7.: Geometric interpretation of the power minimization problem for fixed beamformers

2.3. Uplink Feasibility in the Absence of Power Constraints

In this section, conditions are derived under which the power minimization problem (2.17) is *feasible* in the absence of power constraints. A scenario is called feasible if there exist transmission powers such that SINR target thresholds $\gamma_1 \dots \gamma_K$ are achieved. The achievable balanced SINR margin (2.10) is tightly upper bounded by

$$B_{\text{Inf}}^{\text{UL}}(\tilde{\boldsymbol{U}}) \overset{\text{def}}{=} \sup_{\boldsymbol{q}\colon \boldsymbol{q}>0} \left(\min_{1\le i\le K} \frac{\text{SINR}_i^{\text{UL}}(\tilde{\boldsymbol{u}}_i, \boldsymbol{q})}{\gamma_i} \right) . \tag{2.22}$$

Since $C^{\text{UL}}(\tilde{\boldsymbol{U}}, P_{\max})$ is strictly monotonically increasing in the sum power $\|\boldsymbol{q}\|_1$, the bound $B_{\text{Inf}}^{\text{UL}}$ is asymptotically approached in the high power regime, where crosstalk dominates over noise (see the illustration in Fig. 2.6).

2.3.1. Feasibility of Coupled Users

Let's start by assuming that all users are coupled by crosstalk, as defined in Section 2.1.4. Then, the asymptotic limit $B_{\text{Inf}}^{\text{UL}}$ can be found by dropping the noise term and balancing the signal-to-interference ratios

$$\text{SIR}_i^{\text{UL}}(\boldsymbol{u}_i, \boldsymbol{q}) = \frac{q_i \boldsymbol{u}_i^H \boldsymbol{R}_i \boldsymbol{u}_i}{\boldsymbol{u}_i^H \left(\sum\limits_{\substack{k=1\\k\neq i}}^{K} q_k \boldsymbol{R}_k \right) \boldsymbol{u}_i} , \quad 1 \le i \le K . \tag{2.23}$$

Observe that each SIR is invariant with respect to a scaling of $\boldsymbol{q}$, thus without loss of generality we can assume $\|\boldsymbol{q}\|_1 = 1$. The limit $B_{\text{Inf}}^{\text{UL}}(\tilde{\boldsymbol{U}})$ is obtained by solving the following max-min balancing problem

$$B_{\text{Inf}}^{\text{UL}}(\tilde{\boldsymbol{U}}) = \max_{\boldsymbol{q}} \left(\min_{1\le i\le K} \frac{\text{SIR}_i^{\text{UL}}(\tilde{\boldsymbol{u}}_i, \boldsymbol{q})}{\gamma_i} \right) \quad \text{subject to} \quad \|\boldsymbol{q}\|_1 = 1 . \tag{2.24}$$

Since all SIR are coupled, (2.24) has a solution $\tilde{\boldsymbol{q}}$ that balances all quantities $\text{SIR}_i^{\text{UL}}(\tilde{\boldsymbol{u}}_i, \tilde{\boldsymbol{q}})$ at a level $B_{\text{Inf}}^{\text{UL}}(\tilde{\boldsymbol{U}})$. Using matrix notation, this can be expressed as

$$\boldsymbol{D}\boldsymbol{\Psi}^T(\tilde{\boldsymbol{U}}) \cdot \tilde{\boldsymbol{q}} = \frac{1}{B_{\text{Inf}}^{\text{UL}}} \cdot \tilde{\boldsymbol{q}} . \tag{2.25}$$

It can be observed that $B_{\text{Inf}}^{\text{UL}}(\tilde{\boldsymbol{U}})$ is a reciprocal eigenvalue of the coupling matrix $\boldsymbol{D}\boldsymbol{\Psi}^T(\tilde{\boldsymbol{U}})$. Since coupled users are assumed, the directed graph associated with the non-negative matrix $\boldsymbol{\Psi}^T(\tilde{\boldsymbol{U}})$ is strongly connected (see Section 2.1.4). This implies that $\boldsymbol{D}\boldsymbol{\Psi}^T(\tilde{\boldsymbol{U}})$ is *irreducible* [46]. From the Perron-Frobenius Theorem it can be concluded that $\boldsymbol{D\Psi}^T(\tilde{\boldsymbol{U}})$ has a simple, real and strictly positive maximal eigenvalue $\lambda_{\max}\big(\boldsymbol{D\Psi}^T(\tilde{\boldsymbol{U}})\big)$, which equals the spectral radius. The eigenvector associated with the maximal eigenvalue is strictly positive. Moreover, all other eigenvectors have at least one negative component. Hence, the maximal eigenvalue is the only valid one. It follows that

$$B^{\mathrm{UL}}_{\mathrm{Inf}}(\tilde{\boldsymbol{U}}) = \frac{1}{\lambda_{\max}\big(\boldsymbol{D\Psi}^T(\tilde{\boldsymbol{U}})\big)} \,. \tag{2.26}$$

To conclude, the power minimization problem (2.17) is feasible for a set of coupled users if and only if $\lambda_{\max}\big(\boldsymbol{D\Psi}^T(\tilde{\boldsymbol{U}})\big) < 1$. For $K = 2$ users, condition (2.26) reduces to $\lambda_{\max}(\boldsymbol{D\Psi}^T) = \sqrt{\alpha_{12}\alpha_{21}\gamma_1\gamma_2} < \sqrt{\alpha_{11}\alpha_{22}}$. This is in good agreement with the feasibility condition (2.21) derived for the 2-user case in Section 2.2.2.

Note, that the problem of achieving SINR targets was already studied by Zander [25–27, 29] in the context of classical power control. The result (2.26) was derived in [26], under the implicit assumption that $\boldsymbol{\Psi}$ is irreducible and the Perron-Frobenius Theorem can be applied. This is always fulfilled in the context of classical power control. However, when additional spatial filtering is used, some users may be decoupled by nullsteering beamforming, as discussed in Section 2.1.4.

2.3.2. General Feasibility

Now, consider a mixed scenario with some uncoupled users and (possibly) several subsets of coupled users. The subsets are mutually uncoupled, so each of them can be regarded as a separate system with an individual performance bound. This leads to the following observations:

- If all user are uncoupled then $\lambda_{\max}(\boldsymbol{D\Psi}^T) = 0$, which means that the system is not limited by crosstalk. An example has already been given in Fig. 2.5 on page 12.

- Suppose that there is one subsystem consisting of two or more coupled users, characterized by an irreducible coupling matrix $\boldsymbol{\Psi}_1$. All other users are uncoupled. Then, the performance is limited by the coupled subsystem, i.e., $\lambda_{\max}(\boldsymbol{D\Psi}^T) = \lambda_{\max}(\boldsymbol{D\Psi}_1^T)$.

- Suppose that there are L subsystems with irreducible coupling matrices $\boldsymbol{\Psi}_1, \ldots, \boldsymbol{\Psi}_L$. The systems are mutually uncoupled. Then, the performance is limited by $\lambda_{\max}(\boldsymbol{D\Psi}^T) = \max\big(\lambda_{\max}(\boldsymbol{D\Psi}_1^T), \ldots, \lambda_{\max}(\boldsymbol{D\Psi}_L^T)\big)$.

The results are further specified by the following theorems:

Theorem 1. *Suppose that the power minimization problem (2.17) is feasible for given noise variances $\tilde{\sigma}_i^2 > 0,\ 1 \le i \le K$, that is, there exists a power vector $\tilde{\boldsymbol{q}} > 0$ such that $\mathrm{SINR}_i^{\mathrm{UL}}(\tilde{\boldsymbol{u}}_i, \tilde{\boldsymbol{q}}, \tilde{\sigma}_i^2) \ge \gamma_i$. Then (2.17) is feasible for any $\sigma_i^2 > 0,\ 1 \le i \le K$.*

Proof. See the appendix on page 72. ∎

Theorem 2. *For any noise vector $\boldsymbol{\sigma} > 0$, problem (2.17) has a feasible solution $\tilde{\boldsymbol{q}} > 0$ if and only if $\lambda_{\max}\big(\boldsymbol{D}\boldsymbol{\Psi}^T(\tilde{\boldsymbol{U}})\big) < 1$.*

Proof. See the appendix on page 73. ∎

These results hold for both coupled and uncoupled users. It can be concluded that asymptotic feasibility depends on the one hand on the target thresholds $\gamma_1 \dots \gamma_K$ (included in $\boldsymbol{D}$), on the other hand on the channel properties and spatial filters (included in the cross-talk matrix $\boldsymbol{\Psi}$).

2.4. The Dual Downlink Problem

Now, let's turn our attention to the downlink channel, where M cooperating transmit antennas are used to transmit independent data streams to K non-cooperating receive antennas. As for the uplink, a sum power constraint is imposed and a fixed beamforming matrix $\tilde{\boldsymbol{U}}$ is assumed. Many arguments used for the uplink analysis obviously hold for the downlink as well, thus some proofs can be omitted.

2.4.1. Downlink Power Allocation

A necessary and sufficient condition for the achievability of individual SINR thresholds $\gamma_1 \dots \gamma_K$ under a sum power constraint $\|\boldsymbol{p}\|_1 \leq P_{\max}$ is given by $C^{\mathrm{DL}}(\tilde{\boldsymbol{U}}, P_{\max}) \geq 1$, where

$$C^{\mathrm{DL}}(\tilde{\boldsymbol{U}}, P_{\max}) = \max_{\boldsymbol{p}} \min_{1 \leq i \leq K} \frac{\mathrm{SINR}_i^{\mathrm{DL}}(\tilde{\boldsymbol{U}}, \boldsymbol{p})}{\gamma_i}, \qquad \text{subject to} \quad \|\boldsymbol{p}\|_1 \leq P_{\max} \;\text{ and }\; \boldsymbol{p} \in \mathbb{R}_+^K . \tag{2.27}$$

First, it can be shown that the optimum of (2.27) is balanced:

Lemma 4. *Let $\tilde{\mathbf{p}}$ be a global maximizer of the optimization problem (2.27), then*

$$C^{\mathrm{DL}}(\tilde{\boldsymbol{U}}, P_{\max}) = \frac{\mathrm{SINR}_i^{\mathrm{DL}}(\tilde{\boldsymbol{U}}, \tilde{\boldsymbol{p}})}{\gamma_i}, \quad 1 \leq i \leq K , \tag{2.28}$$

$$P_{\max} = \|\tilde{\boldsymbol{p}}\|_1 . \tag{2.29}$$

Proof. This can be shown in analogy to Lemma 1. ∎

Lemma 5. *The function $C^{\mathrm{DL}}(\tilde{\boldsymbol{U}}, P_{\max})$ is monotonically increasing in $P_{\max}$.*

Proof. This follows from $\mathrm{SINR}_i^{\mathrm{DL}}(\tilde{\boldsymbol{U}}, \alpha\boldsymbol{p}) > \mathrm{SINR}_i^{\mathrm{DL}}(\tilde{\boldsymbol{U}}, \boldsymbol{p})$, with $1 \leq i \leq K$ and $\alpha > 1$. ∎

Hence, the function $C^{\mathrm{DL}}(\tilde{\boldsymbol{U}}, P_{\max})$ has the same properties as the corresponding uplink function $C^{\mathrm{UL}}(\tilde{\boldsymbol{U}}, P_{\max})$ discussed in Section 2.2. Defining

$$\boldsymbol{\Upsilon}(\boldsymbol{U}, P_{\max}) = \begin{bmatrix} \boldsymbol{D}\boldsymbol{\Psi}(\boldsymbol{U}) & \boldsymbol{D}\boldsymbol{\sigma} \\ \frac{1}{P_{\max}}\boldsymbol{1}_K^T\boldsymbol{D}\boldsymbol{\Psi}(\boldsymbol{U}) & \frac{1}{P_{\max}}\boldsymbol{1}_K^T\boldsymbol{D}\boldsymbol{\sigma} \end{bmatrix} , \tag{2.30}$$

the set of equations (2.28) and (2.29) can be written as

$$\boldsymbol{\Upsilon}(\tilde{\boldsymbol{U}}, P_{\max}) \begin{bmatrix} \tilde{\boldsymbol{p}} \\ 1 \end{bmatrix} = \frac{1}{C^{\mathrm{DL}}(\tilde{\boldsymbol{U}}, P_{\max})} \begin{bmatrix} \tilde{\boldsymbol{p}} \\ 1 \end{bmatrix} . \tag{2.31}$$

Using the same monotony argument as in Section 2.2, it can be shown that

$$C^{\mathrm{DL}}\big(\tilde{\boldsymbol{U}}, P_{\max}\big) = \frac{1}{\lambda_{\max}\big(\boldsymbol{\Upsilon}(\tilde{\boldsymbol{U}}, P_{\max})\big)} , \tag{2.32}$$

where $\lambda_{\max}\big(\boldsymbol{\Upsilon}(P_{\max})\big)$ is the maximal eigenvalue of the extended coupling matrix $\boldsymbol{\Upsilon}$.

In analogy to the uplink, the power minimum is achieved for $C^{\mathrm{DL}}\big(\tilde{\boldsymbol{U}}, P_{\max}\big) = 1$. If the SINR requirements are feasible, then a power allocation that minimizes the total transmission power is found by solving

$$\min_{\boldsymbol{p}>0} \|\boldsymbol{p}\|_1 \quad \text{subject to} \quad \mathrm{SINR}_i^{\mathrm{DL}}(\tilde{\boldsymbol{U}}, \boldsymbol{p}) \geq \gamma_i \ , \quad 1 \leq i \leq K \ . \tag{2.33}$$

Problem (2.33) is called feasible if there exists a solution $\tilde{\boldsymbol{p}} > 0$ that fulfills the constraints in (2.33). Moreover, since $\mathrm{SINR}_i^{\mathrm{DL}}$ is strictly monotonically increasing in p_i and monotonically decreasing in p_k, $k \neq i$, this optimum is characterized by $\mathrm{SINR}_i^{\mathrm{DL}}(\tilde{\boldsymbol{U}}, \tilde{\boldsymbol{p}}) = \gamma_i$. Using matrix notation, this point can be found by solving the following set of equations

$$\big(\boldsymbol{I} - \boldsymbol{D}\boldsymbol{\Psi}(\tilde{\boldsymbol{U}})\big)\tilde{\boldsymbol{p}} = \boldsymbol{D}\boldsymbol{\sigma} \ . \tag{2.34}$$

As in the uplink case, an interesting question is: under which conditions is (2.33) feasible in the asymptotic limit for $P_{\max} \to \infty$? This will be answered in the next section.

2.4.2. Feasibility Conditions for the Downlink

Comparing (2.34) and (2.18), it can be observed that the downlink users are coupled by cross-talk matrix $\boldsymbol{\Psi}$, whereas the uplink users are coupled by the transpose $\boldsymbol{\Psi}^T$. Hence, the same arguments that have been used in Section 2.3 to derive a feasibility bound for the uplink, immediately carry over to the downlink. The results are summarized by the following theorems:

Theorem 3. *Suppose that the power minimization problem (2.33) is feasible for given noise variances* $\tilde{\sigma}_i^2 > 0,\ 1 \leq i \leq K$, *that is, there exists a power vector* $\tilde{\boldsymbol{p}} > 0$ *such that* $\mathrm{SINR}_i^{\mathrm{DL}}(\tilde{\boldsymbol{U}}, \tilde{\boldsymbol{p}}, \tilde{\sigma}_i^2) \geq \gamma_i$. *Then (2.33) is feasible for any* $\sigma_i^2 > 0,\ 1 \leq i \leq K$.

Proof. This can be shown by using the same technique as for Theorem 1. ∎

Theorem 4. *For any noise vector* $\boldsymbol{\sigma} > 0$, *problem (2.33) has a feasible solution* $\tilde{\boldsymbol{p}} > 0$ *if and only if* $\lambda_{\max}\big(\boldsymbol{D}\boldsymbol{\Psi}(\tilde{\boldsymbol{U}})\big) < 1$.

Proof. This can be shown by using the same technique as for Theorem 2. ∎

2.4.3. Weak Duality

Now we compare uplink and downlink performance in terms of their feasibility range. To this end we need the following lemma, which will prove very useful throughout the remainder of this thesis.

Lemma 6. *The maximal eigenvalue of any non-negative real matrix* $\boldsymbol{B}_{K\times K}$ *can be expressed as*

$$\lambda_{\max}(\boldsymbol{B}) = \max_{\boldsymbol{x}>0} \min_{\boldsymbol{y}>0} \frac{\boldsymbol{x}^T \boldsymbol{B} \boldsymbol{y}}{\boldsymbol{x}^T \boldsymbol{y}} = \min_{\boldsymbol{x}>0} \max_{\boldsymbol{y}>0} \frac{\boldsymbol{x}^T \boldsymbol{B} \boldsymbol{y}}{\boldsymbol{x}^T \boldsymbol{y}} \ . \tag{2.35}$$

Proof. See [47, p. 28]. ∎

With Lemma 6 the following result can be proven:

Lemma 7. *Let* $\boldsymbol{\Psi}_{K\times K}$ *be non-negative real and* $\boldsymbol{D}$ *as defined in (2.13). Then*

$$\lambda_{\max}(\boldsymbol{D}\boldsymbol{\Psi}) = \lambda_{\max}(\boldsymbol{D}\boldsymbol{\Psi}^T) \ . \tag{2.36}$$

Proof. Using Lemma 6 and $\lambda_{\max}(\boldsymbol{B}) = \lambda_{\max}(\boldsymbol{B}^T)$, we have

$$\begin{aligned} \lambda_{\max}(\boldsymbol{D}\boldsymbol{\Psi}^T) &= \lambda_{\max}(\boldsymbol{\Psi}\boldsymbol{D}) \\ &= \min_{\boldsymbol{y}>0} \max_{\boldsymbol{x}>0} \frac{\boldsymbol{x}^T \boldsymbol{\Psi} \boldsymbol{D} \boldsymbol{y}}{\boldsymbol{x}^T \boldsymbol{y}} \ . \end{aligned} \tag{2.37}$$

The matrix $\boldsymbol{D}$ is regular, thus we can substitute $\boldsymbol{x}_1 \overset{\mathrm{def}}{=} \boldsymbol{D}^{-1}\boldsymbol{x}$ and $\boldsymbol{y}_1 \overset{\mathrm{def}}{=} \boldsymbol{D}\boldsymbol{y}$. Hence, (2.37) can be rewritten as

$$\begin{aligned} \lambda_{\max}(\boldsymbol{D}\boldsymbol{\Psi}^T) &= \min_{\boldsymbol{y}_1>0} \max_{\boldsymbol{x}_1>0} \frac{\boldsymbol{x}_1^T \boldsymbol{D} \boldsymbol{\Psi} \boldsymbol{y}_1}{\boldsymbol{x}_1^T \boldsymbol{y}_1} \\ &= \lambda_{\max}(\boldsymbol{D}\boldsymbol{\Psi}) \ . \end{aligned} \tag{2.38}$$

∎

Lemma 7 shows that the asymptotic feasibility bounds for uplink and downlink are identical. We refer to this result as *weak duality*:

Theorem 5. *The uplink problem (2.17) is feasible if and only if the downlink problem (2.33) is feasible. Then both problems are feasible for arbitrary noise vectors* $\boldsymbol{\sigma} > 0$.

Proof. The theorem follows directly from Theorem 2, Theorem 4, and Lemma 7. ■

An alternative proof for Theorem 5 was provided by Zander [27].

2.4.4. Strong Duality

Next, $\lambda_{\max}\big(\boldsymbol{D}\boldsymbol{\Psi}(\tilde{\boldsymbol{U}})\big) < 1$ is taken for granted, i.e., both uplink and downlink targets are feasible. Let $\boldsymbol{A} \overset{\text{def}}{=} \big(\boldsymbol{D}^{-1} - \boldsymbol{\Psi}(\tilde{\boldsymbol{U}})\big)^{-1}$. It was already shown that the power minimizing uplink and downlink allocation can be found by solving the sets of equations (2.18) and (2.34), respectively. Hence, there exist positive downlink and uplink power vectors

$$\boldsymbol{p} = \boldsymbol{A}\boldsymbol{\sigma}\ , \qquad \text{(downlink)} \tag{2.39}$$

$$\boldsymbol{q} = \boldsymbol{A}^T\boldsymbol{\sigma}\ . \qquad \text{(uplink)} \tag{2.40}$$

We now whish to know under what conditions does the total uplink power equal the total downlink power, i.e.,

$$\|\boldsymbol{p}\|_1 = \sum_{k=1}^{K} p_k = \sum_{k=1}^{K} q_k = \|\boldsymbol{q}\|_1\ . \tag{2.41}$$

If (2.41) holds together with weak duality, i.e., the same SINR levels are achievable in uplink and downlink, then we say that *strong duality* holds.

Theorem 6. *Let* $\boldsymbol{\sigma} = \nu \cdot \mathbf{1}_K$ *with* $\nu \in \mathbb{R}_+$. *Then strong duality is fulfilled for any non-negative* $\boldsymbol{A}$.

Proof. This is an immediate consequence of

$$\|\boldsymbol{q}\|_1 = \mathbf{1}_K^T\boldsymbol{q} = \nu \cdot \mathbf{1}_K^T\boldsymbol{A}^T\mathbf{1}_K = \nu \cdot \mathbf{1}_K^T\boldsymbol{A}\mathbf{1}_K = \mathbf{1}_K^T\boldsymbol{p} = \|\boldsymbol{p}\|_1. \tag{2.42}$$

The result was published by Boche and Schubert in [6] and was independently derived by Tse and Viswanath in [34]. ■

Now, we are interested in a more general characterization of the noise vectors that guarantee strong duality.

Lemma 8. *Let $\boldsymbol{\sigma}^{(1)} > 0$ and $\boldsymbol{\sigma}^{(2)} > 0$ be noise vectors. The resulting downlink and uplink power vectors follow directly from (2.39) and (2.40). They are denoted by $\boldsymbol{p}^{(1)}$, $\boldsymbol{p}^{(2)}$, $\boldsymbol{q}^{(1)}$, and $\boldsymbol{q}^{(2)}$. Also, consider a noise vector $\boldsymbol{\sigma} = \alpha\boldsymbol{\sigma}^{(1)} + \beta\boldsymbol{\sigma}^{(2)}$, where the positive scalars α and β satisfy $\alpha + \beta = 1$. The resulting power vectors are denoted by $\boldsymbol{p}$ and $\boldsymbol{q}$. Then, $\|\boldsymbol{p}\|_1 = \|\boldsymbol{q}\|_1$ holds for all $\alpha, \beta \geq 0$ if and only if $\|\boldsymbol{p}^{(l)}\|_1 = \|\boldsymbol{q}^{(l)}\|_1,\ l = 1, 2$.*

Proof. Assume $\|\boldsymbol{p}\|_1 = \|\boldsymbol{q}\|_1$. Substituting $\boldsymbol{\sigma} = \alpha\boldsymbol{\sigma}^{(1)} + \beta\boldsymbol{\sigma}^{(2)}$ in (2.39) and (2.40) we have $\boldsymbol{p} = \alpha\boldsymbol{p}^{(1)} + \beta\boldsymbol{p}^{(2)}$ and $\boldsymbol{q} = \alpha\boldsymbol{q}^{(1)} + \beta\boldsymbol{q}^{(2)}$, respectively. From the assumption follows $\|\boldsymbol{p}^{(l)}\|_1 = \|\boldsymbol{q}^{(l)}\|_1,\ l = 1, 2$. To prove the reverse direction, assume $\|\boldsymbol{p}^{(l)}\|_1 = \|\boldsymbol{q}^{(l)}\|_1,\ l = 1, 2$. This implies $\|\boldsymbol{p}\|_1 = \alpha\|\boldsymbol{p}_k^{(1)}\|_1 + \beta\|\boldsymbol{p}_k^{(2)}\|_1 = \|\boldsymbol{q}\|_1$. ∎

Lemma 9. *Suppose that $\boldsymbol{p} = \boldsymbol{A}\boldsymbol{\sigma}$ and $\boldsymbol{q} = \boldsymbol{A}^T\boldsymbol{\sigma}$ fulfill (2.41), where $\boldsymbol{\sigma} > 0$ is an arbitrary positive noise vector and $\boldsymbol{A}$ is non-negative. Then (2.41) is fulfilled for* all *noise vectors $\boldsymbol{\sigma} \geq 0$.*

Proof. Let $\hat{\boldsymbol{\sigma}}$ be an arbitrary noise vector with $[\hat{\boldsymbol{\sigma}}]_l = 0$ for some index l. Let $\hat{\boldsymbol{p}} = \boldsymbol{A}\hat{\boldsymbol{\sigma}}$ and $\hat{\boldsymbol{q}} = \boldsymbol{A}^T\hat{\boldsymbol{\sigma}}$. Now, consider the convergent sequence $\hat{\boldsymbol{\sigma}}^{(n)} = \hat{\boldsymbol{\sigma}} + \frac{1}{n}\mathbf{1}_K$ with $[\hat{\boldsymbol{\sigma}}^{(n)}]_l > 0,\ 1 \leq l \leq K$. Since the linear operator $\boldsymbol{A}$ is continuous, the sequences $\hat{\boldsymbol{p}}^{(n)} = \boldsymbol{A}\hat{\boldsymbol{\sigma}}^{(n)}$ and $\hat{\boldsymbol{q}}^{(n)} = \boldsymbol{A}^T\hat{\boldsymbol{\sigma}}^{(n)}$ are also convergent. With the assumption that (2.41) holds for any $\boldsymbol{\sigma} > 0$, we have $\|\hat{\boldsymbol{p}}^{(n)}\|_1 = \|\hat{\boldsymbol{q}}^{(n)}\|_1$ for all n. Hence,

$$\lim_{n\to\infty} \|\hat{\boldsymbol{p}}^{(n)}\|_1 = \|\hat{\boldsymbol{p}}\|_1 = \lim_{n\to\infty} \|\hat{\boldsymbol{q}}^{(n)}\|_1 = \|\hat{\boldsymbol{q}}\|_1 \; .$$

From this we can conclude that (2.41) holds for $\hat{\boldsymbol{\sigma}} \geq 0$. ∎

Lemma 10. *Given a matrix $\boldsymbol{A}$, the relation (2.41) is fulfilled for all $\boldsymbol{\sigma} > 0$ if and only if it is fulfilled for*

$$[\boldsymbol{e}^{(k)}]_l = \begin{cases} 1, & l = k \\ 0, & l \neq k \end{cases} , \quad 1 \leq k \leq K \; . \tag{2.43}$$

Proof. If (2.41) is fulfilled for all $\boldsymbol{\sigma} > 0$, then it follows from Lemma 9 that it is also fulfilled for vectors (2.43). On the other hand, if (2.41) is fulfilled for (2.43), we know from Lemma 8 that it is fulfilled for all linear combinations, i.e., for all $\boldsymbol{\sigma} > 0$. ∎

Using the above results, it can be shown that strong duality holds for *any* noise vector if and only if the matrix $\boldsymbol{A}$ has a specific structure specified by the following theorem (the result was published by Boche and Schubert in [1]).

Theorem 7. *Relation (2.41) holds for all $\boldsymbol{\sigma} > 0$ if and only if*

$$\sum_{l=1}^{K} \boldsymbol{A}_{kl} = \sum_{l=1}^{K} \boldsymbol{A}_{lk} \; , \quad 1 \leq k \leq K \; . \tag{2.44}$$

Proof. This follows directly from Lemma 10 with $\boldsymbol{p}^{(k)} = \boldsymbol{A}\boldsymbol{e}^{(k)} = \sum_{l=1}^{K} \boldsymbol{A}_{lk}$ and $\boldsymbol{q}^{(k)} = \boldsymbol{A}^T\boldsymbol{e}^{(k)} = \sum_{l=1}^{K} \boldsymbol{A}_{kl}$, where $\boldsymbol{e}^{(k)}$ is defined as in (2.43). ∎

2.5. Discussion

In this chapter, a fundamental duality between the downlink point-to-multipoint channel and the uplink multipoint-to-point channel has been found. If one of the conditions formulated by Theorem 6 and Theorem 7 hold true, then identical SINR levels can be achieved in both links with the same total transmission power.

This duality relation is extremely useful, as will be shown in the following. In particular, each SINR-based signaling strategy that is designed for the uplink immediately carries over to the downlink. One merely has to ensure that the condition in Theorem 6 is fulfilled, i.e., all receivers have the same noise level.

For the downlink, this is easily achieved by scaling the SINR (2.5) such that $\boldsymbol{\sigma} = \mathbf{1}_K$. Then, the optimization has to be performed with respect to *scaled* matrices $\boldsymbol{R}_1/\sigma_1^2, \ldots, \boldsymbol{R}_K/\sigma_K^2$. Such a scaling has no impact on the downlink SINR. However, when applying the same matrices to the uplink problem, one has

$$\mathrm{SINR}_i^{\mathrm{UL}}(\boldsymbol{u}_i, \boldsymbol{p}) = \frac{p_i \boldsymbol{u}_i^H \frac{\boldsymbol{R}_i}{\sigma_i^2} \boldsymbol{u}_i}{\boldsymbol{u}_i^H \left(\sum_{\substack{k=1 \\ k \neq i}}^{K} p_k \frac{\boldsymbol{R}_k}{\sigma_k^2} + \boldsymbol{I} \right) \boldsymbol{u}_i} \, , \quad 1 \leq i \leq K \, . \tag{2.45}$$

This scaled SINR may in general be different from the true uplink SINR (2.7). Thus, strong duality only holds between the scaled channels. But by solving the scaled "virtual" uplink problem, one always gets a solution for the "true" downlink problem.

If one is interested in the uplink problem, the condition $\boldsymbol{\sigma} = \mathbf{1}_K$ can likewise be ensured. While the downlink channel is invariant to a scaling of the link gains, the uplink channel is invariant to a scaling of the beamforming weights. By constraining $\sigma_i^2 \boldsymbol{u}_i^H \boldsymbol{u}_i = 1$, it would in principle be possible to achieve target SINR's in the uplink by considering the dual "virtual" downlink problem instead. However, this is less interesting from a practical point of view since the downlink has a more difficult analytical structure.

Finally, note that the duality found in this chapter stands in an interesting relationship to other results in the literature:

- In [39, 40] an iterative algorithm for joint beamforming and power control was proposed which uses *virtual* uplink power control in each iteration step.
- In [48] it was shown that the capacity of the MIMO channel remains the same when reversing the role of transmitter and receiver
- In [33] duality was found in an information theoretical context, between the Gaussian broadcast channel and the multiple access channel.

The generalization of these independent observations is still an open problem. Partial results will be presented later in Chapter 5.

3. Joint Beamforming in the Absence of Noise

In the previous chapter it was shown how the achievable SINR margin is limited by the effects of mutual interference. Assuming coupled users, an upper bound on the system performance can be found by balancing the signal-to-interference ratios (SIR) in the absence of noise.

In this chapter the problem of SIR balancing is studied with additional optimization over the beamforming filters. This problem was first addressed by Gerlach and Paulraj [10] in the context of downlink beamforming. Algorithms have been presented in [10, 43]. However, no proof of global convergence was found so far. One goal of this chapter is to analyze both optimization strategies and to carry out a convergence analysis.

By studying the joint beamforming problem in the absence of noise, necessary and sufficient conditions for feasibility are obtained, as discussed in Section 2.3. Moreover, it is expected that the results provide deeper insight into the analytical structure of the general problem of controlling SINR levels.

3.1. Optimal Interference Balancing based on ℓ_∞-Norm Minimization

We start with the downlink SIR balancing problem, as formulated by Gerlach and Paulraj [10]. For given channel matrices $\boldsymbol{R}_1, \ldots, \boldsymbol{R}_K$, one is interested in the beamforming matrix $\boldsymbol{U}$ and power allocation $\boldsymbol{p}$, which jointly balance the values $\mathrm{SIR}_i^{\mathrm{DL}}/\gamma_i$, $1 \le i \le K$, as high as possible. Each SIR is a function of $\boldsymbol{p}$ and $\boldsymbol{U}$, i.e.,

$$\mathrm{SIR}_i^{\mathrm{DL}}(\boldsymbol{p}, \boldsymbol{U}) = \frac{p_i \boldsymbol{u}_i^H \boldsymbol{R}_i \boldsymbol{u}_i}{\sum\limits_{\substack{k=1 \\ k \neq i}}^{K} p_k \boldsymbol{u}_k^H \boldsymbol{R}_i \boldsymbol{u}_k}, \quad 1 \le i \le K . \tag{3.1}$$

This problem can be expressed mathematically as

$$B_{\mathrm{Inf}}^{\mathrm{DL}} = \max_{\boldsymbol{U},\boldsymbol{p}} \left(\min_{1 \le i \le K} \frac{\mathrm{SIR}_i^{\mathrm{DL}}(\boldsymbol{U}, \boldsymbol{p})}{\gamma_i} \right) \quad \text{subject to} \quad \begin{array}{l} \|\boldsymbol{u}_i\|_2 = 1, \ \ 1 \le i \le K , \\ \|\boldsymbol{p}\|_1 = 1 . \end{array} \tag{3.2}$$

Note, that this problem is only defined as long as each user receives interference, in which case the optimum is characterized by balanced relative SIR levels. Thus, min-max operations are interchangeable and one can equivalently balance the reciprocal quantities $\gamma_i/\mathrm{SIR}_i^{\mathrm{DL}}$. Hence, problem (3.2) is solved by minimizing the ℓ_∞-norm of the vector

$$\boldsymbol{\xi}(\boldsymbol{U},\boldsymbol{p}) = \left[\frac{\gamma_1}{\mathrm{SIR}_1^{\mathrm{DL}}(\boldsymbol{U},\boldsymbol{p})},\ldots,\frac{\gamma_K}{\mathrm{SIR}_K^{\mathrm{DL}}(\boldsymbol{U},\boldsymbol{p})}\right]^T . \tag{3.3}$$

By optimizing over both $\boldsymbol{U}$ and $\boldsymbol{p}$, the optimally balanced level $B_{\mathrm{Inf}}^{\mathrm{DL}}$ is found:

$$\frac{1}{B_{\mathrm{Inf}}^{\mathrm{DL}}} = \min_{\boldsymbol{U},\boldsymbol{p}} \|\boldsymbol{\xi}(\boldsymbol{U},\boldsymbol{p})\|_\infty . \tag{3.4}$$

Note, that (3.4) has a non-differentiable objective function which in general may have many local minima. Thus, there is no obvious way for finding the global optimum. Fortunately, the analytical results of Chapter 2 provide a characterization of the global optimum, which leads to a form that is better suited for optimization. This will be shown in the following section.

3.1.1. Eigenvalue Minimization

In Section 2.3.1 it has been shown that for any fixed beamforming matrix $\tilde{\boldsymbol{U}}$ the balanced optimum is given by the inverse maximal eigenvalue $\lambda_{\max}\big(\boldsymbol{D}\boldsymbol{\Psi}(\tilde{\boldsymbol{U}})\big)$. Hence, the global optimum of the ℓ_∞ optimization problem (3.4) is found by solving an eigenvalue optimization problem

$$B_{\mathrm{Inf}}^{\mathrm{DL}} = \frac{1}{\min\limits_{\boldsymbol{U}} \lambda_{\max}\big(\boldsymbol{D}\boldsymbol{\Psi}(\boldsymbol{U})\big)} \quad \text{subject to} \quad \|\boldsymbol{u}_i\|_2 = 1, \;\; 1 \le i \le K . \tag{3.5}$$

Note, that this problem no longer depends on $\boldsymbol{p}$. Once an optimizer $\boldsymbol{U}^{opt}$ is found, the associated $\boldsymbol{p}^{opt}$ is given as the dominant right-hand eigenvector of the matrix $\boldsymbol{D}\boldsymbol{\Psi}(\boldsymbol{U}^{opt})$, as shown in Section 2.3.1.

Another straightforward observation is that the eigenvalue optimization problem (3.5) not only provides a solution of the ℓ_∞ balancing problem (3.2), but also provides a necessary and sufficient criterion for the feasibility of SINR $\ge \gamma_i$, $1 \le i \le K$. It has been shown in Section 2.3.2, that this does not require the assumption of coupled users, which can therefore be dropped as long as the eigenvalue optimization problem (3.5) is concerned. The maximal eigenvalue is always defined, even if the users are completely decoupled. If (3.5) has a solution $B_{\mathrm{Inf}}^{\mathrm{DL}} = 0$, then SINR $\ge \gamma_i$ is always feasible, but (3.4) is not defined.

While the problem formulation (3.5) has less degrees of freedom than the original problem (3.2), it is still very unlikely to allow for efficient algorithmic solution. As the objective function may generally be non-convex, global optimization may be prevented by local minima.

In this situation one can make use of the weak duality formulated in Section 2.4.3. From this result it is known that instead of balancing the downlink quantities $\mathrm{SIR}_i^{\mathrm{DL}}/\gamma_i$ one can equivalently balance the uplink quantities $\mathrm{SIR}_i^{\mathrm{UL}}/\gamma_i$, where $\mathrm{SIR}_i^{\mathrm{UL}}$ is defined in (2.23). The following balanced level can be achieved by optimizing over both $\boldsymbol{U}$ and $\boldsymbol{q}$:

$$B_{\mathrm{Inf}}^{\mathrm{UL}} = \max_{\boldsymbol{U},\boldsymbol{q}} \left(\min_{1\le i\le K} \frac{\mathrm{SIR}_i^{\mathrm{UL}}(\boldsymbol{u}_i,\boldsymbol{q})}{\gamma_i} \right) \quad \text{subject to} \quad \begin{array}{l} \|\boldsymbol{u}_i\|_2 = 1, \;\; 1 \le i \le K \;, \\ \|\boldsymbol{q}\|_1 = 1 \;. \end{array} \tag{3.6}$$

Note, that $\mathrm{SIR}_i^{\mathrm{UL}}(\boldsymbol{u}_i,\boldsymbol{q})$ is scalable in $\boldsymbol{q}$, thus $\|\boldsymbol{q}\|_1 = 1$ can be assumed without loss of generality. As in the downlink, the max-min balancing problem (3.6) can be equivalently stated as an eigenvalue optimization problem

$$B_{\mathrm{Inf}}^{\mathrm{UL}} = \frac{1}{\min\limits_{\boldsymbol{U}} \lambda_{\max}\big(\boldsymbol{D}\boldsymbol{\Psi}^T(\boldsymbol{U})\big)} \;, \quad \text{subject to} \quad \|\boldsymbol{u}_i\|_2 = 1, \quad 1 \le i \le K \;. \tag{3.7}$$

From Lemma 7 in Section 2.4.3 it is known that $B_{\mathrm{Inf}}^{\mathrm{DL}} = B_{\mathrm{Inf}}^{\mathrm{UL}}$ for any beamforming matrix, including the global minimizers of (3.5) and (3.7). Hence, any beamformer that solves the uplink problem (3.7) also solves the downlink problem (3.5) and vice versa. Note that this one-to-one correspondence pertains to the beamforming solution, but not to the transmission powers. The optimal power allocation in uplink and downlink may in general be different. Having found a global minimizer $\boldsymbol{U}^{opt}$, the power allocations are found by solving the following two eigenvalue problems (see Section 2.3):

$$\boldsymbol{D}\boldsymbol{\Psi}^T(\boldsymbol{U}^{opt}) \cdot \boldsymbol{q}^{opt} = \frac{1}{B_{\mathrm{Inf}}^{\mathrm{UL}}} \cdot \boldsymbol{q}^{opt} \;, \qquad \text{(uplink)} \tag{3.8}$$

$$\boldsymbol{D}\boldsymbol{\Psi}(\boldsymbol{U}^{opt}) \cdot \boldsymbol{p}^{opt} = \frac{1}{B_{\mathrm{Inf}}^{\mathrm{DL}}} \cdot \boldsymbol{p}^{opt} \;. \qquad \text{(downlink)} \tag{3.9}$$

3.1.2. Characterization of the Global Minimizer

Next, the global optimum of (3.7) is characterized. With Lemma 6 we have

$$\lambda_{\max}\big(\boldsymbol{D}\boldsymbol{\Psi}^T(\boldsymbol{U})\big) = \max_{\boldsymbol{x}>0} \min_{\boldsymbol{y}>0} \frac{\boldsymbol{x}^T\boldsymbol{D}\boldsymbol{\Psi}^T(\boldsymbol{U})\boldsymbol{y}}{\boldsymbol{x}^T\boldsymbol{y}} = \min_{\boldsymbol{x}>0} \max_{\boldsymbol{y}>0} \frac{\boldsymbol{x}^T\boldsymbol{D}\boldsymbol{\Psi}^T(\boldsymbol{U})\boldsymbol{y}}{\boldsymbol{x}^T\boldsymbol{y}} \;. \tag{3.10}$$

Using (3.10), the eigenvalue minimization problem (3.7) can be rewritten as

$$\frac{1}{B_{\mathrm{Inf}}^{\mathrm{UL}}} = \min_{\boldsymbol{U}:\,\|\boldsymbol{u}_i\|_2=1} \min_{\boldsymbol{q}>0} \hat{f}(\boldsymbol{U},\boldsymbol{q}), \quad \text{with} \quad \hat{f}(\boldsymbol{U},\boldsymbol{q}) = \max_{\boldsymbol{x}>0} \frac{\boldsymbol{x}^T\boldsymbol{D}\boldsymbol{\Psi}^T(\boldsymbol{U})\boldsymbol{q}}{\boldsymbol{x}^T\boldsymbol{q}} \;. \tag{3.11}$$

Here, $\boldsymbol{x}$ is an auxiliary variable which has no physical meaning. The vector $\boldsymbol{q}$ can be interpreted as the uplink power vector. Now, the idea is to find an alternating optimization scheme that keeps one of the variables $\boldsymbol{U}$ and $\boldsymbol{q}$ fixed while minimizing with respect to the other.

Theorem 8. *For a fixed beamforming matrix* $\hat{\boldsymbol{U}}$ *the objective function* $\hat{f}(\hat{\boldsymbol{U}}, \boldsymbol{q})$ *is minimized by the dominant eigenvalue of* $\boldsymbol{D}\boldsymbol{\Psi}^T(\hat{\boldsymbol{U}})$.

Proof. From (3.10) we know that the minimum of the objective function is $\min_{\boldsymbol{q}>0} \hat{f}(\hat{\boldsymbol{U}}, \boldsymbol{q}) = \lambda_{\max}\big(\boldsymbol{D}\boldsymbol{\Psi}^T(\hat{\boldsymbol{U}})\big)$. Let $\hat{\boldsymbol{q}}$ be a solution of

$$\boldsymbol{D}\boldsymbol{\Psi}^T(\hat{\boldsymbol{U}}) \cdot \hat{\boldsymbol{q}} = \lambda_{\max}\big(\boldsymbol{D}\boldsymbol{\Psi}^T(\hat{\boldsymbol{U}})\big) \cdot \hat{\boldsymbol{q}} \; . \tag{3.12}$$

Then the following relation holds for any $\boldsymbol{x} > 0$:

$$\frac{\boldsymbol{x}^T \boldsymbol{D}\boldsymbol{\Psi}^T(\hat{\boldsymbol{U}})\hat{\boldsymbol{q}}}{\boldsymbol{x}^T\hat{\boldsymbol{q}}} = \lambda_{\max}\big(\boldsymbol{D}\boldsymbol{\Psi}^T(\hat{\boldsymbol{U}})\big) \; .$$

This can be shown by left-hand multiplying both sides of (3.12) with $\boldsymbol{x}^T/\boldsymbol{x}^T\hat{\boldsymbol{q}}$. Hence, $\hat{f}(\hat{\boldsymbol{U}}, \hat{\boldsymbol{q}}) = \lambda_{\max}\big(\boldsymbol{D}\boldsymbol{\Psi}^T(\hat{\boldsymbol{U}})\big)$. ■

Theorem 9. *For a fixed power allocation* $\tilde{\boldsymbol{q}}$ *the objective function* $\hat{f}(\boldsymbol{U}, \tilde{\boldsymbol{q}})$ *is minimized by* $\tilde{\boldsymbol{U}} = [\tilde{\boldsymbol{u}}_1, \dots, \tilde{\boldsymbol{u}}_K]$*, where* $\tilde{\boldsymbol{u}}_i$ *is the dominant eigenvector of the generalized eigenproblem*

$$\boldsymbol{R}_i\boldsymbol{u}_i = \lambda_{\max}\boldsymbol{Q}_i(\tilde{\boldsymbol{q}})\boldsymbol{u}_i \tag{3.13}$$

$$\textit{with} \quad \boldsymbol{Q}_i(\boldsymbol{q}) = \sum_{\substack{k=1\\k\neq i}}^{K} [\boldsymbol{q}]_k \boldsymbol{R}_k \; . \tag{3.14}$$

Proof. There exists an $\boldsymbol{x}_0 > 0$ such that

$$\begin{aligned}\hat{f}(\boldsymbol{U}, \tilde{\boldsymbol{q}}) = \max_{\boldsymbol{x}>0} \frac{\boldsymbol{x}^T\boldsymbol{D}\boldsymbol{\Psi}^T(\boldsymbol{U})\tilde{\boldsymbol{q}}}{\boldsymbol{x}^T\tilde{\boldsymbol{q}}} &= \frac{\boldsymbol{x}_0^T\boldsymbol{D}\boldsymbol{\Psi}^T(\boldsymbol{U})\tilde{\boldsymbol{q}}}{\boldsymbol{x}_0^T\tilde{\boldsymbol{q}}} \\ &= \frac{1}{\boldsymbol{x}_0^T\tilde{\boldsymbol{q}}} \sum_{i=1}^{K} [\boldsymbol{x}_0]_i \gamma_i \frac{\boldsymbol{u}_i^H\boldsymbol{Q}_i(\tilde{\boldsymbol{q}})\boldsymbol{u}_i}{\boldsymbol{u}_i^H\boldsymbol{R}_i\boldsymbol{u}_i} \; . \end{aligned} \tag{3.15}$$

Observe that the minimization with respect to $\boldsymbol{U} = [\boldsymbol{u}_1, \dots, \boldsymbol{u}_K]$ leads to a set of K decoupled problems. The optimizers can equivalently be found by maximizing the reciprocal value, i.e.,

$$\tilde{\boldsymbol{u}}_i = \arg\max_{\boldsymbol{u}_i} \frac{\boldsymbol{u}_i^H\boldsymbol{R}_i\boldsymbol{u}_i}{\boldsymbol{u}_i^H\boldsymbol{Q}_i(\tilde{\boldsymbol{q}})\boldsymbol{u}_i} \quad \text{subject to} \quad \|\boldsymbol{u}_i\|_2 = 1 \; , \;\; 1 \leq i \leq K \; . \tag{3.16}$$

Hence, the i^{th} beamforming vector $\tilde{\boldsymbol{u}}_i$ is given by the dominant generalized eigenvector of the matrix pair $\big(\boldsymbol{R}_i, \boldsymbol{Q}_i(\tilde{\boldsymbol{q}})\big)$. ■

Note, that (3.16) maximizes the ratio between the desired signal power of the i^{th} user and the interference received by all other users, which provides an additional interpretation. Interestingly, the SIR requirements contained in $\boldsymbol{D}$ play no role for the beamforming optimization. However, they are used for each power allocation step, thus they indirectly influence the optimal beamforming solution.

With (3.10) and Theorem 9 we are able to prove the following necessary and sufficient condition for global optimality:

Theorem 10. *A beamforming matrix $\bar{\boldsymbol{U}}$ solves the eigenvalue minimization problem (3.7) if and only if for all $\boldsymbol{x} > 0$*

$$\frac{\boldsymbol{x}^T \boldsymbol{D}\boldsymbol{\Psi}^T(\bar{\boldsymbol{U}})\bar{\boldsymbol{q}}}{\boldsymbol{x}^T\bar{\boldsymbol{q}}} = \min_{\boldsymbol{U}} \frac{\boldsymbol{x}^T \boldsymbol{D}\boldsymbol{\Psi}^T(\boldsymbol{U})\bar{\boldsymbol{q}}}{\boldsymbol{x}^T\bar{\boldsymbol{q}}} , \tag{3.17}$$

$$\text{where } \bar{\boldsymbol{q}} \text{ fulfills} \quad \boldsymbol{D}\boldsymbol{\Psi}^T(\bar{\boldsymbol{U}}) \cdot \bar{\boldsymbol{q}} = \lambda_{\max}\big(\boldsymbol{D}\boldsymbol{\Psi}^T(\bar{\boldsymbol{U}})\big) \cdot \bar{\boldsymbol{q}} \ . \tag{3.18}$$

Proof. See the appendix on page 75. ■

It can be concluded from Theorem 10 that the beamformers $\boldsymbol{U}^{opt}$ and transmission powers $\boldsymbol{q}^{opt}$ that solve the uplink SIR balancing problem (3.6) are always linked in the special way described by (3.17) and (3.18). Hence, the optimum is completely determined if either $\boldsymbol{q}^{opt}$ and $\boldsymbol{U}^{opt}$ is known. This will be exploited in the next section.

3.1.3. Subspace Characterization of the Optimal Beamforming Solutions

Suppose that the power allocation $\boldsymbol{q}^{opt}$ solves the SIR balancing problem (3.6). The optimal beamforming solution that is associated with $\boldsymbol{q}^{opt}$ need not be unique. The set of possible solutions is denoted as $\mathcal{M}_\infty$. From Theorem 10 we know that an optimal beamformer $\boldsymbol{U}^{opt}$ fulfills

$$\boldsymbol{D}\boldsymbol{\Psi}^T(\boldsymbol{U}^{opt}) \cdot \boldsymbol{q}^{opt} = \lambda_{\max}^{opt} \cdot \boldsymbol{q}^{opt} , \tag{3.19}$$

where $\lambda_{\max}^{opt} \stackrel{\text{def}}{=} 1/B_{\text{Inf}}^{\text{UL}}$. The set of equations (3.19) can be rewritten as

$$(\boldsymbol{u}_i^{opt})^H \, \boldsymbol{\Omega}_i(\lambda_{max}^{opt}, \boldsymbol{q}^{opt}) \, \boldsymbol{u}_i^{opt} = 0 \ , \quad 1 \le i \le K \ , \tag{3.20}$$

where the functions $\boldsymbol{\Omega}_i$ are defined as

$$\boldsymbol{\Omega}_i(\lambda, \boldsymbol{q}) = \lambda \, q_i \boldsymbol{R}_i - \gamma_i \sum_{\substack{k=1 \\ k \neq i}}^{K} q_k \boldsymbol{R}_k, \quad 1 \le i \le K \ . \tag{3.21}$$

It can be observed from (3.20) that a solution $\boldsymbol{U}^{opt} \in \mathcal{M}_\infty$ exists as long as the matrices $\boldsymbol{\Omega}_i(\lambda_{max}^{opt}, \boldsymbol{q}^{opt})$ are singular. This provides a new criterion for feasibility. Unlike the criterion used in Section 2.3.1, this criterion is not based on a given set of beamforming weights. Instead, feasibility is characterized for a given power allocation.

Theorem 11. *The constraints* $\mathrm{SINR}_i^{\mathrm{UL}} \geq \gamma_i$, $1 \leq i \leq K$, *are feasible if and only if there exist* $\lambda < 1$ *and* $\tilde{\boldsymbol{q}} > 0$ *such that the matrices* $\boldsymbol{\Omega}_i(\lambda, \tilde{\boldsymbol{q}})$ *are singular. Then, each* $\tilde{\boldsymbol{u}}_i$ *chosen from the nullspace of* $\boldsymbol{\Omega}_i(\lambda, \tilde{\boldsymbol{q}})$ *fulfills* $\mathrm{SIR}_i^{\mathrm{UL}}(\tilde{\boldsymbol{u}}_i, \tilde{\boldsymbol{q}}) > \gamma_i$.

Proof. See the appendix on page 76. ∎

From Theorem 11 some useful properties can be derived:

Corollary 1. *An alternative strategy for solving the eigenvalue optimization problem (3.6) is as follows. Let* $\boldsymbol{\Omega}_i(\lambda, \boldsymbol{q})$ *be singular matrices as defined in (3.21), then*

$$\frac{1}{B_{\mathrm{Inf}}^{\mathrm{UL}}} = \min_{\boldsymbol{q},\lambda} \lambda \qquad \textit{subject to singular matrices} \quad \boldsymbol{\Omega}_i(\lambda, \boldsymbol{q}),\ 1 \leq i \leq K\ , \tag{3.22}$$

which provides the smallest positive λ *for which representation (3.20) holds true.*

Corollary 2. *Let* $(\boldsymbol{U}^{opt}, \boldsymbol{q}^{opt})$ *be a minimizer of (3.6), then* $\boldsymbol{U}^{opt}$ *is unique if and only if the matrix* $\boldsymbol{\Omega}_i(1/B_{\mathrm{Inf}}^{\mathrm{UL}}, \boldsymbol{q}^{opt})$ *has a one-dimensional null space.*

Corollary 3. *If the balancing problem (3.6) has two distinct solutions* $\boldsymbol{U}^I = [\boldsymbol{u}_1^I, \ldots, \boldsymbol{u}_K^I]$ *and* $\boldsymbol{U}^{II} = [\boldsymbol{u}_1^{II}, \ldots, \boldsymbol{u}_K^{II}]$, *then* $\tilde{\boldsymbol{u}}_k = \mu \boldsymbol{u}_k^I + (1-\mu)\boldsymbol{u}_k^{II}$ *with* $0 < \mu < 1$ *is also a solution. All solutions are associated with the same power allocation.*

3.2. A Globally Convergent Algorithm

The analytical results in Section 3.1.2 motivate an alternating optimization strategy for problem (3.6). By keeping either $\boldsymbol{U}$ or $\boldsymbol{q}$ fixed and minimizing $\hat{f}(\boldsymbol{U}, \boldsymbol{q})$ with respect to the other variable, one can expect to approach a minimum. The required optimization steps are provided by Theorems 8 and 9. This motivates Algorithm 1, which was first described in [43], but without proof of convergence. A complete convergence analysis will be provided in the next section. The result was published by Schubert and Boche in [5].

3.2.1. Monotony and Global Convergence

Next, monotony and global convergence of Algorithm 1 will be proven. This is perhaps surprising, since the objective function is non-convex and may have local minima. Similar strategies based on alternating variables are known to have very poor convergence properties and may even get stuck before reaching a minimum.

However, the following results show that this is not the case for Algorithm 1, which exhibits excellent convergence behavior. A key step in the proof is Theorem 10, which shows that each local minimum of the objective $\hat{f}(\boldsymbol{U}, \boldsymbol{q})$ is a global minimum. Hence, it remains to prove convergence.

Algorithm 1 Solution of the eigenvalue minimization problem (3.7)

$n \Leftarrow 0$
$\boldsymbol{q}^{(0)} \Leftarrow [1, \dots, 1]^T$
$\lambda_{\max}(0) \Leftarrow 0$
repeat
  $n \Leftarrow n + 1$
  $\boldsymbol{u}_i^{(n)} \Leftarrow \arg\max_{\boldsymbol{u}_i} \dfrac{\boldsymbol{u}_i^H \boldsymbol{R}_i \boldsymbol{u}_i}{\boldsymbol{u}_i^H \boldsymbol{Q}_i(\boldsymbol{q}^{(n-1)}) \boldsymbol{u}_i}, \quad \text{subject to} \quad \|\boldsymbol{u}_i\|_2 = 1, \quad 1 \leq i \leq K$
  $\big(\lambda_{\max}(n), \boldsymbol{q}^{(n)}\big) \Leftarrow \text{solution of } \boldsymbol{D}\boldsymbol{\Psi}^T(\boldsymbol{U}^{(n)}) \cdot \boldsymbol{q}^{(n)} = \lambda_{\max}(n) \cdot \boldsymbol{q}^{(n)}$
until $|\lambda_{\max}(n) - \lambda_{\max}(n-1)| \leq \epsilon$

Theorem 12. *The iteration sequence $\lambda_{\max}(n)$ provided by Algorithm 1 is monotonically decreasing and converges towards the global optimum of the eigenvalue minimization problem (3.7).*

Proof. Define

$$\tilde{\lambda}_n(\boldsymbol{x}) \stackrel{\text{def}}{=} \frac{\boldsymbol{x}^T \boldsymbol{D}\boldsymbol{\Psi}^T(\boldsymbol{U}^{(n)})\boldsymbol{q}^{(n-1)}}{\boldsymbol{x}^T \boldsymbol{q}^{(n-1)}}, \quad \boldsymbol{x} > 0 . \tag{3.23}$$

By the same argumentation as in the proof of Theorem 9, it can be shown that $\boldsymbol{U}^{(n)}$ is a minimizer of $\boldsymbol{x}^T \boldsymbol{D}\boldsymbol{\Psi}^T(\boldsymbol{U})\boldsymbol{q}^{(n-1)} = \sum_{i=1}^{K} [\boldsymbol{x}]_i \gamma_i \frac{\boldsymbol{u}_i^H \boldsymbol{Q}_i(\boldsymbol{q}^{(n-1)})\boldsymbol{u}_i}{\boldsymbol{u}_i^H \boldsymbol{R}_i \boldsymbol{u}_i}$ for any $\boldsymbol{x} > 0$. Thus

$$\tilde{\lambda}_n(\boldsymbol{x}) \leq \frac{\boldsymbol{x}^T \boldsymbol{D}\boldsymbol{\Psi}^T(\boldsymbol{U}^{(n-1)})\boldsymbol{q}^{(n-1)}}{\boldsymbol{x}^T \boldsymbol{q}^{(n-1)}} = \lambda_{\max}(n-1) . \tag{3.24}$$

This follows directly from $\boldsymbol{D}\boldsymbol{\Psi}^T(\boldsymbol{U}^{(n)}) \cdot \boldsymbol{q}^{(n)} = \lambda_{\max}(n) \cdot \boldsymbol{q}^{(n)}$. Combining (3.10) and (3.23), we have

$$\begin{aligned} \lambda_{\max}(n) &= \max_{\boldsymbol{x}>0} \min_{\boldsymbol{y}>0} \frac{\boldsymbol{x}^T \boldsymbol{D}\boldsymbol{\Psi}^T(\boldsymbol{U}^{(n)})\boldsymbol{y}}{\boldsymbol{x}^T \boldsymbol{y}} \\ &\leq \max_{\boldsymbol{x}>0} \frac{\boldsymbol{x}^T \boldsymbol{D}\boldsymbol{\Psi}^T(\boldsymbol{U}^{(n)})\boldsymbol{q}^{(n-1)}}{\boldsymbol{x}^T \boldsymbol{q}^{(n-1)}} = \max_{\boldsymbol{x}>0} \tilde{\lambda}_n(\boldsymbol{x}) . \end{aligned} \tag{3.25}$$

Likewise, it can be shown that $\lambda_{\max}(n)$ is lower bounded:

$$\begin{aligned} \lambda_{\max}(n) &= \min_{\boldsymbol{x}>0} \max_{\boldsymbol{y}>0} \frac{\boldsymbol{x}^T \boldsymbol{D}\boldsymbol{\Psi}^T(\boldsymbol{U}^{(n)})\boldsymbol{y}}{\boldsymbol{x}^T \boldsymbol{y}} \\ &\geq \min_{\boldsymbol{x}>0} \frac{\boldsymbol{x}^T \boldsymbol{D}\boldsymbol{\Psi}^T(\boldsymbol{U}^{(n)})\boldsymbol{q}^{(n-1)}}{\boldsymbol{x}^T \boldsymbol{q}^{(n-1)}} = \min_{\boldsymbol{x}>0} \tilde{\lambda}_n(\boldsymbol{x}) . \end{aligned} \tag{3.26}$$

Combining (3.24), (3.25), and (3.26) we have

$$\min_{\boldsymbol{x}>0} \tilde{\lambda}_n(\boldsymbol{x}) \leq \lambda_{\max}(n) \leq \max_{\boldsymbol{x}>0} \tilde{\lambda}_n(\boldsymbol{x}) \leq \lambda_{\max}(n-1) . \tag{3.27}$$

Hence, the iteration sequence $\lambda_{\max}(n)$ is monotonically decreasing and there exists a limit value $\lambda^{\infty} \stackrel{\text{def}}{=} \lim_{n\to\infty} \lambda_{\max}(n)$. Using the fact that the quantities $\boldsymbol{q}^{(n)}$ and $\boldsymbol{U}^{(n)}$ are both bounded, there must exist limit values $\boldsymbol{q}^{\infty}$ and $\boldsymbol{U}^{\infty}$ such that

$$\begin{aligned} \lim_{n\to\infty} \|\boldsymbol{U}^{(n)} - \boldsymbol{U}^{\infty}\|_F &= 0 \\ \lim_{n\to\infty} \|\boldsymbol{q}^{(n)} - \boldsymbol{q}^{\infty}\|_1 &= 0 \,. \end{aligned}$$

Since $\boldsymbol{\Psi}(\boldsymbol{U})$ is continuous, we have

$$\lim_{n\to\infty} \|\boldsymbol{D}\boldsymbol{\Psi}^T(\boldsymbol{U}^{(n)}) - \boldsymbol{D}\boldsymbol{\Psi}^T(\boldsymbol{U}^{\infty})\|_F = 0$$

and therefore

$$\begin{aligned} \lim_{n\to\infty} \boldsymbol{D}\boldsymbol{\Psi}^T(\boldsymbol{U}^{(n)})\boldsymbol{q}^{(n)} &= \boldsymbol{D}\boldsymbol{\Psi}^T(\boldsymbol{U}^{\infty})\boldsymbol{q}^{\infty} \\ \lim_{n\to\infty} \lambda_{\max}(n)\boldsymbol{q}^{(n)} &= \lambda^{\infty}\boldsymbol{q}^{\infty} \,. \end{aligned}$$

Consequently, λ^{∞} is a solution of $\boldsymbol{D}\boldsymbol{\Psi}^T(\boldsymbol{U}^{\infty})\boldsymbol{q}^{\infty} = \lambda^{\infty}\boldsymbol{q}^{\infty}$ and

$$\boldsymbol{U}^{\infty} = \arg\min_{\boldsymbol{U}} \frac{\boldsymbol{x}^T\boldsymbol{D}\boldsymbol{\Psi}^T(\boldsymbol{U})\boldsymbol{q}^{\infty}}{\boldsymbol{x}^T\boldsymbol{q}^{\infty}} \,.$$

From Theorem 10 we know that $\boldsymbol{U}^{\infty}$ fulfills the condition for global optimality. Thus it solves the ℓ_{∞}-norm minimization problem (3.4). ∎

3.2.2. Stopping Criterion

The above results show that the iteration sequence is strictly monotonically decreasing as long as the global optimum is not found. A stopping criterion is needed that allows to control the desired accuracy by defining a threshold ϵ. Obviously, $\lambda_{\max}(n-1) - \lambda_{\max}(n) \le \epsilon$ is such a criterion. Necessary and sufficient conditions for the optimality of a solution $\boldsymbol{U}^{(n)}$ are provided in the following.

Firstly, a solution $\boldsymbol{U}^{(n)}$ solves the eigenvalue minimization problem (3.7) if and only if $\lambda_{\max}(n) = \lambda_{\max}(n+1)$, which follows directly from Theorem 10. This criterion, however, requires the computation of $\boldsymbol{U}^{(n+1)}$, which means that an additional iteration step has to be carried out. It is therefore desirable to assess the optimality of $\boldsymbol{U}^{(n)}$ directly, without the need of additional eigenvalue decompositions.

Theorem 13. *$\boldsymbol{U}^{(n)}$ is a global minimizer of the eigenvalue minimization problem (3.7) if and only if $\tilde{\lambda}_n(\boldsymbol{x}) = \lambda_{\max}(n)$ for any $\boldsymbol{x} > 0$.*

Proof. See the appendix on page 77. ∎

Theorem 13 implies that the global optimum is achieved if and only if $\max_{\boldsymbol{x}} \tilde{\lambda}_n(\boldsymbol{x}) = \min_{\boldsymbol{x}} \tilde{\lambda}_n(\boldsymbol{x})$. If this is fulfilled then $\lambda_{\max}(n) = \lambda_{\max}(n+1)$. The converse also holds, thus both conditions are equivalent.

Lemma 11. *Let $\boldsymbol{x}$, $\boldsymbol{b}$, and $\boldsymbol{c}$ be positive, K-dimensional vectors, then the following two equalities hold:*

$$\max_{\boldsymbol{x}} \frac{\boldsymbol{x}^T \boldsymbol{b}}{\boldsymbol{x}^T \boldsymbol{c}} = \max_{1 \le k \le K} \frac{[\boldsymbol{b}]_k}{[\boldsymbol{c}]_k} \tag{3.28}$$

$$\min_{\boldsymbol{x}} \frac{\boldsymbol{x}^T \boldsymbol{b}}{\boldsymbol{x}^T \boldsymbol{c}} = \min_{1 \le k \le K} \frac{[\boldsymbol{b}]_k}{[\boldsymbol{c}]_k} . \tag{3.29}$$

Proof. See the appendix on page 70. ■

Applying Lemma 11 to the function $\tilde{\lambda}_n(\boldsymbol{x})$, as defined in (3.23), and using the monotony result (3.27), we have

$$\min_{1 \le k \le K} \left(\frac{\gamma_k}{\mathrm{SIR}_k^{\mathrm{UL}}(\boldsymbol{q}^{(n-1)}, \boldsymbol{u}_k^{(n)})} \right) \le \lambda_{\max}(n) \le \max_{1 \le k \le K} \left(\frac{\gamma_k}{\mathrm{SIR}_k^{\mathrm{UL}}(\boldsymbol{q}^{(n-1)}, \boldsymbol{u}_k^{(n)})} \right) \le \lambda_{\max}(n-1).$$

Combining Lemma 11 with Theorem 13, it becomes clear how the optimality of a solution $\boldsymbol{U}^{(n)}$ is related to the SIR balancing problem (3.6). The global optimum is achieved if and only if all relative SIR are balanced at the same level after the beamforming step. Note, that the upper bound for $\lambda_{\max}(n)$ is always smaller than $\lambda_{\max}(n-1)$. This explains the rapid convergence of the algorithm. Typically, only a few iteration steps are required. The convergence behavior is illustrated in Fig. 3.1.

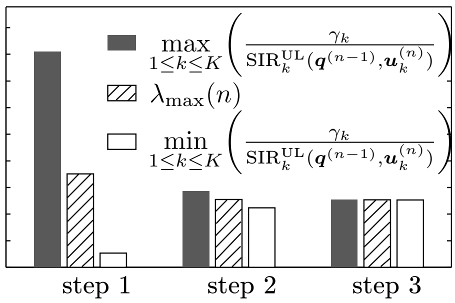

Figure 3.1.: Typical convergence behavior of the proposed Algorithm 1

3.3. Alternative Strategy based on ℓ_1-Norm Minimization

Gerlach and Paulraj [10] proposed a different strategy for solving the downlink SIR balancing problem (3.2). Instead of minimizing the non-differentiable objective function $\|\boldsymbol{\xi}(\boldsymbol{U}, \boldsymbol{p})\|_\infty$ defined in (3.3), they proposed to minimize the ℓ_1-norm $\|\boldsymbol{\xi}(\boldsymbol{U}, \boldsymbol{p})\|_1$

instead. In general, this approach has the advantage that one has a smoother objective

$$F_1(\boldsymbol{U}, \boldsymbol{p}) = \frac{1}{K}\|\boldsymbol{\xi}(\boldsymbol{U}, \boldsymbol{p})\|_1 = \frac{1}{K}\sum_{i=1}^{K} p_i \boldsymbol{u}_i^H \boldsymbol{G}_i(\boldsymbol{p})\boldsymbol{u}_i \;, \tag{3.30}$$

$$\text{where} \quad \boldsymbol{G}_i(\boldsymbol{p}) = \sum_{\substack{k=1\\k\neq i}}^{K} \frac{\gamma_k \boldsymbol{R}_k}{p_k} \;. \tag{3.31}$$

The following optimization problem has been considered in [10]:

$$B_1 = \min_{\boldsymbol{U},\,\boldsymbol{p}} F_1(\boldsymbol{U}, \boldsymbol{p}) \quad \text{subject to} \quad \begin{array}{l} \boldsymbol{u}_i \boldsymbol{R}_i \boldsymbol{u}_i = 1, \;\; 1 \leq i \leq K \;, \\ \|\boldsymbol{p}\|_1 = 1 \;. \end{array} \tag{3.32}$$

This will now be compared with the ℓ_∞ approach

$$B_{\mathrm{Inf}}^{\mathrm{DL}} = \max_{\boldsymbol{U},\boldsymbol{p}} \left(\min_{1\leq i\leq K} \frac{\mathrm{SIR}_i^{\mathrm{DL}}(\boldsymbol{U}, \boldsymbol{p})}{\gamma_i} \right) \quad \text{subject to} \quad \begin{array}{l} \boldsymbol{u}_i \boldsymbol{R}_i \boldsymbol{u}_i = 1, \;\; 1 \leq i \leq K \;, \\ \|\boldsymbol{p}\|_1 = 1 \;. \end{array} \tag{3.33}$$

Note, that both (3.32) and (3.33) pose quadratic constraints on the beamforming vectors $\boldsymbol{u}_i$, whereas the ℓ_∞ approach (3.2) studied in Section 3.1 uses a different constraint $\|\boldsymbol{u}_i\|_2 = 1$. This, however, will not affect the level on which the relative SIR are be balanced, but only the transmission powers and the scaling of the vectors $\boldsymbol{u}_i$. Quadratic constraints will be assumed exclusively in the remainder of this section in order to compare the ℓ_∞ and ℓ_1 based strategies proposed in [10].

In the following we denote $\mathcal{M}_1$ the set of beamforming matrices $\boldsymbol{U}$ that solve (3.32). Also $(\hat{\boldsymbol{U}}, \hat{\boldsymbol{p}})$ is a global minimizer of (3.32), thus $B_1 = F_1(\hat{\boldsymbol{U}}, \hat{\boldsymbol{p}})$. The set of optimizers of the ℓ_∞ problem (3.33) is denoted by $\mathcal{M}_\infty$.

It was conjectured in [10] that each $\hat{\boldsymbol{U}} \in \mathcal{M}_1$ solves the original SIR balancing problem (3.33), i.e., $\mathcal{M}_1 \subseteq \mathcal{M}_\infty$. Now, an interesting question is, whether or not this is fulfilled. This was not ultimately answered in [10]. In order to find an answer, we start by characterizing the optimum of the ℓ_1 problem. The ℓ_∞ problem was already studied in Section 3.1.

3.3.1. Characterization of the ℓ_1 Minimizer

We start by assuming a fixed beamforming matrix $\boldsymbol{U}$. The power vector $\boldsymbol{p}$ that minimizes the cost function $F_1(\boldsymbol{U}, \boldsymbol{p})$ is characterized by the following lemma:

Lemma 12. *For any fixed $\boldsymbol{U}$ the optimization problem $\min_{\boldsymbol{p}} F_1(\boldsymbol{U}, \boldsymbol{p})$ has a unique solution $\tilde{\boldsymbol{p}} = [\tilde{p}_1, \ldots, \tilde{p}_K]^T$ with $\|\tilde{\boldsymbol{p}}\|_1 = 1$. This solution is characterized by*

$$\frac{\tilde{p}_i}{\sum_{\substack{k=1\\k\neq i}}^{K} \tilde{p}_k \boldsymbol{u}_k^H \gamma_i \boldsymbol{R}_i \boldsymbol{u}_k} = \frac{1}{\tilde{p}_i \boldsymbol{u}_i^H \left(\sum_{\substack{k=1\\k\neq i}}^{K} \frac{\gamma_k \boldsymbol{R}_k}{\tilde{p}_k} \right) \boldsymbol{u}_i} \;. \tag{3.34}$$

Proof. See the appendix on page 71. ∎

Next, assume that $\boldsymbol{p}$ is the given parameter and that $F_1(\boldsymbol{U}, \boldsymbol{p})$ is minimized with respect to $\boldsymbol{U}$. From (3.30) it can be observed that this leads to a set of K decoupled problems

$$\min_{\boldsymbol{u}_i} \boldsymbol{u}_i^H \boldsymbol{G}_i(\boldsymbol{p}) \boldsymbol{u}_i \ , \quad \text{s.t.} \quad \boldsymbol{u}_i^H \boldsymbol{R}_i \boldsymbol{u}_i = 1, \ \ 1 \le i \le K \ . \tag{3.35}$$

The optimizers are given as the dominant generalized eigenvectors of the matrix pairs $(\boldsymbol{R}_i, \boldsymbol{G}_i(\boldsymbol{p}))$. With these results we are able to characterize the optimal solution $(\hat{\boldsymbol{U}}, \hat{\boldsymbol{p}})$ that solves (3.32):

Theorem 14. *The global minimizer* $(\hat{\boldsymbol{U}}, \hat{\boldsymbol{p}})$ *of the cost function* $F_1(\boldsymbol{U}, \boldsymbol{p})$ *is characterized by the following two equations:*

$$\boldsymbol{R}_i \ \hat{\boldsymbol{u}}_i = \lambda_{\max}\big(\boldsymbol{R}_i, \boldsymbol{G}_i(\hat{\boldsymbol{p}})\big) \cdot \boldsymbol{G}_i(\hat{\boldsymbol{p}}) \ \hat{\boldsymbol{u}}_i \ , \quad 1 \le i \le K \ , \tag{3.36}$$

$$\frac{\hat{p}_i}{\sum\limits_{\substack{k=1 \\ k \neq i}}^{K} \hat{p}_k \hat{\boldsymbol{u}}_k^H \gamma_i \boldsymbol{R}_i \hat{\boldsymbol{u}}_k} = \frac{1}{\hat{p}_i \hat{\boldsymbol{u}}_i^H \boldsymbol{G}_i(\hat{\boldsymbol{p}}) \hat{\boldsymbol{u}}_i} \ , \quad 1 \le i \le K \ . \tag{3.37}$$

Proof. This can be shown by combining (3.35) and Lemma 12. ∎

3.3.2. Optimality Conditions

Next, necessary and sufficient conditions will be derived for the optimality of the ℓ_1 solution $(\hat{\boldsymbol{U}}, \hat{\boldsymbol{p}})$ with respect to the original ℓ_∞ problem (3.33). Then, a necessary and sufficient condition will be derived for the optimality of the beamforming solution $\hat{\boldsymbol{U}}$ alone.

The optimality of $\hat{\boldsymbol{U}}$ was conjectured in [10], where it was proposed to solve (3.32), then to solve an eigenproblem

$$\boldsymbol{\Gamma\Psi}(\hat{\boldsymbol{U}}) \ \boldsymbol{p}^g = \lambda_{\max}\big(\boldsymbol{\Gamma\Psi}(\hat{\boldsymbol{U}})\big) \ \boldsymbol{p}^g \ , \tag{3.38}$$

where $\boldsymbol{\Gamma} = \text{diag}\{\gamma_1, \ldots, \gamma_K\}$. Note, that the power allocation $\boldsymbol{p}^g$ balances the quantities $\text{SIR}_i^{\text{DL}}/\gamma_i$ at the same level.

Now, consider the ℓ_∞ solution $(\boldsymbol{U}^{opt}, \boldsymbol{p}^{opt})$, which also balances all $\text{SIR}_i^{\text{DL}}/\gamma_i$ at the same level, thus $1/B_{\text{Inf}}^{\text{DL}} = \lambda_{\max}^{opt} = F_1(\boldsymbol{U}^{opt}, \boldsymbol{p}^{opt})$. This optimal level can be compared with the ℓ_1 optimum $B_1 = F_1(\hat{\boldsymbol{U}}, \hat{\boldsymbol{p}})$ by using the following relation:

$$\begin{aligned} B_1 &= \frac{1}{K} \min_{\boldsymbol{U}, \boldsymbol{p}} \sum_{i=1}^{K} \frac{\gamma_i}{\text{SIR}_i^{\text{DL}}(\boldsymbol{U}, \boldsymbol{p})} \\ &\le \frac{1}{K} \min_{\boldsymbol{U}, \boldsymbol{p}} \sum_{i=1}^{K} \max_{1 \le k \le K} \frac{\gamma_k}{\text{SIR}_k^{\text{DL}}(\boldsymbol{U}, \boldsymbol{p})} = \lambda_{\max}^{opt} \ . \end{aligned} \tag{3.39}$$

It can be concluded that

$$\begin{array}{ccccc} B_1 & \leq & \lambda_{\max}^{opt} & \leq & \lambda_{\max}\big(\boldsymbol{\Gamma\Psi}(\hat{\boldsymbol{U}})\big) \\ \parallel & & \parallel & & \parallel \\ F_1(\hat{\boldsymbol{U}},\hat{\boldsymbol{p}}) & \leq & F_1(\boldsymbol{U}^{opt},\boldsymbol{p}^{opt}) & \leq & F_1(\hat{\boldsymbol{U}},\boldsymbol{p}^{g}) \; . \end{array} \tag{3.40}$$

Using this result the following theorem can be proven:

Theorem 15. *The global minimizer $(\hat{\boldsymbol{U}},\hat{\boldsymbol{p}})$ of the cost function $F_1(\boldsymbol{U},\boldsymbol{p})$ solves the ℓ_∞-problem (3.33), i.e., $F_1(\hat{\boldsymbol{U}},\hat{\boldsymbol{p}}) = F_1(\boldsymbol{U}^{opt},\boldsymbol{p}^{opt})$, if and only if one of the following two equivalent conditions holds true:*

$$\boldsymbol{\Gamma\Psi}(\hat{\boldsymbol{U}}) \cdot \hat{\boldsymbol{p}} = \lambda_{\max}\big(\boldsymbol{\Gamma\Psi}(\hat{\boldsymbol{U}})\big) \cdot \hat{\boldsymbol{p}} \; , \tag{3.41}$$

$$\big(\hat{\boldsymbol{p}}^{-1}\big)^T \cdot \boldsymbol{\Gamma\Psi}(\hat{\boldsymbol{U}}) = \big(\hat{\boldsymbol{p}}^{-1}\big)^T \cdot \lambda_{\max}\big(\boldsymbol{\Gamma\Psi}(\hat{\boldsymbol{U}})\big) \; . \tag{3.42}$$

where $\hat{\boldsymbol{p}}^{-1} \overset{\text{def}}{=} [\hat{p}_1^{-1}, \ldots \hat{p}_K^{-1}]^T$.

Proof. See the appendix on page 78. ■

From Theorem 15 we can conclude that the ℓ_1 solution solves the ℓ_∞ problem if and only if the resulting levels $\mathrm{SIR}_i^{\mathrm{DL}}(\hat{\boldsymbol{U}},\hat{\boldsymbol{p}})/\gamma_i$ are balanced. It was shown in Section 3.1.1 that this corresponds to the case where $\hat{\boldsymbol{p}}$ is the right-hand eigenvector of $\boldsymbol{\Gamma\Psi}(\hat{\boldsymbol{U}})$. Now, Theorem 15 shows that this is equivalently fulfilled when $\hat{\boldsymbol{p}}^{-1}$ is the left-hand eigenvector. Comparison with (3.8) reveals that $\hat{\boldsymbol{p}}^{-1}$ is the optimal power allocation of the dual uplink problem. This provides additional insight in how uplink and downlink transmission powers are related.

Theorem 15 can also be expressed in terms of the quantities B_1 and $\lambda_{\max}^{opt}$, which leads to the following corollary:

Corollary 4. *The global minimizer $(\hat{\boldsymbol{U}},\hat{\boldsymbol{p}})$ of the cost function $F_1(\boldsymbol{U},\boldsymbol{p})$ solves the ℓ_∞-problem (3.33) if and only if $B_1 = \lambda_{\max}^{opt}$.*

Proof. From (3.39) it can be concluded that $B_1 = \lambda_{\max}^{opt}$ if and only if the quantities $\mathrm{SIR}_i^{\mathrm{DL}}(\hat{\boldsymbol{U}},\hat{\boldsymbol{p}})/\gamma_i$ are balanced. Then $\hat{\boldsymbol{p}}$ is the right-hand eigenvector of $\boldsymbol{\Gamma\Psi}(\hat{\boldsymbol{U}})$. From Theorem 15 follows that $(\hat{\boldsymbol{U}},\hat{\boldsymbol{p}})$ solves (3.33). In the reverse direction assume that $(\hat{\boldsymbol{U}},\hat{\boldsymbol{p}})$ solves the ℓ_∞ problem (3.33). Theorem 15 implies that $\hat{\boldsymbol{p}}$ solves (3.41), from which we can conclude that $\lambda_{\max}^{opt} = B_1$. ■

Further insight is gained by multiplying both sides of (3.38) with $(\hat{\boldsymbol{p}}^{-1})^T$, i.e.,

$$\begin{aligned} (\hat{\boldsymbol{p}}^{-1})^T \lambda_{\max}\big(\boldsymbol{\Gamma\Psi}(\hat{\boldsymbol{U}})\big)\boldsymbol{p}^g &= (\hat{\boldsymbol{p}}^{-1})^T \boldsymbol{\Gamma\Psi}(\hat{\boldsymbol{U}})\boldsymbol{p}^g \\ &= \sum_{i=1}^{K} p_i^g \hat{\boldsymbol{u}}_i^H \boldsymbol{G}_i(\hat{\boldsymbol{p}})\hat{\boldsymbol{u}}_i \; . \end{aligned} \tag{3.43}$$

Multiplying (3.30) by K and subtracting the result from both sides of (3.43) we obtain

$$\left(\sum_{i=1}^{K}\frac{p_i^g}{\hat{p}_i}\right)\lambda_{\max}\big(\boldsymbol{\Gamma\Psi}(\hat{\boldsymbol{U}})\big) - K\cdot B_1 = \sum_{i=1}^{K}(p_i^g-\hat{p}_i)\hat{\boldsymbol{u}}_i^H\boldsymbol{G}(\hat{\boldsymbol{p}})\hat{\boldsymbol{u}}_i\ . \tag{3.44}$$

It can be observed from (3.44) that for small $p_i^g-\hat{p}_i$, we can approximate

$$\lambda_{\max}\big(\boldsymbol{\Gamma\Psi}(\hat{\boldsymbol{U}})\big) \approx B_1\ . \tag{3.45}$$

This provides additional interpretation for Theorem 15 and Corollary 4.

Next, a necessary and sufficient condition for the optimality of the balanced ℓ_1 solution $(\hat{\boldsymbol{U}},\boldsymbol{p}^g)$ with respect to the ℓ_∞ problem (3.33) is provided:

Theorem 16. *Let $\hat{\boldsymbol{U}}\in\mathcal{M}_1$. Furthermore, let $\boldsymbol{q}^g$ and $\boldsymbol{p}^g$ denote the dominant left- and right-hand eigenvectors of the matrix $\boldsymbol{\Gamma\Psi}(\hat{\boldsymbol{U}})$, respectively. Let $(\boldsymbol{q}^g)^{-1}\overset{\text{def}}{=}[(q_1^g)^{-1},\dots,(q_K^g)^{-1}]^T$. The solution $(\hat{\boldsymbol{U}},\boldsymbol{p}^g)$ solves the ℓ_∞-problem (3.33) if and only if*

$$\min_{\boldsymbol{U}} F_1(\boldsymbol{U},(\boldsymbol{q}^g)^{-1}) = F_1(\hat{\boldsymbol{U}},(\boldsymbol{q}^g)^{-1})\ . \tag{3.46}$$

Proof. See the appendix on page 78. ■

If $\hat{\boldsymbol{U}}$ fulfills the condition in Theorem 16, then the right side of inequality (3.40) is satisfied with equality. The same, however, need not be true for the left side. That is, $\hat{\boldsymbol{U}}$ may be an optimizer of the ℓ_∞ problem although the quantities $\mathrm{SIR}_i(\hat{\boldsymbol{U}},\hat{\boldsymbol{p}})/\gamma_i$ are not balanced.

Up to this point, necessary and sufficient conditions have been given for the optimality of the ℓ_1 solution $(\hat{\boldsymbol{U}},\hat{\boldsymbol{p}})$ and the balanced ℓ_1 solution $(\hat{\boldsymbol{U}},\boldsymbol{p}^g)$ with respect to the ℓ_∞ optimization problem (3.33). Now we are interested in finding out whether these problems are actually equivalent or not.

3.3.3. Closed-Form Solution for the 2-User Scenario

For $K=2$, the ℓ_1 minimization problem (3.32) reduces to

$$B_1 = \min_{p_1,p_2,\boldsymbol{u}_1,\boldsymbol{u}_2}\frac{1}{2}\left(\frac{\gamma_1 p_2\boldsymbol{u}_2^H\boldsymbol{R}_1\boldsymbol{u}_2}{p_1}+\frac{\gamma_2 p_1\boldsymbol{u}_1^H\boldsymbol{R}_2\boldsymbol{u}_1}{p_2}\right)\quad \text{s.t.}\quad \begin{array}{l}\boldsymbol{u}_i\boldsymbol{R}_i\boldsymbol{u}_i=1,\ \ \forall i\ ,\\ \|\boldsymbol{p}\|_1=1\ .\end{array} \tag{3.47}$$

It can be observed that the minimization with respect to $\boldsymbol{u}_1$ and $\boldsymbol{u}_2$ does not depend on the transmission powers. Each summand of the cost function can be minimized independently. The minimizers $\hat{\boldsymbol{u}}_1,\hat{\boldsymbol{u}}_2$ are obtained by solving the following two generalized eigenproblems

$$\boldsymbol{R}_2\hat{\boldsymbol{u}}_2 = \lambda_{\max}^{(2)}\boldsymbol{R}_1\hat{\boldsymbol{u}}_2\ , \tag{3.48}$$

$$\boldsymbol{R}_2\hat{\boldsymbol{u}}_1 = \lambda_{\min}^{(2)}\boldsymbol{R}_1\hat{\boldsymbol{u}}_1\ , \tag{3.49}$$

where $\lambda_{\max}^{(2)}$ and $\lambda_{\min}^{(2)}$ denote the maximal and minimal generalized eigenvalue of the matrix pair $(\boldsymbol{R}_2, \boldsymbol{R}_1)$, respectively. Considering the constraint $\boldsymbol{u}_i^H \boldsymbol{R}_i \boldsymbol{u}_i = 1$, we have $\lambda_{\max}^{(2)} = 1/\hat{\boldsymbol{u}}_2^H \boldsymbol{R}_1 \hat{\boldsymbol{u}}_2$ and $\lambda_{\min}^{(2)} = \hat{\boldsymbol{u}}_1^H \boldsymbol{R}_2 \hat{\boldsymbol{u}}_1$, which can be substituted back into (3.47). This leads to a new cost function

$$C(p_1, p_2) = \frac{1}{2}\left(\frac{\gamma_1 p_2}{p_1 \lambda_{\max}^{(2)}} + \frac{\gamma_2 p_1 \lambda_{\min}^{(2)}}{p_2}\right) . \tag{3.50}$$

Since $\mathrm{SIR}_i^{\mathrm{DL}}(\boldsymbol{U}, \boldsymbol{p})$ is scalable in $\boldsymbol{p}$, we can set $\boldsymbol{p} = [\mu, 1]$, where μ denotes the ratio between the transmission powers p_1 and p_2. This leads to a 1-dimensional optimization problem

$$B_1 = \min_{\mu} \frac{1}{2}\left(\frac{\gamma_1}{\mu \lambda_{\max}^{(2)}} + \mu \gamma_2 \lambda_{\min}^{(2)}\right) . \tag{3.51}$$

The unique minimizer

$$\hat{\mu} = \sqrt{\frac{\gamma_1}{\gamma_2 \lambda_{\max}^{(2)} \lambda_{\min}^{(2)}}} \tag{3.52}$$

is obtained from computing the derivative of the cost function. Putting (3.52) into (3.51) it can be observed that

$$\frac{\mathrm{SIR}_1^{\mathrm{DL}}([\hat{\boldsymbol{u}}_1, \hat{\boldsymbol{u}}_2], \left[\begin{smallmatrix}\hat{\mu}\\ 1\end{smallmatrix}\right])}{\gamma_1} = \frac{\mathrm{SIR}_2^{\mathrm{DL}}([\hat{\boldsymbol{u}}_1, \hat{\boldsymbol{u}}_2], \left[\begin{smallmatrix}\hat{\mu}\\ 1\end{smallmatrix}\right])}{\gamma_2} = \sqrt{\frac{\lambda_{\max}^{(2)}}{\gamma_1 \gamma_2 \lambda_{\min}^{(2)}}} . \tag{3.53}$$

The SIR levels are balanced. From the results in Section 3.3.2 we know that in this case the ℓ_1 solution solves the optimal ℓ_∞ problem. Thus, for the 2-user case both problems are indeed equivalent.

An additional interpretation is obtained by rewriting (3.53) as an eigenvalue decomposition

$$\boldsymbol{\Gamma\Psi}([\hat{\boldsymbol{u}}_1, \hat{\boldsymbol{u}}_2]) \cdot \begin{bmatrix} \hat{\mu}^{1/2} \\ \hat{\mu}^{-1/2} \end{bmatrix} = \sqrt{\frac{\gamma_1 \gamma_2 \lambda_{\min}^{(2)}}{\lambda_{\max}^{(2)}}} \cdot \begin{bmatrix} \hat{\mu}^{1/2} \\ \hat{\mu}^{-1/2} \end{bmatrix} .$$

Hence, $[\hat{\mu}^{1/2}, \hat{\mu}^{-1/2}]^T$ is a (scaled) eigenvector of the coupling matrix $\boldsymbol{\Gamma\Psi}$. Likewise, it can be shown that $[\hat{\mu}^{-1/2}, \hat{\mu}^{1/2}]^T$ is a dominant eigenvector of $(\boldsymbol{\Gamma\Psi})^T$. From Theorem 15 it can be concluded, that the closed-form solution $(\hat{\boldsymbol{u}}_1, \hat{\boldsymbol{u}}_2, \hat{p}_1, \hat{p}_2)$ not only solves the ℓ_1-problem (3.32), but also the ℓ_∞-problem (3.33). Thus we have

$$B_{\mathrm{Inf}}^{\mathrm{DL}} = 1/B_1 = \sqrt{\lambda_{\max}^{(2)}/(\gamma_1 \gamma_2 \lambda_{\min}^{(2)})} . \tag{3.54}$$

Now, assume that $\mathrm{SIR}_i^{\mathrm{DL}} \geq \gamma_i$ is required for $i = 1, 2$. These requirements can only be fulfilled if $B_{\mathrm{Inf}}^{\mathrm{DL}} \geq 1$ holds. This leads to the following condition

$$\lambda_{\max}^{(2)} / \lambda_{\min}^{(2)} \geq \gamma_1 \gamma_2 \ . \tag{3.55}$$

Thus, the feasibility of a certain scenario, characterized by the channel covariance matrices $\boldsymbol{R}_1, \boldsymbol{R}_2$ and SIR requirements γ_1, γ_2, is determined by (3.55). An illustration of this result is given in Fig. 3.2.

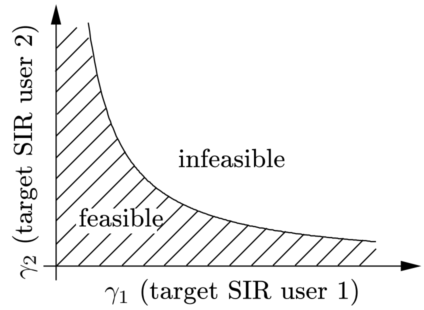

Figure 3.2.: 2-user scenario: tradeoff between SIR requirements γ_1 and γ_2

From (3.55) it becomes clear that we must avoid situations where the ratio $\lambda_{\max}^{(2)} / \lambda_{\min}^{(2)}$ becomes small. Clearly, the worst case is given for $\boldsymbol{R}_1 = \boldsymbol{R}_2$, where $\lambda_{\min}^{(2)} = \lambda_{\min}^{(1)}$ holds. This corresponds to a situation where the users cannot be distinguished by spatial filtering.

3.3.4. Numerical Counterexample for $K > 2$

Now, consider the general case $K > 2$. Even when assuming the most simple scenario $K = 3$ and $M = 1$, the ℓ_∞ problem becomes quite complicated and there is no obvious way to decide whether or not it is equivalent to the ℓ_1 approach. Fortunately, optimal numerical solutions are known for the ℓ_1 problem (see [10]) and the ℓ_∞ problem (see Section 3.2 and the corresponding paper [5]). Thus, together with the optimality conditions derived in Section 3.3.2, it is possible to find a numerical counterexample that disproves general equivalence. The results for a specific channel scenario are illustrated in Fig. 3.3.

From Fig. 3.3.a it can be observed that the SIR levels resulting from $(\hat{\boldsymbol{U}}, \hat{\boldsymbol{p}})$ are not balanced. From Theorem 15 it can be concluded that in this case the ℓ_1 solution does not solve the ℓ_∞ optimization problem (3.33). Hence, both problems are not equivalent.

Is it possible that the balanced ℓ_1 solution $(\hat{\boldsymbol{U}}, \boldsymbol{p}^g)$ is optimal? From Corollary 4 it is known that this holds true as long as ℓ_1 and ℓ_∞ balancing achieves the same level. A counterexample is depicted in Fig. 3.3.b, where $F_1(\boldsymbol{U}^{opt}, \boldsymbol{p}^{opt}) < F_1(\hat{\boldsymbol{U}}, \boldsymbol{p}^g)$ holds. Hence, $\hat{\boldsymbol{U}}$ is not always an optimizer of the ℓ_∞ optimization problem (3.33).

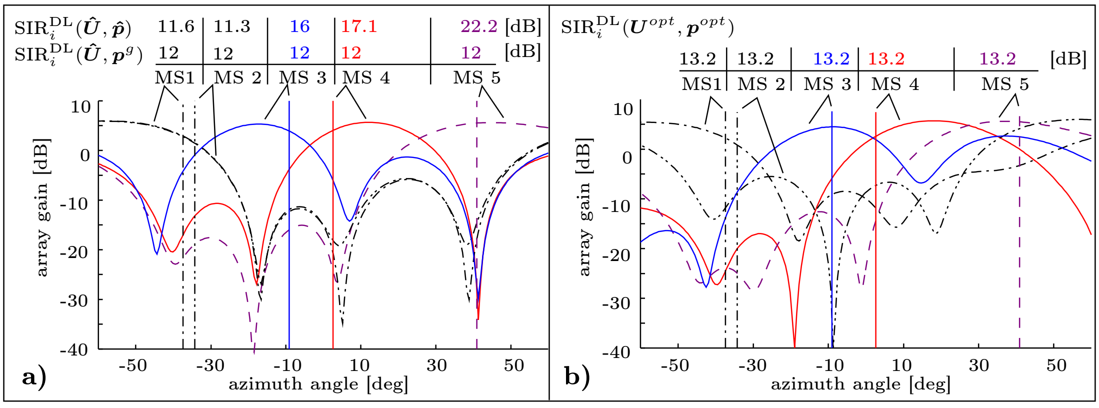

Figure 3.3.: Comparison of **a)** ℓ_1 optimization **b)** ℓ_∞ optimization strategies in the absence of noise. The normalized beam patterns are depicted for a 5-user scenario. The results have been found with the ℓ_1-based algorithm proposed in [10] and the optimal ℓ_∞ optimization scheme summarized on p. 30. The same simulation parameters were assumed for both optimization techniques.

While the observations in Fig. 3.3 only hold for a specific scenario, the statistical analysis in Fig. 3.4 shows, that the same behavior holds for most other scenarios as well, including the case $K = 3$. However, the difference becomes smaller as the number of users increases. It can be concluded that for most scenarios the ℓ_1-based strategy proposed in [10] only approximates the ℓ_∞ optimum. In the next section, a modified algorithm will be proposed that always converges to the ℓ_∞ optimum.

3.3.5. Optimal Algorithm Based on ℓ_1-Optimization

From Theorem 16 it is known that the global optimum of the ℓ_∞ problem (3.33) is characterized in two different ways: An optimal solution $\boldsymbol{U}^{opt} \in \mathcal{M}_\infty$ can be found by minimizing the cost function $F_1\big(\boldsymbol{U}, (\boldsymbol{q}^g)^{-1}\big)$, which requires knowledge of the optimal $\boldsymbol{q}^g$. On the other hand, if $\boldsymbol{U}^{opt}$ is known, then the associated $\boldsymbol{q}^g$ is given as the dominant left-hand eigenvector of the matrix $\boldsymbol{\Gamma\Psi}(\boldsymbol{U}^{opt})$. This provides intuition for a new alternating optimization scheme, which is based on the ℓ_1 cost function F_1, as proposed by Gerlach and Paulraj in [10], but which uses a different way of adjusting the power vector in each iteration step. Instead of minimizing $F_1(\boldsymbol{U}, \boldsymbol{p})$ with respect to $\boldsymbol{p}$, the power update is done by solving the eigenvalue problem (3.38). The algorithm is summarized below. It was published by Boche and Schubert in [4]. The optimal beamforming strategy for given $\boldsymbol{q}^{(n-1)}$ is found by evaluating

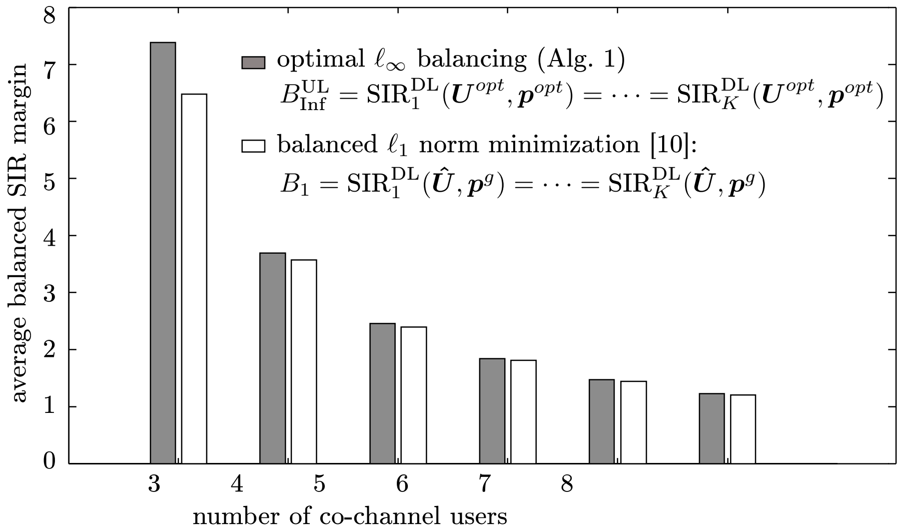

Figure 3.4.: Achievable levels B_1 and $B_{\text{Inf}}^{\text{UL}}$ averaged over 1000 Monte Carlo runs. Random channel matrices are assumed and $\gamma_1 = \cdots = \gamma_K = 1$

$$\begin{aligned}
\boldsymbol{U}^{(n)} &= \arg\min_{\boldsymbol{U}} F(\boldsymbol{U}, (\boldsymbol{q}^{(n-1)})^{-1}) \;, \quad \text{s.t.} \quad \boldsymbol{u}_i^H \boldsymbol{R}_i \boldsymbol{u}_i = 1, \;\; 1 \le i \le K \\
&= \arg\min_{\boldsymbol{U}} \sum_{i=1}^{K} [\boldsymbol{x}]_i \boldsymbol{u}_i^H \Bigg(\sum_{\substack{k=1 \\ k \neq i}}^{K} [\boldsymbol{q}^{(n-1)}]_k \gamma_k \boldsymbol{R}_k \Bigg) \boldsymbol{u}_i \;, \quad \text{for any } \boldsymbol{x} \in \mathbb{R}_+^K \\
&= \arg\min_{\boldsymbol{U}} \frac{\boldsymbol{x}^T \big(\boldsymbol{\Gamma\Psi}(\boldsymbol{U})\big)^T \boldsymbol{q}^{(n-1)}}{\boldsymbol{x}^T \boldsymbol{q}^{(n-1)}} \;. \qquad (3.58)
\end{aligned}$$

This strategy is similar to the approach chosen for Algorithm 1 on p. 30. However, it differs in the way the targets $\gamma_1 \dots \gamma_K$ affect the iteration process. In Algorithm 2, they influence both beamforming and power control steps, while in Algorithm 1 only the power control step is involved.

Global convergence of Algorithm 2 can be shown by defining a function

$$\check{\lambda}_n(\boldsymbol{x}) \stackrel{\text{def}}{=} \frac{\boldsymbol{x}^T \big(\boldsymbol{\Gamma\Psi}(\boldsymbol{U}^{(n)})\big)^T \boldsymbol{q}^{(n-1)}}{\boldsymbol{x}^T \boldsymbol{q}^{(n-1)}} \;, \quad \text{where } \boldsymbol{x} > 0. \qquad (3.59)$$

It follows from (3.58) that

$$\begin{aligned}
\check{\lambda}_n(\boldsymbol{x}) &= \min_{\boldsymbol{U}} \frac{\boldsymbol{x}^T \big(\boldsymbol{\Gamma\Psi}(\boldsymbol{U})\big)^T \boldsymbol{q}^{(n-1)}}{\boldsymbol{x}^T \boldsymbol{q}^{(n-1)}} \\
&\le \frac{\boldsymbol{x}^T \big(\boldsymbol{\Gamma\Psi}(\boldsymbol{U}^{(n-1)})\big)^T \boldsymbol{q}^{(n-1)}}{\boldsymbol{x}^T \boldsymbol{q}^{(n-1)}} = \lambda_{\max}(n-1)
\end{aligned}$$

Algorithm 2 Optimal SIR balancing based on ℓ_1 optimization.

1: $n \Leftarrow 0$
2: $\boldsymbol{q}^{(0)} \Leftarrow [1, \dots, 1]^T$
3: $\lambda_{\max}(0) \Leftarrow 0$
4: **repeat**
5: $\quad n \Leftarrow n + 1$
6: $\quad$ for given $\boldsymbol{q}^{(n)}$ minimize the ℓ_1 cost function

$$\boldsymbol{U}^{(n)} \Leftarrow \arg\min_{\boldsymbol{U}} F_1(\boldsymbol{U}, (\boldsymbol{q}^{(n-1)})^{-1}) , \quad \text{s.t.} \quad \boldsymbol{u}_i^H \boldsymbol{R}_i \boldsymbol{u}_i = 1,\ 1 \leq i \leq K \tag{3.56}$$

7: $\quad$ for given $\boldsymbol{U}^{(n)}$ solve the eigenproblem

$$\big(\boldsymbol{\Gamma\Psi}(\boldsymbol{U}^{(n)})\big)^T \cdot \boldsymbol{q}^{(n)} = \lambda_{\max}(n) \cdot \boldsymbol{q}^{(n)} . \tag{3.57}$$

8: **until** $\lambda_{\max}(n-1) - \lambda_{\max}(n) \leq \epsilon$

for any $\boldsymbol{x} > 0$. Hence,

$$\begin{aligned} \lambda_{\max}(n) &= \max_{\boldsymbol{x}>0} \min_{\boldsymbol{y}>0} \frac{\boldsymbol{x}^T \big(\boldsymbol{\Gamma\Psi}(\boldsymbol{U}^{(n)})\big)^T \boldsymbol{y}}{\boldsymbol{x}^T \boldsymbol{y}} \\ &\leq \max_{\boldsymbol{x}>0} \frac{\boldsymbol{x}^T \big(\boldsymbol{\Gamma\Psi}(\boldsymbol{U}^{(n)})\big)^T \boldsymbol{q}^{(n-1)}}{\boldsymbol{x}^T \boldsymbol{q}^{(n-1)}} \\ &= \max_{\boldsymbol{x}>0} \check{\lambda}_n(\boldsymbol{x}) \leq \lambda_{\max}(n-1) . \end{aligned} \tag{3.60}$$

The sequence $\lambda_{\max}(n)$ is strictly monotonically decreasing and converges to $\lambda_{\max}^{opt}$. In analogy to the proof in Section 3.2.1, it can be shown that the optimality condition (3.46) is fulfilled after convergence. The resulting beamforming solution $\boldsymbol{U}^{opt}$ is an optimizer of the ℓ_∞ problem (3.33).

3.4. Discussion

Joint beamforming and power allocation in the absence of noise consists of minimizing the ℓ_∞ norm of the vector (3.3). This objective function is non-differentiable, so at first sight it seems unlikely that a globally convergent algorithm can be found. The equivalent eigenvalue optimization problem has a smoother objective function, but may still have local minima. So a key result of this chapter is to prove that each local minimum is a global minimum. This allows to develop a rapidly converging algorithm, which typically requires only a few iteration steps. These results complete the studies in [43], where the same problem was studied.

An interesting aspect of the solution is, that it need not be unique. Knowing the optimal allocation, all optimal beamforming solutions can be found by the subspace characterization proposed in Section 3.1.3. This is practically relevant since it allows to choose the solution that is best suited, e.g. with respect to additional design criteria, like the peak to average ratio of the beamforming filters.

Finally, the ℓ_1-norm based optimization strategy proposed in [10] is studied. By providing necessary and sufficient conditions for optimality along with counterexamples, it is shown that this approach is in general not equivalent to the original ℓ_∞ norm optimization problem. A modified version of the ℓ_1 strategy is proposed. This new algorithm has the same convergence properties as the one above and always converges to the global ℓ_∞ optimum.

4. Power-Aware Spatial Multiplexing under a Sum Power Constraint

Next, the results are extended to the case where each receiver has a certain noise level and a sum power constraint is imposed. The goal is to achieve SINR thresholds $\gamma_1 \dots \gamma_K$ by jointly optimizing over all beamforming vectors and transmission powers. The solution builds on the duality result in Chapter 2 and the interference balancing technique in the absence of noise, which has been derived in Chapter 3. From the discussion in Section 2.5 it becomes clear that multiuser channels can always be scaled, so without loss of generality, $\boldsymbol{\sigma} = \mathbf{1}_K$ can be assumed in the remainder of this thesis.

4.1. Joint Beamforming and Power Allocation

4.1.1. SINR Balancing in the Downlink

The design goal $\min_{1 \le i \le K} \mathrm{SINR}_i^{\mathrm{DL}} \ge \gamma_i$ motivates the following optimization strategy:

$$\begin{aligned} C_{\mathrm{opt}}^{\mathrm{DL}}(P_{\max}) = \max_{\boldsymbol{U},\boldsymbol{p}} \min_{1 \le i \le K} & \frac{\mathrm{SINR}_i^{\mathrm{DL}}(\boldsymbol{U},\boldsymbol{p})}{\gamma_i}, \\ \text{subject to} \quad & \|\boldsymbol{p}\|_1 \le P_{\max} \\ & \|\boldsymbol{u}_i\|_2 = 1, \quad 1 \le i \le K \,. \end{aligned} \tag{4.1}$$

The achievable level $C_{\mathrm{opt}}^{\mathrm{DL}}(P_{\max})$ provides a single performance measure for the quality of several spatially multiplexed channels. Individual targets $\gamma_1 \dots \gamma_K$ can be achieved if and only if $C_{\mathrm{opt}}^{\mathrm{DL}}(P_{\max}) \ge 1$. Each beamforming solution obtained by (4.1) is optimal in the sense that no other beamforming algorithm can achieve a balanced level larger than $C_{\mathrm{opt}}^{\mathrm{DL}}(P_{\max})$ under the same power constraint. Since $C_{\mathrm{opt}}^{\mathrm{DL}}(P_{\max})$ is monotonically increasing in $P_{\max}$, the SINR levels $\mathrm{SINR}_i^{\mathrm{DL}} = C_{\mathrm{opt}}^{\mathrm{DL}}(P_{\max})\gamma_i$ are achieved with minimal transmission power.

In Section 2.2.1 it was shown that for any fixed $\boldsymbol{U}$ the maximal balanced level $C^{\mathrm{DL}}(\boldsymbol{U}, P_{\max})$ is given by the reciprocal maximal eigenvalue of the extended coupling matrix $\boldsymbol{\Upsilon}(\boldsymbol{U}, P_{\max})$. Hence, the global optimum $C^{\mathrm{DL}}_{\mathrm{opt}}(P_{\max}) = \max_{\boldsymbol{U}} C^{\mathrm{DL}}(\boldsymbol{U}, P_{\max})$ is found by solving

$$C^{\mathrm{DL}}_{\mathrm{opt}}(P_{\max}) = \frac{1}{\min\limits_{\boldsymbol{U}} \lambda_{\max}\big(\boldsymbol{\Upsilon}(\boldsymbol{U}, P_{\max})\big)} \; . \tag{4.2}$$

Any $\boldsymbol{U}^{opt}$ that solves (4.2) is an optimizer of the SINR balancing problem (4.1).

The eigenvalue minimization problem (4.2) has a reduced dimensionality as compared to the original problem (4.1). Yet, it is still very unlikely to allow for an efficient and global algorithmic solution because the objective is typically non-convex in $\boldsymbol{U}$ and may have many local minima.

4.1.2. The Dual Uplink Problem

The same SINR balancing problem that was discussed for the downlink in Section 4.1.1 can be formulated for the uplink:

$$\begin{aligned} C^{\mathrm{UL}}_{\mathrm{opt}}(P_{\max}) = \max_{\boldsymbol{U}, \boldsymbol{q}} \; &\min_{1 \le i \le K} \frac{\mathrm{SINR}^{\mathrm{UL}}_i(\boldsymbol{u}_i, \boldsymbol{q})}{\gamma_i}, \\ \text{subject to} \quad & \|\boldsymbol{q}\|_1 \le P_{\max} \\ & \|\boldsymbol{u}_i\|_2 = 1, \;\; 1 \le i \le K \; . \end{aligned} \tag{4.3}$$

Again, this leads to a beamforming solution, which is optimal in terms of the design goal $\mathrm{SINR}^{\mathrm{UL}}_i \ge \gamma_i$. For given $P_{\max}$, a maximal balanced level $C^{\mathrm{UL}}_{\mathrm{opt}}(P_{\max})$ is achieved. The associated levels $\mathrm{SINR}^{\mathrm{UL}}_i = C^{\mathrm{UL}}_{\mathrm{opt}}(P_{\max})\gamma_i$ are achieved with minimal power. The global optimum $C^{\mathrm{UL}}_{\mathrm{opt}}(P_{\max}) = \max_{\boldsymbol{U}} C^{\mathrm{UL}}(\boldsymbol{U}, P_{\max})$ is found by solving an eigenvalue optimization problem

$$C^{\mathrm{UL}}_{\mathrm{opt}}(P_{\max}) = \frac{1}{\min\limits_{\boldsymbol{U}} \lambda_{\max}\big(\boldsymbol{\Lambda}(\boldsymbol{U}, P_{\max})\big)} \; . \tag{4.4}$$

The relationship between the downlink problem (4.2) and the uplink problem (4.4) is described by the following corollary, which is an immediate consequence of the duality observed in Section 7.

Corollary 5. *Suppose that strong duality, as defined in Section 2.4.4, holds. Then, the same balanced level $C^{\mathrm{DL}}_{\mathrm{opt}}(P_{\max}) = C^{\mathrm{UL}}_{\mathrm{opt}}(P_{\max})$ can be achieved in uplink and downlink under the same sum power constraint $\|\boldsymbol{q}\|_1 = \|\boldsymbol{p}\|_1 = P_{\max}$. This implies that each beamforming solution which solves the uplink problem (4.4) also solves the downlink problem (4.2) and vice versa.*

As discussed in Section 2.5, the downlink channel can always be scaled such that $\boldsymbol{\sigma} = \mathbf{1}_K$ holds. Hence, without loss of generality the downlink beamforming problem (4.2) can be solved by considering the dual uplink problem (4.4) instead. This approach is motivated by the results of Chapter 3, where it was observed that the uplink has a "smoother" analytical structure.

Finally, it is important to notice that the optimizer of (4.4) need not be unique. Let $\mathcal{M}$ denote the set of optimal solutions, then $\boldsymbol{U}^{opt} \in \mathcal{M}$ solves the uplink balancing problem (4.3). Hence, $\boldsymbol{U}^{opt}$ is characterized by $C_{\mathrm{opt}}^{\mathrm{UL}} = \mathrm{SINR}_i^{\mathrm{UL}}(\boldsymbol{U}^{opt}, \boldsymbol{q}^{opt})/\gamma_i$, which can be rewritten as

$$(\boldsymbol{u}_i^{opt})^H \left(\frac{1}{C_{\mathrm{opt}}^{\mathrm{UL}}} q_i^{opt} \boldsymbol{R}_i - \gamma_i \boldsymbol{Z}_i(\boldsymbol{q}^{opt}) \right) \boldsymbol{u}_i^{opt} = 0 \; , \quad 1 \le i \le K \; , \tag{4.5}$$

where $\boldsymbol{Z}_i$ is the spatial interference+noise covariance matrix

$$\boldsymbol{Z}_i(\boldsymbol{q}) = \sum_{\substack{k=1 \\ k \neq i}}^{K} [\boldsymbol{q}]_k \boldsymbol{R}_k + \boldsymbol{I} \; , \quad 1 \le i \le K \; . \tag{4.6}$$

In analogy to Theorem 11 it can be shown that all vectors $\tilde{\boldsymbol{u}}_i$ that are chosen from the nullspace of $\left(\frac{1}{C_{\mathrm{opt}}^{\mathrm{UL}}} q_i^{opt} \boldsymbol{R}_i - \gamma_i \boldsymbol{Z}_i(\boldsymbol{q}^{opt})\right)$ are elements of $\mathcal{M}$. This important characterization is discussed in more detail in Section 3.1.3, where the same result has been derived in the absence of noise.

4.1.3. Problem Reformulation

Using (2.35), the maximal eigenvalue of the extended coupling matrix $\boldsymbol{\Lambda}$ can be expressed as

$$\lambda_{\max}(\boldsymbol{\Lambda}) = \max_{\boldsymbol{x}>0} \min_{\boldsymbol{y}>0} \frac{\boldsymbol{x}^T \boldsymbol{\Lambda} \boldsymbol{y}}{\boldsymbol{x}^T \boldsymbol{y}} = \min_{\boldsymbol{x}>0} \max_{\boldsymbol{y}>0} \frac{\boldsymbol{x}^T \boldsymbol{\Lambda} \boldsymbol{y}}{\boldsymbol{x}^T \boldsymbol{y}} \; . \tag{4.7}$$

Introducing a function

$$\hat{\lambda}_n(\boldsymbol{U}, \boldsymbol{y}) = \max_{\boldsymbol{x}>0} \frac{\boldsymbol{x}^T \boldsymbol{\Lambda}(\boldsymbol{U}, P_{\max}) \boldsymbol{y}}{\boldsymbol{x}^T \boldsymbol{y}} \; , \tag{4.8}$$

problem (4.4) can be rewritten as

$$C_{\mathrm{opt}}^{\mathrm{DL}}(P_{\max}) = \frac{1}{\min\limits_{\boldsymbol{U}} \min\limits_{\boldsymbol{q}_{\mathrm{ext}}>0} \hat{\lambda}_n(\boldsymbol{U}, \boldsymbol{q}_{\mathrm{ext}})} \; . \tag{4.9}$$

Here, $\boldsymbol{q}_{\mathrm{ext}} = \left[\begin{smallmatrix} \boldsymbol{q} \\ 1 \end{smallmatrix}\right]$ is the extended uplink power vector, as introduced in (2.15), whereas the auxiliary variable $\boldsymbol{x} > 0$ has no physical meaning. The global optimum is found by minimizing the cost function $\hat{\lambda}_n(\boldsymbol{U}, \boldsymbol{q}_{\mathrm{ext}})$ over all $\boldsymbol{U}$ and $\boldsymbol{q}_{\mathrm{ext}} > 0$. At first sight, the problem (4.9) seems to be more complicated than the original problem (4.4), since it depends on more variables. However, the representation (4.9) allows for an efficient algorithmic solution. By keeping either $\boldsymbol{U}$ or $\boldsymbol{q}_{\text{ext}}$ fixed and minimizing $\hat{\lambda}_n(\boldsymbol{U}, \boldsymbol{q}_{\text{ext}})$ with respect to the other variable, the minimum of (4.9) is approached.

For fixed $\tilde{\boldsymbol{U}}$, the cost function $\hat{\lambda}_n(\tilde{\boldsymbol{U}}, \boldsymbol{q}_{\text{ext}})$ is minimized by the vector $\hat{\boldsymbol{q}}_{\text{ext}}$, which fulfills

$$\boldsymbol{\Lambda}(\tilde{\boldsymbol{U}}, P_{\max}) \cdot \hat{\boldsymbol{q}}_{\text{ext}} = \lambda_{\max}\big(\boldsymbol{\Lambda}(\tilde{\boldsymbol{U}}, P_{\max})\big) \cdot \hat{\boldsymbol{q}}_{\text{ext}} \quad \text{with} \quad [\hat{\boldsymbol{q}}_{\text{ext}}]_{K+1} = 1 \; . \tag{4.10}$$

This can easily be shown by multiplying both sides of (4.10) by $\boldsymbol{x}^T \in \mathbb{R}_+^{K+1}$ and dividing by $\boldsymbol{x}^T \hat{\boldsymbol{q}}_{\text{ext}}$. Combining (4.7) and (4.8) we have

$$\begin{aligned} \frac{\boldsymbol{x}^T \boldsymbol{\Lambda}(\tilde{\boldsymbol{U}}, P_{\max}) \hat{\boldsymbol{q}}_{\text{ext}}}{\boldsymbol{x}^T \hat{\boldsymbol{q}}_{\text{ext}}} &= \lambda_{\max}\big(\boldsymbol{\Lambda}(\tilde{\boldsymbol{U}}, P_{\max})\big) \\ &= \min_{\boldsymbol{q}_{\text{ext}}} \hat{\lambda}_n(\tilde{\boldsymbol{U}}, \boldsymbol{q}_{\text{ext}}) \; . \end{aligned}$$

Having found the optimal power control strategy, we are now interested in finding the beamformer $\hat{\boldsymbol{U}}$ that is optimal for given $\hat{\boldsymbol{q}}_{\text{ext}}$, i.e.,

$$\hat{\boldsymbol{U}} = \arg\min_{\boldsymbol{U}} \hat{\lambda}_n(\boldsymbol{U}, \hat{\boldsymbol{q}}_{\text{ext}}) \; . \tag{4.11}$$

To this end we need the following lemma:

Lemma 13. *The cost function $\hat{\lambda}_n(\boldsymbol{U}, \boldsymbol{q}_{\text{ext}})$ does not depend on the last row of the extended coupling matrix $\boldsymbol{\Lambda}$, i.e.,*

$$\begin{aligned} \max_{\boldsymbol{x}>0} \frac{\boldsymbol{x}^T \boldsymbol{\Lambda}(\boldsymbol{U}, P_{\max}) \boldsymbol{q}_{\text{ext}}}{\boldsymbol{x}^T \boldsymbol{q}_{\text{ext}}} &= \max_{\boldsymbol{x}\colon [\boldsymbol{x}]_{K+1}=0} \frac{\boldsymbol{x}^T \boldsymbol{\Lambda}(\boldsymbol{U}, P_{\max}) \boldsymbol{q}_{\text{ext}}}{\boldsymbol{x}^T \boldsymbol{q}_{\text{ext}}} \\ &= \max_{1 \le i \le K} \frac{\gamma_i}{\text{SINR}_i^{\text{UL}}(\boldsymbol{u}_i, \boldsymbol{q})} \; , \quad \textit{where } \boldsymbol{q} = [\boldsymbol{q}_{\text{ext}}]_{1:K} \; . \end{aligned} \tag{4.12}$$

The same relation holds when replacing max *by* min.

Proof. See the appendix on page 71. ∎

A beneficial consequence from Lemma 13 is that minimizing the cost function $\hat{\lambda}_n(\boldsymbol{U}, \boldsymbol{q}_{\text{ext}})$ with respect to $\boldsymbol{U}$ (keeping $\boldsymbol{q}_{\text{ext}} = \left[\begin{smallmatrix} \boldsymbol{q} \\ 1 \end{smallmatrix}\right]$ fixed) leads to a set of K decoupled problems

$$\begin{aligned} \hat{\boldsymbol{u}}_i &= \arg\max_{\boldsymbol{u}_i} \text{SINR}_i^{\text{UL}}(\boldsymbol{u}_i, \boldsymbol{q}) \\ &= \arg\max_{\boldsymbol{u}_i} \frac{\boldsymbol{u}_i^H \boldsymbol{R}_i \boldsymbol{u}_i}{\boldsymbol{u}_i^H \boldsymbol{Z}_i(\boldsymbol{q}) \boldsymbol{u}_i} \; , \quad 1 \le i \le K \; . \end{aligned} \tag{4.13}$$

The matrices $\boldsymbol{Z}_i$, as defined in (4.6), are non-singular and symmetric, thus (4.13) is solved by the dominant generalized eigenvectors of the matrix pairs $\big(\boldsymbol{R}_i, \boldsymbol{Z}_i(\boldsymbol{q})\big)$, $1 \le i \le K$.

4.1.4. Necessary and Sufficient Condition for Global Optimality

Using Lemma 13, a characterization of each global optimizer $\boldsymbol{U}^{opt} \in \mathcal{M}$ can be found. The result is summarized by the following theorem, which will prove very useful in Section 4.2, where an iterative solution will be derived.

Theorem 17. *A matrix $\hat{\boldsymbol{U}} = [\hat{\boldsymbol{u}}_1, \ldots, \hat{\boldsymbol{u}}_K]$ is optimal, i.e., $\hat{\boldsymbol{U}} \in \mathcal{M}$ if and only if there exists a $\hat{\boldsymbol{q}}_{\text{ext}}$ such that*

$$\hat{\lambda}_n(\hat{\boldsymbol{U}}, \hat{\boldsymbol{q}}_{\text{ext}}) = \min_{\boldsymbol{U}} \hat{\lambda}_n(\boldsymbol{U}, \hat{\boldsymbol{q}}_{\text{ext}}) \;, \tag{4.14}$$

$$\textit{and} \quad \boldsymbol{\Lambda}(\hat{\boldsymbol{U}}, P_{\max})\, \hat{\boldsymbol{q}}_{\text{ext}} = \lambda_{\max}\big(\boldsymbol{\Lambda}(\hat{\boldsymbol{U}}, P_{\max})\big)\, \hat{\boldsymbol{q}}_{\text{ext}} \;. \tag{4.15}$$

Proof. Assume that (4.14) and (4.15) hold. Let $\boldsymbol{x} \in \mathbb{R}_+^{K+1}$ be an arbitrary vector. Left-hand multiplication on both sides of (4.15) with $\boldsymbol{x}^T/\boldsymbol{x}^T\hat{\boldsymbol{q}}_{\text{ext}}$ leads to

$$\frac{\boldsymbol{x}^T\boldsymbol{\Lambda}(\hat{\boldsymbol{U}}, P_{\max})\hat{\boldsymbol{q}}_{\text{ext}}}{\boldsymbol{x}^T\hat{\boldsymbol{q}}_{\text{ext}}} = \lambda_{\max}\big(\boldsymbol{\Lambda}(\hat{\boldsymbol{U}}, P_{\max})\big) \;. \tag{4.16}$$

The same $\hat{\boldsymbol{U}}$ that minimizes $\hat{\lambda}_n(\boldsymbol{U}, \hat{\boldsymbol{q}}_{\text{ext}}) = \max_{1 \le i \le K} \frac{\gamma_i}{\text{SINR}_i^{\text{UL}}(\boldsymbol{u}_i, \hat{\boldsymbol{q}})}$ is also a minimizer of $\min_{1 \le i \le K} \frac{\gamma_i}{\text{SINR}_i^{\text{UL}}(\boldsymbol{u}_i, \hat{\boldsymbol{q}})}$. It follows from Lemma 13 that

$$\min_{\boldsymbol{x}>0} \frac{\boldsymbol{x}^T\boldsymbol{\Lambda}(\hat{\boldsymbol{U}}, P_{\max})\hat{\boldsymbol{q}}_{\text{ext}}}{\boldsymbol{x}^T\hat{\boldsymbol{q}}_{\text{ext}}} = \min_{\boldsymbol{U}} \min_{\boldsymbol{x}>0} \frac{\boldsymbol{x}^T\boldsymbol{\Lambda}(\boldsymbol{U}, P_{\max})\hat{\boldsymbol{q}}_{\text{ext}}}{\boldsymbol{x}^T\hat{\boldsymbol{q}}_{\text{ext}}} \;. \tag{4.17}$$

Since (4.16) holds for any $\boldsymbol{x} > 0$, relation (4.17) can be rewritten as

$$\min_{\boldsymbol{U}} \min_{\boldsymbol{x}>0} \frac{\boldsymbol{x}^T\boldsymbol{\Lambda}(\boldsymbol{U}, P_{\max})\hat{\boldsymbol{q}}_{\text{ext}}}{\boldsymbol{x}^T\hat{\boldsymbol{q}}_{\text{ext}}} = \lambda_{\max}\big(\boldsymbol{\Lambda}(\hat{\boldsymbol{U}}, P_{\max})\big) \;. \tag{4.18}$$

Combining (4.4), (4.7), and (4.18) we have

$$\begin{aligned} 1/C_{\text{opt}}^{\text{UL}}(P_{\max}) &= \min_{\boldsymbol{U}} \lambda_{\max}\big(\boldsymbol{\Lambda}(\boldsymbol{U}, P_{\max})\big) \\ &= \min_{\boldsymbol{U}} \min_{\boldsymbol{x}>0} \max_{\boldsymbol{y}>0} \frac{\boldsymbol{x}^T\boldsymbol{\Lambda}(\boldsymbol{U}, P_{\max})\boldsymbol{y}}{\boldsymbol{x}^T\boldsymbol{y}} \\ &\ge \min_{\boldsymbol{U}} \min_{\boldsymbol{x}>0} \frac{\boldsymbol{x}^T\boldsymbol{\Lambda}(\boldsymbol{U}, P_{\max})\hat{\boldsymbol{q}}_{\text{ext}}}{\boldsymbol{x}^T\hat{\boldsymbol{q}}_{\text{ext}}} = \lambda_{\max}\big(\boldsymbol{\Lambda}(\hat{\boldsymbol{U}}, P_{\max})\big) \;. \end{aligned} \tag{4.19}$$

Inequality (4.19) can only be satisfied with equality, since $1/C_{\text{opt}}^{\text{DL}}(P_{\max})$ is the global minimum. From this we can conclude that $\hat{\boldsymbol{U}} \in \mathcal{M}$ holds.

To prove the reverse direction, suppose that $\hat{\boldsymbol{U}}$ is optimal, i.e., $\hat{\boldsymbol{U}} \in \mathcal{M}$. This implies $\lambda_{\max}\big(\boldsymbol{\Lambda}(\hat{\boldsymbol{U}}, P_{\max})\big) \le \lambda_{\max}\big(\boldsymbol{\Lambda}(\boldsymbol{U}, P_{\max})\big)$ for all $\boldsymbol{U}$. Let $\hat{\boldsymbol{q}}_{\text{ext}}$ be the dominant eigenvector of $\boldsymbol{\Lambda}(\hat{\boldsymbol{U}}, P_{\max})$ with $\hat{\boldsymbol{q}}_{\text{ext}} = \left[\begin{smallmatrix}\hat{\boldsymbol{q}}\\ 1\end{smallmatrix}\right]$ and $\|\hat{\boldsymbol{q}}\|_1 = P_{\max}$. With (4.7) and (4.8) the following inequality is obtained:

$$\begin{aligned}\lambda_{\max}\big(\boldsymbol{\Lambda}(\hat{\boldsymbol{U}}, P_{\max})\big) &\leq \lambda_{\max}\big(\boldsymbol{\Lambda}(\boldsymbol{U}, P_{\max})\big)\\ &= \min_{\boldsymbol{y}>0}\max_{\boldsymbol{x}>0} \frac{\boldsymbol{x}^T\boldsymbol{\Lambda}(\boldsymbol{U}, P_{\max})\boldsymbol{y}}{\boldsymbol{x}^T\boldsymbol{y}}\\ &\leq \max_{\boldsymbol{x}>0} \frac{\boldsymbol{x}^T\boldsymbol{\Lambda}(\boldsymbol{U}, P_{\max})\hat{\boldsymbol{q}}_{\text{ext}}}{\boldsymbol{x}^T\hat{\boldsymbol{q}}_{\text{ext}}}\\ &= \hat{\lambda}_n(\boldsymbol{U}, \hat{\boldsymbol{q}}_{\text{ext}})\ . \end{aligned} \tag{4.20}$$

This holds for any $\boldsymbol{U}$. Thus, using (4.16) it follows that

$$\begin{aligned}\min_{\boldsymbol{U}} \hat{\lambda}_n(\boldsymbol{U}, \hat{\boldsymbol{q}}_{\text{ext}}) &\geq \lambda_{\max}\big(\boldsymbol{\Lambda}(\hat{\boldsymbol{U}}, P_{\max})\big)\\ &= \max_{\boldsymbol{z}>0} \frac{\boldsymbol{z}^T\boldsymbol{\Lambda}(\hat{\boldsymbol{U}}, P_{\max})\hat{\boldsymbol{q}}_{\text{ext}}}{\boldsymbol{z}^T\hat{\boldsymbol{q}}_{\text{ext}}}\\ &= \hat{\lambda}_n(\hat{\boldsymbol{U}}, \hat{\boldsymbol{q}}_{\text{ext}})\ . \end{aligned} \tag{4.21}$$

Inequality (4.21) can only be fulfilled with equality, which concludes the proof. ■

4.2. Global Optimization with Alternating Variables

The method of alternating variables in its simplest form keeps all but one variable fixed and seeks a value of this variable so as to minimize the objective function. This is repeated successively for all variables. In general, this strategy is know to approach the optimum very slowly and may even get stuck. The variant proposed in this section, however, exploits the analytical structure of the given problem and therefore rapidly converges towards the global optimum of the eigenvalue minimization problem (4.4).

4.2.1. Algorithm Summary

In Section 4.1.4 it was shown how the objective function $\hat{\lambda}_n(\boldsymbol{U}, \boldsymbol{q}_{\text{ext}})$ is minimized when either $\boldsymbol{U}$ or $\boldsymbol{q}_{\text{ext}}$ is kept fixed. Also, a necessary and sufficient condition for global optimality is provided by Theorem 17. This motivates the alternating algorithm summarized below. The quantities associated with the n^{th} iteration step are denoted by the superscript $(\cdot)^{(n)}$.

4.2.2. Monotony and Global Convergence

Theorem 18. *The iteration sequence $\lambda_{\max}(n)$ obtained from Algorithm 3 is monotonically decreasing and converges to the global optimum of the eigenvalue minimization problem (4.4), regardless of the chosen initialization.*

Algorithm 3 Algorithmic solution of the eigenvalue minimization problem (4.4)

1: $n \Leftarrow 0$
2: $\boldsymbol{q}_{\text{ext}}^{(0)} \Leftarrow [0, \ldots, 0, 1]^T$
3: **repeat**
4: $\quad n \Leftarrow n + 1$
5: $\quad$ for given $\boldsymbol{q}_{\text{ext}}^{(n-1)}$ compute $\boldsymbol{U}^{(n)} = [\boldsymbol{u}_1^{(n)}, \ldots, \boldsymbol{u}_K^{(n)}]$ as the solution of

$$\boldsymbol{u}_i^{(n)} = \arg\max_{\boldsymbol{u}_i} \frac{\boldsymbol{u}_i^H \boldsymbol{R}_i \boldsymbol{u}_i}{\boldsymbol{u}_i^H \boldsymbol{Z}_i(\boldsymbol{q}_{\text{ext}}^{(n-1)}) \boldsymbol{u}_i} \;, \quad 1 \leq i \leq K \tag{4.22}$$

6: $\quad$ for given $\boldsymbol{U}^{(n)}$ compute $\boldsymbol{q}_{\text{ext}}^{(n)}$ as the solution of

$$\boldsymbol{\Lambda}(\boldsymbol{U}^{(n)}, P_{\max})\, \boldsymbol{q}_{\text{ext}}^{(n)} = \lambda_{\max}(n)\, \boldsymbol{q}_{\text{ext}}^{(n)} \;, \quad \text{with} \quad [\boldsymbol{q}_{\text{ext}}^{(n)}]_{K+1} = 1$$

7: **until** $\lambda_{\max}(n-1) - \lambda_{\max}(n) < \epsilon$

Proof. From Lemma 13 follows that for given $\boldsymbol{q}_{\text{ext}}^{(n-1)}$, the solution $\boldsymbol{U}^{(n)}$ minimizes the cost function $\hat{\lambda}_n(\boldsymbol{U}, \boldsymbol{q}_{\text{ext}}^{(n-1)})$, i.e,

$$\hat{\lambda}_n(\boldsymbol{U}^{(n)}, \boldsymbol{q}_{\text{ext}}^{(n-1)}) \leq \hat{\lambda}_n(\boldsymbol{U}^{(n-1)}, \boldsymbol{q}_{\text{ext}}^{(n-1)}) = \lambda_{\max}(n-1) \;. \tag{4.23}$$

Using (4.7) and (4.23) we have

$$\begin{aligned} \lambda_{\max}(n) &= \min_{\boldsymbol{y}>0} \max_{\boldsymbol{x}>0} \frac{\boldsymbol{x}^T \boldsymbol{\Lambda}(\boldsymbol{U}^{(n)}, P_{\max}) \boldsymbol{y}}{\boldsymbol{x}^T \boldsymbol{y}} \\ &\leq \hat{\lambda}_n(\boldsymbol{U}^{(n)}, \boldsymbol{q}_{\text{ext}}^{(n-1)}) \\ &\leq \lambda_{\max}(n-1) \;. \end{aligned} \tag{4.24}$$

Hence, the iteration sequence $\lambda_{\max}(n)$ is monotonically decreasing. Using (4.7), it can be shown that the quantity $\lambda_{\max}(n)$ is lower bounded:

$$\begin{aligned} \lambda_{\max}(n) &= \max_{\boldsymbol{y}>0} \min_{\boldsymbol{x}>0} \frac{\boldsymbol{x}^T \boldsymbol{\Lambda}(\boldsymbol{U}^{(n)}, P_{\max}) \boldsymbol{y}}{\boldsymbol{x}^T \boldsymbol{y}} \\ &\geq \min_{\boldsymbol{x}>0} \frac{\boldsymbol{x}^T \boldsymbol{\Lambda}(\boldsymbol{U}^{(n)}, P_{\max}) \boldsymbol{q}_{\text{ext}}^{(n-1)}}{\boldsymbol{x}^T \boldsymbol{q}_{\text{ext}}^{(n-1)}} \;. \end{aligned} \tag{4.25}$$

Combining (4.12), (4.24), and (4.25) we have

$$\min_{1 \leq i \leq K} \frac{\gamma_i}{\text{SINR}_i^{\text{UL}}(\boldsymbol{u}_i^{(n)}, \boldsymbol{q}^{(n-1)})} \leq \lambda_{\max}(n) \leq \max_{1 \leq i \leq K} \frac{\gamma_i}{\text{SINR}_i^{\text{UL}}(\boldsymbol{u}_i^{(n)}, \boldsymbol{q}^{(n-1)})} \leq \lambda_{\max}(n-1) \;. \tag{4.26}$$

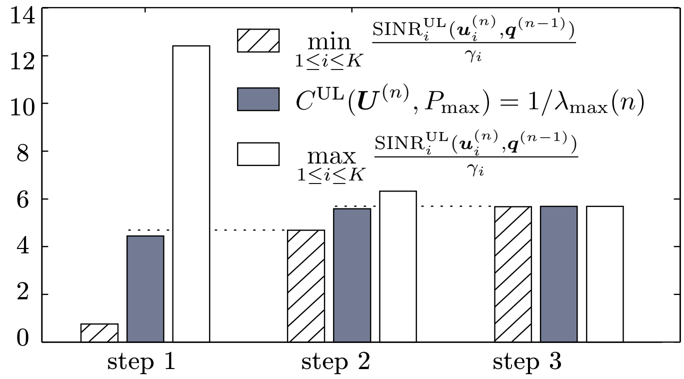

Figure 4.1.: Typical convergence behavior of Algorithm 3

The monotony result (4.26) implies the existence of a limit $\lambda^\infty = \lim_{n\to\infty} \lambda_{\max}(n)$ (an illustration is given in Fig. 4.1). Using the continuity of $\boldsymbol{\Lambda}(\boldsymbol{U})$, as well as the fact that both $\|\boldsymbol{q}_{\mathrm{ext}}^{(n)}\|_1$ and $\|\boldsymbol{U}^{(n)}\|_F$ are bounded, it can be shown in the same way as in Section 3.2.1, that λ^∞ is a solution of $\boldsymbol{\Lambda}(\boldsymbol{U}^\infty)\boldsymbol{q}_{\mathrm{ext}}^\infty = \lambda^\infty \boldsymbol{q}_{\mathrm{ext}}^\infty$. Thus,

$$\min_{\boldsymbol{U}} \hat{\lambda}_n(\boldsymbol{U}, \boldsymbol{q}_{\mathrm{ext}}^\infty) = \hat{\lambda}_n(\boldsymbol{U}^\infty, \boldsymbol{q}_{\mathrm{ext}}^\infty) . \tag{4.27}$$

From Theorem 17 we know that (4.27) is necessary and sufficient for the optimality of $\boldsymbol{U}^\infty$. ■

4.2.3. Stopping Criteria

Next, stopping criteria are derived in analogy to the noiseless case (see Section 3.2.2).

A solution $\boldsymbol{U}^{(n)}$ is a global optimizer of the eigenvalue minimization problem (4.4) if and only if $\lambda_{\max}(n) = \lambda_{\max}(n+1)$. This is an immediate consequence from Theorem 17. Thus, the algorithm can be stopped as soon as the difference $\lambda_{\max}(n) - \lambda_{\max}(n+1)$ falls below a threshold ϵ.

A drawback of this approach is that the quantity $\boldsymbol{U}^{(n+1)}$ must be computed in order to assess the optimality of $\boldsymbol{U}^{(n)}$, which means that an additional iteration step must be carried out. A more direct stopping criterion can be found by considering the ratios $\mathrm{SINR}_i^{\mathrm{UL}}(\boldsymbol{U}^{(n)}, \boldsymbol{q}^{(n-1)})/\gamma_i$, where $\boldsymbol{q} = [\boldsymbol{q}_{\mathrm{ext}}]_{1:K}$. If they are balanced at the same level, the global optimum is reached.

Theorem 19. *A solution $\boldsymbol{U}^{(n)}$ is optimal with respect to (4.4), i.e., $\boldsymbol{U}^{(n)} \in \mathcal{M}$, if and only if*

$$\min_{1\le i\le K} \frac{\mathrm{SINR}_i^{\mathrm{UL}}(\boldsymbol{U}^{(n)}, \boldsymbol{q}^{(n-1)})}{\gamma_i} = \max_{1\le i\le K} \frac{\mathrm{SINR}_i^{\mathrm{UL}}(\boldsymbol{U}^{(n)}, \boldsymbol{q}^{(n-1)})}{\gamma_i} . \tag{4.28}$$

Proof. See the appendix on page 80. ■

Theorem 19 provides an additional interpretation in terms of SINR balancing. As long as the optimum is not reached, the quantity $C^{\mathrm{UL}}(\boldsymbol{U}^{(n)}, P_{\max}) = 1/\lambda_{\max}(n)$ is lower and upper bounded as in (4.26). The iteration process can be stopped as soon as the difference between the relative SINR levels in (4.28) is smaller than a threshold ϵ.

4.3. Minimizing Excess Transmission Power

If $C^{\mathrm{UL}}_{\mathrm{opt}}(P_{\max}) > 1$, then there are excess degrees of freedom which can be used to minimize the total transmission power:

$$\min_{\boldsymbol{U},\,\boldsymbol{q}} \sum_{i=1}^{K} q_i \quad \text{subject to} \quad \begin{array}{l} \mathrm{SINR}_i^{\mathrm{UL}} \geq \gamma_i\,, \quad 1 \leq i \leq K \\[1ex] \|\boldsymbol{u}_i\|_2 = 1, \;\; 1 \leq i \leq K\,. \end{array} \tag{4.29}$$

In Section 2.2.2 it was shown that (4.29) can be seen as a special case of the SINR balancing problem (4.1). Thus, the global optimum (4.29) can be found by extending Algorithm 3.

4.3.1. Iterative Power Minimization

The first step for solving the power minimization problem (4.29) is to make sure that the constraints $\mathrm{SINR}_i^{\mathrm{UL}} \geq \gamma_i$ can be fulfilled. As discussed in Section 2.2, this is exactly the case when there exists a beamforming solution $\boldsymbol{U}^{(n)}$ such that $C^{\mathrm{UL}}(\boldsymbol{U}^{(n)}, P_{\max}) \geq 1$ (the function C^{UL} is defined by (2.10) and illustrated in Fig. 2.6). The problem is infeasible if and only if Algorithm 3 yields a solution $C^{\mathrm{UL}}(\boldsymbol{U}^{(n)}, P_{\max}) < 1$ for $n \to \infty$. Such a situation should be avoided by proper countermeasures taken by the dynamic resource management.

As soon as it turns out that the problem is feasible, the global power minimum (4.29) can be found by changing the power control policy. Instead of computing the power allocation which maximizes the balanced ratio $\mathrm{SINR}_i^{\mathrm{UL}}/\gamma_i$ for given $P_{\max}$, we are now interested in finding the allocation that minimizes the total tranmission power while satisfying $\mathrm{SINR}_i^{\mathrm{UL}}/\gamma_i = 1$. This problem was already discussed in Section 2.2.2. The solution is found by solving the set of linear equations (2.18). These steps are repeated until convergence. The algorithm is summarized below and illustrated in Fig. 4.2.

Theorem 20. *Suppose that the power minimization problem (4.29) is feasible, then Algorithm 4 approximates the global power minimum up to a desired accuracy.*

Proof. Suppose that (4.29) is feasible. In Section 2.2.2 it was shown that for given $\boldsymbol{U}^{(n)}$ the allocation $\boldsymbol{q}^{(n)} = \big(\boldsymbol{I} - \boldsymbol{D}\boldsymbol{\Psi}^T(\boldsymbol{U}^{(n)})\big)^{-1}\boldsymbol{D}\boldsymbol{\sigma}$ achieves the SINR targets with

Algorithm 4 Algorithmic solution of the power minimization problem (4.29)

initialize: $n \Leftarrow 0$, $\boldsymbol{q}^{(0)} \Leftarrow [0, \dots, 0]^T$, $C^{(0)} \Leftarrow 0$
repeat
  $n \Leftarrow n + 1$
  $\boldsymbol{U}^{(n)} = [\boldsymbol{u}_1^{(n)}, \dots, \boldsymbol{u}_K^{(n)}] \Leftarrow \arg\max_{\boldsymbol{u}_i} \frac{\boldsymbol{u}_i^H \boldsymbol{R}_i \boldsymbol{u}_i}{\boldsymbol{u}_i^H \boldsymbol{Z}_i(\boldsymbol{q}^{(n-1)}) \boldsymbol{u}_i}$, $1 \le i \le K$
  if $C^{(n)} < 1$ **then**
    $P_{sum}^{(n)} \Leftarrow P_{\max}$
    solve $\boldsymbol{\Lambda}(\boldsymbol{U}^{(n)}, P_{sum}^{(n)}) \begin{bmatrix} \boldsymbol{q}^{(n)} \\ 1 \end{bmatrix} = \lambda_{\max}(n) \begin{bmatrix} \boldsymbol{q}^{(n)} \\ 1 \end{bmatrix}$
    $C^{(n)} \Leftarrow 1/\lambda_{\max}(n)$
  else
    $\boldsymbol{q}^{(n)} \Leftarrow \left(\boldsymbol{I} - \boldsymbol{D}\boldsymbol{\Psi}^T(\boldsymbol{U}^{(n)})\right)^{-1} \boldsymbol{D}\boldsymbol{\sigma}$
    $P_{sum}^{(n)} \Leftarrow \|\boldsymbol{q}^{(n)}\|_1$
    $C^{(n)} \Leftarrow 1$
  end if
until $\max_{1 \le i \le K} \mathrm{SINR}_i^{\mathrm{UL}}(\boldsymbol{u}_i^{(n)}, \boldsymbol{q}^{(n-1)}) - \min_{1 \le i \le K} \mathrm{SINR}_i^{\mathrm{UL}}(\boldsymbol{u}_i^{(n)}, \boldsymbol{q}^{(n-1)}) < \epsilon$

minimal transmission power. Hence, $P_{sum}^{(n)} \le P_{sum}^{(n-1)}$, as illustrated in Fig 4.2. The algorithm converges towards a solution $P_{sum}^{(\infty)}$. That is, for a given sum power $P_{sum}^{(\infty)}$, the beamforming step achieves no further improvement. With the results in Section 4.2 it can be concluded that

$$C^{\mathrm{UL}}(\boldsymbol{U}^{(\infty)}, P_{sum}^{(\infty)}) = \max_{\boldsymbol{U}} C^{\mathrm{UL}}(\boldsymbol{U}, P_{sum}^{(\infty)}) . \tag{4.30}$$

Now, assume that there exists a beamforming solution $\tilde{\boldsymbol{U}}$ which fulfills the SINR constraints with a minimal power level $\tilde{P} < P_{sum}^{(\infty)}$. Since C^{UL} is strictly monotonically increasing in the total power, this implies $C^{\mathrm{UL}}(\tilde{\boldsymbol{U}}, P_{sum}^{(\infty)}) > C^{\mathrm{UL}}(\boldsymbol{U}^{(\infty)}, P_{sum}^{(\infty)})$, which is a contradiction to (4.30). ∎

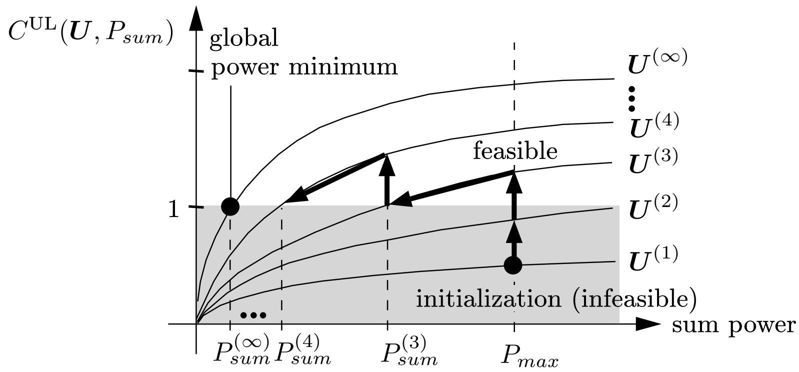

Figure 4.2.: Schematic illustration of Algorithm 4 (iterative power minimization)

If the power minimization problem (4.29) is not feasible, then convergence is achieved with $C^{(\infty)} < 1$. Then, the algorithm does not differ from the SINR balancing algorithm in Table 3. As discussed before, $C^{(\infty)} \geq 1$ is a necessary and sufficient condition for feasibility required by the dynamic resource allocation.

4.3.2. Closed-Form Solution for the 2-User Scenario

Consider a 2-user scenario with perfect channel information $\boldsymbol{R}_i = \boldsymbol{h}_i \boldsymbol{h}_i^H$, $i = 1, 2$, and equal noise levels $\sigma_1^2 = \sigma_2^2 = 1$. The goal is to balance the quantities $C_i^{\mathrm{UL}} = \mathrm{SINR}_i^{\mathrm{UL}}(\boldsymbol{u}_i, q_1, q_2)/\gamma_i$, $i = 1, 2$, with minimal transmission power. The first user achieves a level

$$C_1^{\mathrm{UL}} = \frac{\mathrm{SINR}_1^{\mathrm{UL}}(\boldsymbol{u}_1, q_1, q_2)}{\gamma_1} = \frac{q_1 |\boldsymbol{u}_1^H \boldsymbol{h}_1|^2}{\gamma_1 (q_2 |\boldsymbol{u}_1^H \boldsymbol{h}_2|^2 + 1)} \ . \tag{4.31}$$

This is maximized by the normalized MMSE solution

$$\boldsymbol{u}_1^{opt} = \frac{\left(q_2 \boldsymbol{h}_2 \boldsymbol{h}_2^H + \boldsymbol{I}\right)^{-1} \boldsymbol{h}_1}{\|\left(q_2 \boldsymbol{h}_2 \boldsymbol{h}_2^H + \boldsymbol{I}\right)^{-1} \boldsymbol{h}_1\|_2} \ . \tag{4.32}$$

Putting (4.32) in (4.31) we have

$$C_1^{\mathrm{UL}} = \frac{q_1 \boldsymbol{h}_1^H \left(q_2 \boldsymbol{h}_2 \boldsymbol{h}_2^H + \boldsymbol{I}\right)^{-1} \boldsymbol{h}_1}{\gamma_1} \ .$$

Using the Sherman-Morrison inversion lemma (see e.g. [46]) this can be rewritten as

$$C_1^{\mathrm{UL}} = \frac{q_1}{\gamma_1} \left(\boldsymbol{h}_1^H \boldsymbol{h}_1 - \frac{q_2 |\boldsymbol{h}_1^H \boldsymbol{h}_2|^2}{1 + q_2 \boldsymbol{h}_2^H \boldsymbol{h}_2} \right) \ . \tag{4.33}$$

Likewise, the level of the second user is given by

$$C_2^{\mathrm{UL}} = \frac{q_2}{\gamma_2} \left(\boldsymbol{h}_2^H \boldsymbol{h}_2 - \frac{q_1 |\boldsymbol{h}_2^H \boldsymbol{h}_1|^2}{1 + q_1 \boldsymbol{h}_1^H \boldsymbol{h}_1} \right) \ . \tag{4.34}$$

Now, assume that both users are balanced at the same level $C_1^{\mathrm{UL}} = C_2^{\mathrm{UL}} = 1$. Solving (4.33) for q_1, then putting q_1 in (4.34), then solving for q_2 yields

$$q_2 = \frac{-a_2 + \sqrt{a_2^2 + 4 b_2 c_2}}{2 c_2} \tag{4.35}$$

$$\begin{aligned} \text{where} \quad & a_2 = \|\boldsymbol{h}_2\|^2 \|\boldsymbol{h}_1\|^2 (1 + \gamma_1 - \gamma_2 - \gamma_1 \gamma_2) + \gamma_2 |\boldsymbol{h}_1^H \boldsymbol{h}_2|^2 - \gamma_1 |\boldsymbol{h}_2^H \boldsymbol{h}_1|^2 \\ & b_2 = \gamma_2 \|\boldsymbol{h}_1\|^2 (1 + \gamma_1) \\ & c_2 = \|\boldsymbol{h}_2\|^4 \|\boldsymbol{h}_1\|^2 (1 + \gamma_1) - \|\boldsymbol{h}_2\|^2 |\boldsymbol{h}_1^H \boldsymbol{h}_2|^2 - \gamma_1 \|\boldsymbol{h}_2\|^2 |\boldsymbol{h}_2^H \boldsymbol{h}_1|^2 \ . \end{aligned}$$

Likewise, we can derive a closed form expression for user 1:

$$q_1 = \frac{-a_1 + \sqrt{a_1^2 + 4b_1c_1}}{2c_1} \tag{4.36}$$

$$\begin{aligned}
\text{where} \quad a_1 &= \|\boldsymbol{h}_1\|^2\|\boldsymbol{h}_2\|^2(1+\gamma_2-\gamma_1-\gamma_2\gamma_1) + \gamma_1|\boldsymbol{h}_2^H\boldsymbol{h}_1|^2 - \gamma_2|\boldsymbol{h}_1^H\boldsymbol{h}_2|^2 \\
b_1 &= \gamma_1\|\boldsymbol{h}_2\|^2(1+\gamma_2) \\
c_1 &= \|\boldsymbol{h}_1\|^4\|\boldsymbol{h}_2\|^2(1+\gamma_2) - \|\boldsymbol{h}_1\|^2|\boldsymbol{h}_2^H\boldsymbol{h}_1|^2 - \gamma_2\|\boldsymbol{h}_1\|^2|\boldsymbol{h}_1^H\boldsymbol{h}_2|^2\ .
\end{aligned}$$

The power levels (4.35) and (4.36) achieve the targets γ_1 and γ_2 with minimum total transmission power $P_{\max} = q_1 + q_2$. The optimal beamformer $\boldsymbol{u}_1^{opt}$ is obtained from (4.32). Likewise, $\boldsymbol{u}_2^{opt}$ can be computed. With the duality stated in Theorem 6 it is known that $\boldsymbol{u}_1^{opt}$ and $\boldsymbol{u}_2^{opt}$ are optimal for both uplink and downlink. Finally, the optimal downlink powers can be found by the power control strategy discussed in Section 2.2.1.

4.4. Discussion

In this chapter the problem of joint beamforming and power control under a sum power constraint has been solved. A generic solution has been presented, which shares the available power resource in a fair manner, taking into account individual SINR targets. This technique can be used in two different ways:

1. by maximizing the balanced SINR margin $C^{\mathrm{UL}}(\boldsymbol{U}, P_{\max})$ while maintaining a sum power constraint $\|\boldsymbol{q}\|_1 \leq P_{\max}$,
2. by minimizing the total power $\|\boldsymbol{q}\|_1$ while ensuring target SINR's $\gamma_1 \dots \gamma_K$.

Both design goals are closely linked. If the latter is infeasible, this can be detected by the necessary and sufficient condition provided by Algorithm 3. Infeasible scenarios must be handled by proper resource management.

Given an optimal beamforming solution, an optimal power allocation follows directly from (4.15). On the other hand, an optimal beamforming solution is obtained from (4.14) if an optimal power allocation is known. This fundamental relationship will prove useful in the next chapter in order to find the maximum throughput of the Gaussian multiuser channel.

The solution derived in this chapter is general enough to hold for spatial covariance matrices of arbitrary rank. This is important, since perfect spatial channel knowledge is rarely available, due to channel fluctuations in time. Incoherent beamforming can be performed based on knowledge of the spatial covariance matrices that are obtained by averaging over several fading cycles (see Section 2.1.1). Such a "long-term" approach is robust due to the slowly changing geometry of the multipath directions. The rapid convergence behavior of the algorithm makes this approach suitable for real time applications.

5. Rate Balancing for Gaussian Broadcast and Multiple Access Channels

In this chapter we study the SINR balancing problem in an information theoretical context with i.i.d. Gaussian signaling under a sum power constraint. Assuming perfect channel knowledge at the base station, the multiplexed data streams can be decoupled by a combination of linear equalization and successive coding for known interference. This leads to a triangularized channel structure, which is a special case of the general scenario considered so far. As will be shown in this chapter, the triangular structure allows for an efficient solution based on back substitution. By defining threshold targets, rate tuples can be controlled according to individual capacity needs. Such a strategy is required when strict delay constraints are imposed and throughput has to be traded off against fairness.

The results presented in this chapter were published by Boche and Schubert in [1, 2].

5.1. Duality between Broadcast and Multiple Access Channel

5.1.1. Multiple Access Channel with Successive Decoding

We start by considering a Multiple Access Channel (MAC) with K scalar inputs and a vector output. The K independent transmitters use i.i.d. Gaussian random codebooks. The M receive antennas are jointly processed. From the discussion in Section 2.5 it is clear that a noise vector $\boldsymbol{\sigma} = \mathbf{1}_K$ can be assumed without loss of generality.

An optimal receiver structure for the MAC has been found in [35], where it was shown that the vertices of the capacity region can be achieved by using a combination of successive decoding and linear MMSE receivers $\boldsymbol{u}_i^{\text{MMSE}}$, $i = 1, \ldots, K$. Assuming a decoding order $K \dots 1$, the following signal is obtained at the i^{th} cancellation step:

$$y_i(t) = s_i(t)\boldsymbol{u}_i^H \boldsymbol{h}_i + \sum_{k=1}^{i-1} s_k(t)(\boldsymbol{u}_i^{\text{MMSE}})^H \boldsymbol{h}_k + n_i(t) \ , \ \ 1 \leq i \leq K \ . \tag{5.1}$$

This leads to "coded" SINR's

$$\text{SINR}_i^{UL,SD}(\boldsymbol{u}_i^{\text{MMSE}}, q_1 \dots q_i) = \frac{q_i|(\boldsymbol{u}_i^{\text{MMSE}})^H \boldsymbol{h}_i|^2}{(\boldsymbol{u}_i^{\text{MMSE}})^H \hat{\boldsymbol{Z}}_i(q_1 \dots q_{i-1})\boldsymbol{u}_i^{\text{MMSE}}} = q_i \boldsymbol{h}_i^H \hat{\boldsymbol{Z}}_i^{-1} \boldsymbol{h}_i \ . \tag{5.2}$$

where $\boldsymbol{u}_i^{\text{MMSE}} = \hat{\boldsymbol{Z}}_i^{-1} \boldsymbol{h}_i / \|\hat{\boldsymbol{Z}}_i^{-1} \boldsymbol{h}_i\|_2$ and

$$\hat{\boldsymbol{Z}}_i(q_1 \dots q_{i-1}) = \boldsymbol{I} + \sum_{k=1}^{i-1} q_k \boldsymbol{h}_k \boldsymbol{h}_k^H \ . \tag{5.3}$$

There is a one-to-one correspondence between (5.2) and the maximal spectral efficiency

$$\begin{aligned}
\mathcal{R}_i^{\text{UL}} &= \log_2 |q_i \boldsymbol{h}_i \boldsymbol{h}_i^H + \hat{\boldsymbol{Z}}_i| - \log_2 |\hat{\boldsymbol{Z}}_i| \\
&= \log_2 |\boldsymbol{I} + q_i \hat{\boldsymbol{Z}}_i^{-1/2} \boldsymbol{h}_i \boldsymbol{h}_i^H \hat{\boldsymbol{Z}}_i^{-1/2}| \\
&= \log_2(1 + q_i \boldsymbol{h}_i^H \hat{\boldsymbol{Z}}_i^{-1} \boldsymbol{h}_i) \\
&= \log_2(1 + \text{SINR}_i^{UL,SD}(\boldsymbol{u}_i^{\text{MMSE}}, q_1 \dots q_i)) \ .
\end{aligned} \tag{5.4}$$

For simplicity we will also refer to $\mathcal{R}_i$ as the *rate* in the following.

Hence, data rates can be controlled by jointly adjusting transmission powers and MMSE beamformers. By defining target thresholds $\gamma_1 \dots \gamma_K$, the SINR balancing strategy developed in Chapter 4 can be used to achieve rate tuples within the capacity region, including the maximal sum capacity. Provided that $\gamma_1 \dots \gamma_K$ are achievable under the given power constraint, the optimal power allocation and the optimal MMSE filters can be found by solving the power minimization problem

$$\min_{\boldsymbol{q},\boldsymbol{U}} \sum_{i=1}^{K} q_i \quad \text{subject to} \ \ \text{SINR}_i^{UL,SD}(\boldsymbol{u}_i, q_1, \dots, q_i) \geq \gamma_i, \quad 1 \leq i \leq K \ . \tag{5.5}$$

Note, that each optimizer $(\boldsymbol{U}^{opt}, \boldsymbol{q}^{opt})$ of the joint power minimization problem (5.5) is characterized by Theorem 17 (with Lemma 13) in two different ways:

1. Given $\boldsymbol{q}^{opt}$, the optimal beamformer $\boldsymbol{U}^{opt}$ is found by K independent SINR maximization problems.

2. Given $\boldsymbol{U}^{opt}$, the optimal power allocation $\boldsymbol{q}^{opt}$ can be found by the power control strategies described in Section 2.2.

Unlike the general problem treated in Chapter 4, problem (5.5) *always* feasible in the absence of power constraints. This is due to the triangular channel structure imposed by the successive decoding (see the discussion in Section 2.3 and the example in Fig. 2.5).

5.1.2. Broadcast Channel with 'Dirty Paper' Precoding

Next, consider a Gaussian broadcast channel (BC) with M cooperating transmit antennas and K non-cooperating receivers. This channel belongs to the class of non-degraded broadcast channels for which the general capacity region is not known [49].

A partial solution was recently found by Caire and Shamai [30] for the special case of two users and two transmit antennas. The result shows that throughput-wise optimal transmission is possible by using a combination of linear pre-filtering and coding for non-causally known interference at the transmitter. Such a precoder triangularizes the channel in a similar way as the decision-feedback equalizer does. The channel capacity is the same as if the non-causal interference would not exist. No further power enhancement is caused as long as optimal precoding is assumed.

The existence of such a an optimal precoder was first shown by Costa [50] for a Gaussian channel with Gaussian interference. More recently, this was expanded to the case of non-Gaussian interference [51]. Also, strategies for achieving this capacity were proposed [32, 51]. The principle is very much reminiscent of classical Tomlinson/Harashima precoding [52, 53], which can also be expanded to vector broadcast channels [54].

In this work we make use of these results, i.e., we assume that perfect channel state information is available at the transmitter and an optimal precoding scheme exists. We refer to this optimal strategy as "Dirty Paper" precoding after Costa's famous title "Writing on Dirty Paper" [50].

Assume a precoding order $1 \dots K$. Having chosen a codeword for the first user, the interference experienced by the users $2 \dots K$ is known non-causally at the receiver and can be taken into account when precoding the following users. Repeating this strategy for all users, a channel with a triangular structure is created (see Fig. 2.5).

The K receiving mobiles are non-cooperating and thus independently decoded. Multi-user interference appears as independent, zero-mean and non-Gaussian additive noise. It was shown in [55] that in this case the capacity of the i^{th} user is given by

$$\mathcal{R}_i^{\text{DL}} = \log_2(1 + \text{SINR}_i^{DL,CO}) , \quad 1 \le i \le K , \tag{5.6}$$

where

$$\text{SINR}_i^{DL,CO}(\boldsymbol{U}, \boldsymbol{p}) = \frac{p_i |\boldsymbol{u}_i^H \boldsymbol{h}_i|^2}{\sum\limits_{k=i+1}^{K} p_k |\boldsymbol{u}_k^H \boldsymbol{h}_i|^2 + 1} , \quad 1 \le i \le K . \tag{5.7}$$

Again, by jointly adjusting the beamformers $\boldsymbol{U} = [\boldsymbol{u}_1 \dots \boldsymbol{u}_K]$ and transmission power $\boldsymbol{p} = [p_1 \dots p_K]^T$, individual capacities can be controlled. Individual targets $\gamma_1 \dots \gamma_K$ can be achieved by solving the optimization problem

$$\min_{\boldsymbol{p}, \boldsymbol{U}} \sum_{i=1}^{K} p_i \quad \text{subject to} \quad \text{SINR}_i^{DL,CO}(\boldsymbol{U}, \boldsymbol{p}) \ge \gamma_i . \tag{5.8}$$

As for the MAC, this problem is always feasible in the absence of power constraints, which is a consequence of the triangular channel structure (see Section 2.3).

5.1.3. Duality

Suppose that both MAC and BC have the same sum power constraint. From Theorem 7 follows that certain SINR targets $\gamma_1 \dots \gamma_K$ can be achieved in the uplink if and only if the same targets can be achieved in the downlink. The optimization problems (5.5) and (5.8) have the same global optimum, which is achieved by the same uplink MMSE beamforming solution, but with different power allocations.

For the Gaussian channel studied here, this duality immediately carries over to a duality in terms of achievable rates. Hence, the MAC capacity region has a direct counterpart in the BC. This coincides with recent results [33, 56], where a similar duality was observed by using a different approach. It is still not clear, however, whether the "dirty paper" achievable region is actually the capacity region of the BC or not.

In the following, the theoretical framework of SINR balancing is used to solve the optimization problems (5.5) and (5.8). The general solution for this power minimization problem was already given in Chapter 4. An even more efficient approach will be derived in the next section, by exploiting the special triangular channel structure imposed by successive decoding and "dirty paper" precoding.

5.2. Rate Balancing under a Sum Power Constraint

Having shown the duality between the rate balancing problems (5.8) and (5.5), we can now focus on the multiple access channel, which has a less complicated analytical structure.

5.2.1. Joint Beamforming and Power Control via Back-Substitution

Consider the power minimization problem (5.5) with a decoding order $K \dots 1$. It was already shown in Section 2.2.2 that the global minimizer $(\boldsymbol{U}^{opt}, \boldsymbol{q}^{opt})$ fulfills all SINR constraints with equality, i.e.,

$$\mathrm{SINR}_i^{UL,SD}(\boldsymbol{u}_i^{opt}, q_1^{opt} \dots q_i^{opt}) = \gamma_i, \quad 1 \le i \le K \ . \tag{5.9}$$

It can be exploited that the solution of the power minimization problem is a special case of the more general SINR balancing problem (see discussion in Section 2.2.2). Theorem 17 states that for given $\boldsymbol{q}^{opt}$, the optimal beamforming matrix $\boldsymbol{U}^{opt}$ can be found directly by solving K decoupled optimization problems

$$\boldsymbol{u}_i^{opt} = \arg\max_{\boldsymbol{u}_i} \mathrm{SINR}_i^{UL,SD}(\boldsymbol{u}_i, q_1 \dots q_i), \quad 1 \le i \le K \ . \tag{5.10}$$

Now, we exploit that the interference of the first user is completely canceled out, thus

$$\mathrm{SINR}_1^{UL,SD}(\boldsymbol{u}_1, q_1) = q_1 |\boldsymbol{u}_1^H \boldsymbol{h}_1|^2 \ . \tag{5.11}$$

This provides a way to find a globally optimal beamforming solution directly, without the need of iterative beamforming and power adjustment, as it is required for coupled user (see Chapter 4). The strategy that maximizes (5.11) is the spatial matched filter $\boldsymbol{u}_1^{opt} = \boldsymbol{h}_1/\|\boldsymbol{h}_1\|_2$. With (5.2), the minimal transmission power q_1^{opt}, that is needed to achieve $\mathrm{SINR}_1^{UL,SD} = \gamma_1$ is given by

$$q_1^{opt} = \frac{\gamma_1}{(\|\boldsymbol{h}_1\|_2)^2} \ . \tag{5.12}$$

Note, that the transmission power (5.12) is optimal with respect to *all* users, because the functions $\mathrm{SINR}_2^{UL,SD}, \ldots \mathrm{SINR}_K^{UL,SD}$ are monotonically decreasing in q_1^{opt}.

With q_1^{opt}, the SINR of the 2nd user becomes

$$\mathrm{SINR}_2^{UL,SD}(\boldsymbol{u}_2, q_1, q_2) = \frac{q_2 |\boldsymbol{u}_2^H \boldsymbol{h}_2|^2}{\boldsymbol{u}_2^H \hat{\boldsymbol{Z}}_2(q_1^{opt}) \boldsymbol{u}_2}, \quad \text{with} \quad \hat{\boldsymbol{Z}}_2(q_1^{opt}) = q_1^{opt} \boldsymbol{h}_1 \boldsymbol{h}_1^H + \boldsymbol{I} \ . \tag{5.13}$$

This is maximized by the normalized MMSE solution

$$\boldsymbol{u}_2^{opt} = \frac{\hat{\boldsymbol{Z}}_2^{-1}(q_1^{opt}) \boldsymbol{h}_2}{\|\hat{\boldsymbol{Z}}_2^{-1}(q_1^{opt}) \boldsymbol{h}_2\|_2} \ . \tag{5.14}$$

Putting (5.14) in (5.13) leads to

$$\mathrm{SINR}_2^{UL,SD}(\boldsymbol{u}_2, q_1, q_2) = q_2 \, \boldsymbol{h}_2^H \hat{\boldsymbol{Z}}_2^{-1}(q_1^{opt}) \boldsymbol{h}_2 \ . \tag{5.15}$$

Hence, the minimal transmission power q_2^{opt} needed for the 2nd user to achieve an SINR level γ_2 is given by

$$q_2^{opt} = \frac{\gamma_2}{\boldsymbol{h}_2^H \hat{\boldsymbol{Z}}_2^{-1}(q_1^{opt}) \boldsymbol{h}_2} \ . \tag{5.16}$$

Using the same monotony argument as above, the solution (5.16) is optimal for all users in the sense that it causes the least interference. Continuing this strategy, all optimal beamformers $\boldsymbol{u}_1^{opt} \ldots \boldsymbol{u}_K^{opt}$ and uplink transmission powers $q_1^{opt} \ldots q_K^{opt}$ are found successively. The algorithm is summarized below: The beamforming matrix $\boldsymbol{U}^{opt} = [\boldsymbol{u}_1^{opt}, \ldots, \boldsymbol{u}_K^{opt}]$ yielded by Algorithm 5 is optimal for both, uplink and downlink. However, the same does not hold for the power allocation. Thus, it remains to find the optimal downlink power allocation $\boldsymbol{p}^{opt} = [p_1^{opt}, \ldots, p_K^{opt}]^T$, which fulfills $\mathrm{SINR}_i^{DL,CO}(\boldsymbol{U}^{opt}, \boldsymbol{p}^{opt}) = \gamma_i$, where $\mathrm{SINR}_i^{DL,CO}$ is defined as in (5.7).

It is important to note that a MAC decoding order $K \ldots 1$ corresponds to a BC pre-coding order $1 \ldots K$. Only then does the duality between both channels hold

Algorithm 5 Rate balancing for the multiple access channel, decoding order $K \dots 1$

1: **for** $i = 1$ to K **do**
2: $\quad \hat{\boldsymbol{Z}}_i(q_1^{opt}, \dots, q_{i-1}^{opt}) \Leftarrow \sum_{k=1}^{i-1} q_k^{opt} \boldsymbol{h}_k \boldsymbol{h}_k^H + \boldsymbol{I}$
3: $\quad \boldsymbol{u}_i^{opt} \Leftarrow \frac{\hat{\boldsymbol{Z}}_i^{-1} \boldsymbol{h}_i}{\|\hat{\boldsymbol{Z}}_i^{-1} \boldsymbol{h}_i\|_2}$
4: $\quad q_i^{opt} \Leftarrow \gamma_i / (\boldsymbol{h}_i^H \hat{\boldsymbol{Z}}_i^{-1} \boldsymbol{h}_i)$
5: **end for**

true. Under this assumption, the K^{th} user in both channels sees no interference, which implies that the same transmission power $p_K^{opt} = \gamma_K / (\|\boldsymbol{h}_K\|_2)^2$ is required to fulfill the target γ_K. Having found p_K^{opt}, all other power levels $p_{(K-1)}^{opt} \dots p_1^{opt}$ can be determined in descending order of their indices. This leads to Algorithm 6, which is summarized below:

Algorithm 6 Rate balancing for the broadcast channel, precoding order $1 \dots K$

1: optimal beamformers $\boldsymbol{U}^{opt}$ are obtained by Algorithm 5 with inverse decoding order $K \dots 1$
2: **for** $i = K$ to 1 **do**
3: $\quad p_i^{opt} \Leftarrow \frac{\gamma_i}{|\boldsymbol{u}_i^H \boldsymbol{h}_i|^2} \left(\sum_{k=i+1}^{K} p_k |\boldsymbol{u}_k^H \boldsymbol{h}_i|^2 + 1 \right)$
4: **end for**

5.2.2. Closed Form Solution for the 2-User Case

Now, a closed form solution is derived for $K = 2$. The solution balances individual targets γ_1 and γ_2 with minimal power consumption. The solution is derived for the MAC. From the duality result discussed in Section 5.1.3 it is known that each MAC optimizer also solves the equivalent BC problem.

Assume a decoding order $2, 1$. Thus, the first user sees no interference after demodulation. By adjusting the transmission power q_1, the following relative SINR value can be achieved:

$$\frac{\text{SINR}_1^{UL,SD}(\boldsymbol{u}_1, q_1)}{\gamma_1} = \frac{q_1 |\boldsymbol{u}_1^H \boldsymbol{h}_1|^2}{\gamma_1} . \tag{5.17}$$

The spatial matched filter $\boldsymbol{u}_1^{opt} = \boldsymbol{h}_1 / \|\boldsymbol{h}_1\|_2$ is optimal among all possible beamforming solutions, since it maximizes (5.17). Hence, a target threshold C_1 is achieved with minimal transmission power

$$q_1^{opt} = \frac{C_1 \gamma_1}{(\|\boldsymbol{h}_1\|_2)^2} . \tag{5.18}$$

Thus, the individual solution $\boldsymbol{u}_1^{opt}$ causes the least interference to all other users. In analogy to Section 5.2.1, it can be concluded that $\boldsymbol{u}_1^{opt}$ is globally optimal with respect to the joint optimization problem (5.5).

The second user is interfered by the first user, i.e.,

$$\frac{\mathrm{SINR}_2^{UL,SD}(\boldsymbol{u}_2, q_1, q_2)}{\gamma_2} = \frac{q_2|\boldsymbol{u}_2^H \boldsymbol{h}_2|^2}{\gamma_2(q_1|\boldsymbol{u}_2^H \boldsymbol{h}_1|^2 + 1)} \ . \tag{5.19}$$

The optimal beamformer is the MMSE solution

$$\boldsymbol{u}_2^{opt} = \frac{\left(q_1 \boldsymbol{h}_1 \boldsymbol{h}_1^H + \boldsymbol{I}\right)^{-1} \boldsymbol{h}_2}{\|\left(q_1 \boldsymbol{h}_1 \boldsymbol{h}_1^H + \boldsymbol{I}\right)^{-1} \boldsymbol{h}_2\|_2} \ . \tag{5.20}$$

Putting (5.20) in (5.19) and applying the Sherman-Morrison formula (see e.g. [46]), we have

$$\begin{aligned} \frac{\mathrm{SINR}_2^{UL,SD}(\boldsymbol{u}_2, q_1, q_2)}{\gamma_2} &= \frac{q_2 \boldsymbol{h}_2^H \left(q_1 \boldsymbol{h}_1 \boldsymbol{h}_1^H + \boldsymbol{I}\right)^{-1} \boldsymbol{h}_2}{\gamma_2} \\ &= \frac{q_2}{\gamma_2} \left(\boldsymbol{h}_2^H \boldsymbol{h}_2 - \frac{q_1 |\boldsymbol{h}_2^H \boldsymbol{h}_1|^2}{1 + q_1 \boldsymbol{h}_1^H \boldsymbol{h}_1} \right) \ . \end{aligned} \tag{5.21}$$

Assume that target thresholds C_1 and C_2 are given for (5.17) and (5.21), respectively. These targets can are jointly achieved with minimal transmission power q_1^{opt} and

$$q_2^{opt} = \frac{\gamma_2 C_2 (1 + C_1 \gamma_1)}{\boldsymbol{h}_2^H \boldsymbol{h}_2 (1 + C_1 \gamma_1) - C_1 \gamma_1 \frac{|\boldsymbol{h}_2^H \boldsymbol{h}_1|^2}{\boldsymbol{h}_1^H \boldsymbol{h}_1}} \ . \tag{5.22}$$

This can be verified by putting (5.18) in (5.21), setting (5.21) to C_2 and solving for q_2.

Now, assume that both users are balanced at the same level $C = C_1 = C_2$ and the transmission powers are constrained to fulfill $P_{\max} = q_1 + q_2$. Defining

$$\begin{aligned} a &\stackrel{\mathrm{def}}{=} \frac{\|\boldsymbol{h}_2\|^2}{\|\boldsymbol{h}_1\|^2} - \frac{|\boldsymbol{h}_2^H \boldsymbol{h}_1|^2}{\|\boldsymbol{h}_1\|^4} \ , \\ b &\stackrel{\mathrm{def}}{=} \frac{\|\boldsymbol{h}_2\|^2}{\|\boldsymbol{h}_1\|^2} + \frac{P_{\max} |\boldsymbol{h}_2^H \boldsymbol{h}_1|^2}{\|\boldsymbol{h}_1\|^2} - P_{\max} \|\boldsymbol{h}_2\|^2 \ , \end{aligned}$$

and combining (5.18) and (5.22), we obtain a unique positive solution

$$\begin{aligned} C = &\frac{-\gamma_1 b - \gamma_2}{2(\gamma_1^2 a + \gamma_1 \gamma_2)} \\ &+ \sqrt{\frac{(\gamma_1 b + \gamma_2)^2}{4(\gamma_1^2 a + \gamma_1 \gamma_2)^2} + \frac{P_{\max} \|\boldsymbol{h}_2\|^2}{(\gamma_1^2 a + \gamma_1 \gamma_2)}} \ . \end{aligned} \tag{5.23}$$

As discussed in Chapter 2, individual SINR targets γ_1, γ_2 can be fulfilled if and only if $C \geq 1$. With this additional constraint, (5.23) can be rewritten as an inequality that characterizes the achievable SINR region under a given sum power constraint $q_1 + q_2 \leq P_{\max}$ and a coding order $2, 1$. As shown before, this result immediately carries over to the problem of balancing data rates $\mathcal{R}_i = \log_2(1+\gamma_i)$ in both MAC and BC. By taking the convex hull of the regions resulting from both coding orders, an achievable rate region is found. This regions contains all rates that can be achieved by a combination of linear equalization and successive coding. The duality result of Chapter 2 implies that these rates can be achieved in both MAC and BC (see discussion in Section 5.1.3). Two examples are illustrated in Fig. 5.1.

Note, that the region can always be expanded by increasing the total transmission power. Thus, arbitrary rate tuples can be achieved in the absence of power constraints. This behavior differs from the one observed for the interference limited scenarios in Chapter 3 and Chapter 4.

5.2.3. Maximizing the Sum Rate

The uplink/downlink duality can be used to find a strategy that maximizes the downlink throughput (rate sum) under a given power constraint $\|\boldsymbol{p}\|_1 \leq P_{\max}$.

The maximal throughput of the downlink broadcast channel was characterized in [31], where it was shown that this point lies on the closure of the "Dirty Paper" region and can be achieved by a combination of decision feedback precoding and beamforming. The rate-sum

$$\mathcal{C}_{sum}^{\mathrm{DL}} = \max_{\substack{\boldsymbol{U} \\ \|\boldsymbol{p}\|_1 \leq P_{\max}}} \sum_{i=1}^{K} \mathcal{R}_i^{\mathrm{DL}} \tag{5.24}$$

is achieved by optimizing over all beamformers $\boldsymbol{U}$ and power allocations $\boldsymbol{p}$.

The optimization problem (5.24) has a complicated analytical structure. Fortunately, a solution can be found indirectly by exploiting the one-to-one monotonic relationship between $\mathcal{R}_i^{\mathrm{DL}}$ and $\mathrm{SINR}_i^{DL,CO}(\boldsymbol{U}, \boldsymbol{p})$. The optimum $\mathcal{C}_{sum}^{\mathrm{DL}}$ can be achieved by controlling the SINR levels (5.7) such that $\mathrm{SINR}_i^{DL,CO} = \tilde{\gamma}_i$ for the given power constraint. Here $\tilde{\gamma}_1 \ldots \tilde{\gamma}_K$ denote the unknown target thresholds that lead to the maximal throughput (5.24).

The duality theory states that the same targets $\tilde{\gamma}_1 \ldots \tilde{\gamma}_K$ are achievable for BC and MAC. By using a combination of beamforming and successive interference cancellation, we can achieve

$$\tilde{\gamma}_i = \mathrm{SINR}_i^{UL,CO} = \frac{q_i |\boldsymbol{u}_i^H \boldsymbol{h}_i|^2}{\boldsymbol{u}_i^H \boldsymbol{Z}_i(q_1, \ldots, q_{i-1}) \boldsymbol{u}_i}, \quad 1 \leq i \leq K \,. \tag{5.25}$$

In particular, $\tilde{\gamma}_1 \ldots \tilde{\gamma}_K$ also maximize the uplink rate sum $\mathcal{C}_{sum}^{\mathrm{UL}} = \mathcal{C}_{sum}^{\mathrm{DL}}$, which is

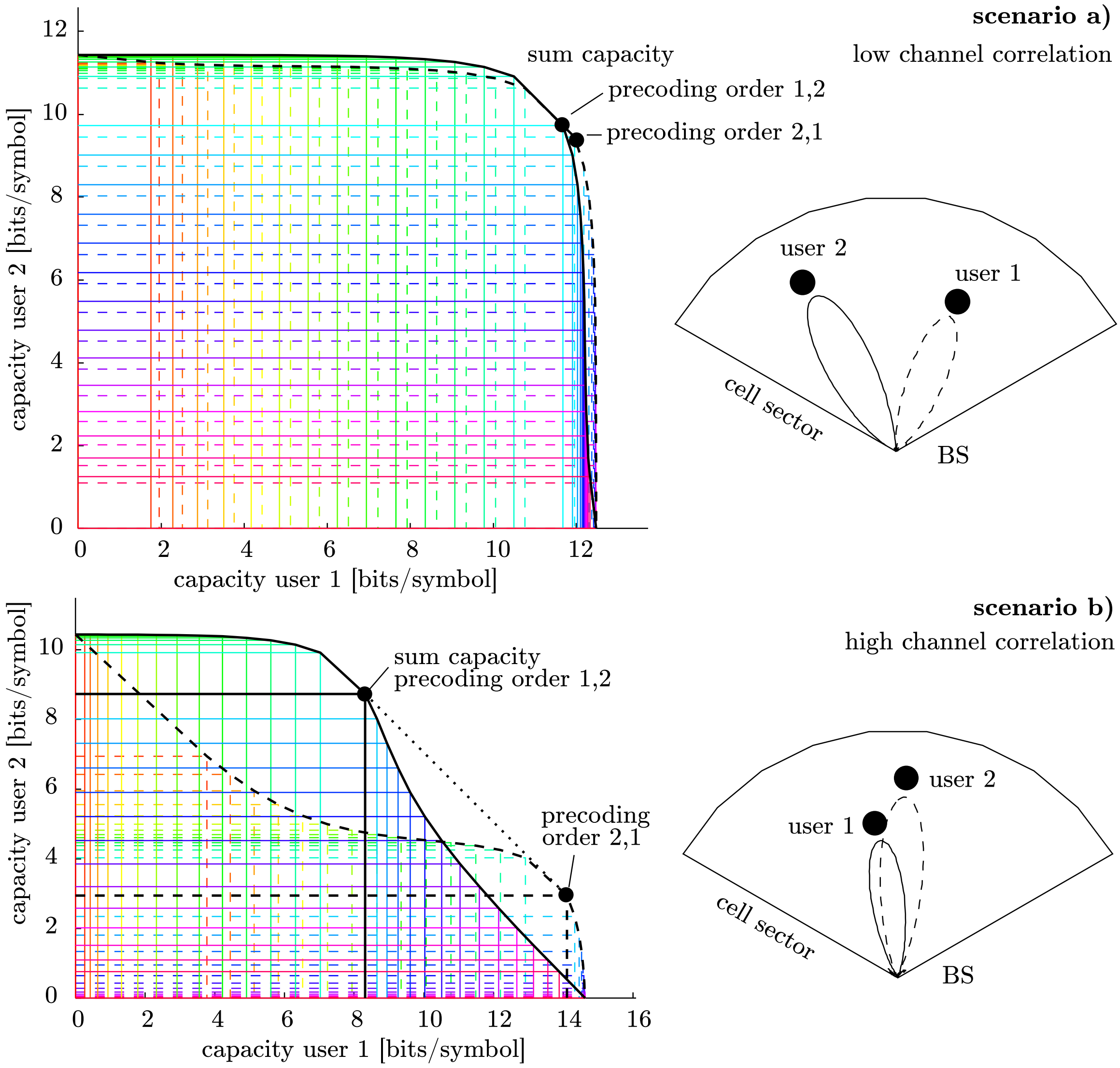

Figure 5.1.: "Dirty paper" achievable regions obtained by combined beamforming and precoding for non-causally known interference for a micro-cell cellular environment. In **scenario a)** interference is suppressed by the linear beamformer, thus the users are nearly decoupled, in which case precoding has only little impact. In **scenario b)**, linear spatial filtering is ineffective because of the small angular separation of the mobiles. In this case the impact of precoding is more pronounced. Within the "Dirty paper" region, the corresponding MAC regions for individual power constraints are depicted for each power pair.

given by

$$\mathcal{C}_{sum}^{\mathrm{UL}} = \max_{\substack{\boldsymbol{U} \\ \|\boldsymbol{q}\|_1 \le P_{\max}}} \sum_{i=1}^{K} \mathcal{R}_i^{\mathrm{UL}}$$

$$= \max_{\|\boldsymbol{q}\|_1 \le P_{\max}} \log_2 \Big| \boldsymbol{I} + \sum_{k=1}^{K} q_k \boldsymbol{h}_k \boldsymbol{h}_k^H \Big| . \tag{5.26}$$

The objective in (5.26) is concave in the transmission powers. The optimal power allocation $\boldsymbol{q}^{opt}$, with $\|\boldsymbol{q}^{opt}\|_1 = P_{\max}$, can be found, e.g. by using the interior point technique proposed in [57]. Knowing $\boldsymbol{q}^{opt}$, the optimal MAC spatial receivers are given by

$$\boldsymbol{u}_i^{opt} = \frac{\boldsymbol{Z}_i(q_1, \ldots, q_{i-1})^{-1} \boldsymbol{h}_i}{\|\boldsymbol{Z}_i(q_1, \ldots, q_{i-1})^{-1} \boldsymbol{h}_i\|_2} , \quad 1 \le i \le K . \tag{5.27}$$

Here, a coding order $K \ldots 1$ has been assumed. However, the sum capacity (5.26) does not depend on the coding order (cf. Fig. 5.1). Additional optimizers are found for other coding orders.

From the duality result in Section 2.4.4 we know that the solutions (5.27) are optimal for both uplink and downlink. Thus, it remains to find the optimal downlink power allocation $\boldsymbol{p}$ that achieves $\mathrm{SINR}_i^{DL,CO} = \tilde{\gamma}_i$. This can be done with Algorithm 6.

5.3. Discussion

In this chapter it was shown how the generic results from Sections 2-4 can be used to solve existing problems in communication theory. By studying the Shannon capacity of the multi-user channel, we can find theoretical limits and understand how to achieve those limits with practical schemes.

Considering Gaussian signaling and coding for known interference, the problem of controlling SINR levels is equivalent to the one of controlling data rates. By properly choosing target thresholds $\gamma_1 \ldots \gamma_K$, rate tuples within the capacity region of the Gaussian MAC can be achieved with the algorithm derived in Chapter 4. The duality result found in Chapter 2 implies that this strategy immediately carries over to the downlink. Thus, the MAC capacity region has a direct equivalence in the broadcast channel, where a combination of downlink beamforming and precoding for non-causally known interference is used. It is still unknown, however, whether this is the actual BC capacity region or not.

The throughput-wise optimal transmission strategy proposed in Section 5.2.3 achieves the capacity of a fully cooperating MIMO system under a worst case noise covariance. This follows from the results in [31, 58]. Hence, cooperation between transmitters (or receivers) need not always be beneficial. Under certain conditions, beamforming is the optimal strategy. This is an interesting aspect, which may influence the design of future multi-user MIMO communication systems.

The choice of the optimal coding order is still an open problem. Here, 'optimal' means that certain target rates are achieved with minimum total transmission power. The error propagation issue is neglected since perfect channel knowledge and optimal power control is assumed. Numerical simulations indicate that for the MAC it is almost always a good choice to decode the channels in decreasing order of their average path gains $\|\boldsymbol{h}_i\|_2$, $1 \leq i \leq K$. For the broadcast channel, the inverse order seems to be preferable.

6. Conclusions

This thesis provides the solution to the problem of spatial multiplexing for a multi-antenna system, if either the transmit antennas or the receive antennas are not allowed to cooperate and a sum power constraint is imposed. The solution proposed here is power-aware, in a sense that each channel is allocated only as much power as it needs to fulfill individual SINR requirements. This allows to trade-off capacities between the multiplexed channels and provides necessary and sufficient conditions for feasibility.

6.1. Summary and Discussion of the Main Results

- In Section 2.4.4 it is shown that there is a fundamental duality between the downlink point-to-multipoint channel and the uplink multipoint-to-point channel. This duality holds as long as either all receiver noise levels are equal or the crosstalk-matrix $\mathbf{\Psi}$ satisfies the symmetry condition in Theorem 7. If this is fulfilled, SINR targets are achievable in the downlink if and only if the same targets are achievable in the uplink under the same sum power constraint.

  This result is very useful in that many results known for the uplink immediately carry over to the downlink. For a longtime, very few results appeared for downlink processing due to the more complicated analytical structure. The uplink has a smoother structure, which allows for the design of efficient algorithms. This has been exploited in the Chapters 3, 4, and 5, where globally convergent algorithmic solutions have been derived.

- The problem of SIR balancing in the absence of noise [10, 43] has been solved in Chapter 3. This not only provides insight into the analytical structure of the general problem, but also yields a necessary and sufficient condition for the achievability of certain SINR targets in the high SNR regime.

  It is proven that the global optimum can be achieved by an iterative strategy, as conjectured in [43]. This is perhaps surprising, since the original problem consists of minimizing an ℓ_∞ norm objective function that is highly non-smooth and non-differentiable. The other algorithm proposed in [10], which is based on a smoother ℓ_1-norm objective, however, is in general not globally convergent. This could be shown by providing necessary and sufficient conditions for optimality along with a numerical counter-example. An exception is the 2-user scenario for which ℓ_1-norm minimization and ℓ_∞-norm are indeed equivalent.

Finally, it is shown how the algorithm proposed in [10] should be modified in order to solve the original SIR balancing problem. This new algorithm is presented in Section 3.3.

- The general problem of controlling SINR levels under a sum power constraint is solved in Chapter 4. A simple iterative solution is proposed, which rapidly converges to the global optimum. The first key step in the convergence analysis is the characterization of the iteration sequence in Section 4.1.4. It turns out that each local minimum is also a global one. Monotony and global convergence are proven in Section 18. The algorithm, which is summarized in Section 4.2, can be applied to systems with both perfect and covariance channel information.

  Important aspects of the solution are:

  - A necessary and sufficient condition for the achievability of SINR targets under a given sum power constraint is provided. The targets are achievable if and only if the global optimum of the iterative solution is greater than one. This plays an important role for the resource management. Only if this condition is fulfilled, the power minimization problem studied in [36–42] has a solution.
  - A modified version of the iterative technique is proposed, which minimizes the total power while satisfying SINR constraints (see Section 4.3). In combination with the necessary and sufficient condition for feasibility described above, this provides a complete solution of the problem studied in [36–42]. Minimizing the total power is preferable from an operator's perspective, since it maximizes the number of users that can be accommodated per cell.

- A power aware rate balancing strategy for Gaussian multiuser channels with unilateral antenna cooperation is proposed in Chapter 5. The algorithm exploits the triangular channel structure imposed by decision feedback decoding/precoding. For this specific case, all users are uncoupled and the SINR control problem can be solved very efficiently by back-substitution. As compared to the algorithm proposed in Chapter 4, the solution is not found iteratively, but can be computed directly. By properly choosing targets $\gamma_1 \dots \gamma_K$, it is possible to achieve arbitrary rate tuples within the MAC capacity region. With the above duality result, this strategy immediately carries over to the BC, where rates within the "dirty paper" achievable region can be achieved.

Whether or not this achievable region is the actual BC capacity region remains to be shown.

- Finally, closed-form solutions for the 2-user case are derived for all scenarios under consideration.

6.2. Future Work

- The generic solution for power aware spatial multiplexing presented in Chapter 4 can be applied to related vector systems with unilateral cooperation, e.g.,
  - synchronous CDMA systems with random sequences [18]
  - wireline communication systems such as digital subscriber lines (DSL), where co-channel interference is caused by electromagnetic coupling and cooperation is only possible at one side [59].
  - Bell Laboratory Layered Space-Time (BLAST) architecture [45] with additional power control at the transmitter
- While multiplexing aims at optimizing throughput, diversity is often required in oder to make the transmission more robust. Hence, an optimal trade-off between multiplexing and diversity is desirable (see, e.g., the work in [60–62] and the reference therein). The technique proposed here can be seen as a step in this direction, in a sense that it allows to smoothly trade-off throughput against robustness by varying the noise parameter.
- If the base station only has covariance channel knowledge, the information theoretical capacity may be achieved by transmitting several independent data streams per user. In this case, the beamforming strategy proposed here is suboptimal. The optimality range depends on the channel properties as well as the SNR, as was recently shown for a single user scenario in [63, 64]. Optimal balancing strategies for multiuser scenarios are still unknown.
- Similarly, the general problem of controlling data rates in a multiuser MIMO channel with minimum total transmission power is still open. A partial result is the iterative waterfilling solution [65], which maximizes the sum rate under independent power constraints.
- Multiuser diversity can be exploited by a scheduler, which transmits only to the user with the best channel at any time. This is optimal in an information theoretical sense as long as the base station is equipped with a single antenna [66, 67]. When several antennas are employed, however, the maximal throughput may be achieved by simultaneously multiplexing severals users in space

[30]. The algorithm proposed in Section 4.2 provides a single measure for the quality of the instantaneous spatially multiplexed channel. This could lead to the development of new space-time scheduling strategies.

Proofs

P.1. Proof of Lemma 11

Substituting $[\boldsymbol{z}]_k \stackrel{\text{def}}{=} [\boldsymbol{x}]_k \cdot [\boldsymbol{c}]_k,\ 1 \leq k \leq K$, we have

$$\max_{\boldsymbol{x}} \frac{\boldsymbol{x}^T \boldsymbol{b}}{\boldsymbol{x}^T \boldsymbol{c}} = \max_{\boldsymbol{z}} \frac{\sum\limits_{k=1}^{K} [\boldsymbol{z}]_k \frac{[\boldsymbol{b}]_k}{[\boldsymbol{c}]_k}}{\sum\limits_{k=1}^{K} [\boldsymbol{z}]_k} . \tag{P.1}$$

Observe that (P.1) is invariant with respect to a scaling of $\boldsymbol{z}$, hence the maximization can be restricted to the set $\{\boldsymbol{z} :\ \|\boldsymbol{z}\|_1 = 1\}$, i.e.,

$$\max_{\boldsymbol{x}} \frac{\boldsymbol{x}^T \boldsymbol{b}}{\boldsymbol{x}^T \boldsymbol{c}} = \max_{\|\boldsymbol{z}\|_1 = 1} \sum_{k=1}^{K} [\boldsymbol{z}]_k \frac{[\boldsymbol{b}]_k}{[\boldsymbol{c}]_k} .$$

Next, we have

$$\begin{aligned} \sum_{k=1}^{K} [\boldsymbol{z}]_k \frac{[\boldsymbol{b}]_k}{[\boldsymbol{c}]_k} &\leq \max_{1 \leq l \leq K} \frac{[\boldsymbol{b}]_l}{[\boldsymbol{c}]_l} \sum_{k=1}^{K} [\boldsymbol{z}]_k \\ &= \max_{1 \leq l \leq K} \frac{[\boldsymbol{b}]_l}{[\boldsymbol{c}]_l} . \end{aligned} \tag{P.2}$$

Denote by k_0 the index that fulfills

$$\frac{[\boldsymbol{b}]_{k_0}}{[\boldsymbol{c}]_{k_0}} = \max_{1 \leq k \leq K} \frac{[\boldsymbol{b}]_k}{[\boldsymbol{c}]_k} .$$

Now, we use $\tilde{\boldsymbol{z}}$ with

$$[\tilde{\boldsymbol{z}}]_k = \begin{cases} 1 & k = k_0 \\ 0\ , & k \neq k_0 \end{cases} .$$

With $\tilde{\boldsymbol{z}}$ the inequality (P.2) is always satisfied with equality, hence (3.28) is fulfilled. Relation (3.29) can be proven in the same way, by replacing the max operator by min.

P.2. Proof of Lemma 12

For arbitrary $\boldsymbol{U}$ and $\boldsymbol{p} > 0$ we have

$$\begin{aligned} F_1(\boldsymbol{U},\boldsymbol{p}) &\geq \frac{1}{K}\frac{\gamma_i}{\mathrm{SIR}_i^{\mathrm{DL}}(\boldsymbol{U},\boldsymbol{p})}\;, \quad 1 \leq i \leq K, \\ &= \frac{\gamma_i}{Kp_i}\sum_{\substack{k=1\\k\neq i}}^{K} p_k \boldsymbol{u}_k^H \boldsymbol{R}_i \boldsymbol{u}_k > 0\;,\;\; 1 \leq i \leq K\;. \end{aligned}$$

For fixed $p_k,\ k \neq i$, we have

$$\lim_{p_i \to 0} F_1(\boldsymbol{U},\boldsymbol{p}) = +\infty\;, \quad 1 \leq i \leq K\;.$$

Thus, there exists a component-wise positive optimizer $\tilde{\boldsymbol{p}} > 0$ with $\|\tilde{\boldsymbol{p}}\|_1 = 1$ such that

$$\min_{\boldsymbol{p}:\|\tilde{\boldsymbol{p}}\|_1=1} F_1(\boldsymbol{U},\boldsymbol{p}) = \inf_{\boldsymbol{p}} F_1(\boldsymbol{U},\boldsymbol{p}) = F_1(\boldsymbol{U},\tilde{\boldsymbol{p}})\;.$$

Hence, the function F_1, as defined in (3.30), is infinitely often differentiable with respect to $\boldsymbol{p}$. The first partial derivative is given by

$$\frac{\partial F_1(\boldsymbol{U},\boldsymbol{p})}{\partial p_l} = \frac{1}{K}\boldsymbol{u}_l^H \boldsymbol{G}_l(\boldsymbol{p})\boldsymbol{u}_l - \frac{1}{Kp_l^2}\sum_{\substack{k=1\\k\neq l}}^{K} p_k \boldsymbol{u}_k^H \gamma_l \boldsymbol{R}_l \boldsymbol{u}_k \quad 1 \leq l \leq K\;. \tag{P.3}$$

Setting (P.3) to zero finally leads to (3.34).

P.3. Proof of Lemma 13

From Lemma 11 we know that

$$\hat{\lambda}_n(\boldsymbol{U},\boldsymbol{q}_{\mathrm{ext}}) = \max_{1\leq k\leq K+1} \frac{\boldsymbol{e}_k^T \boldsymbol{\Lambda}(\boldsymbol{U})\boldsymbol{q}_{\mathrm{ext}}}{\boldsymbol{e}_k^T \boldsymbol{q}_{\mathrm{ext}}}\;,$$

where $\boldsymbol{e}_k$ is defined as a vector whose k^{th} component equals one, while all other components are zero. The same relation can be formulated for the minimum.

With $\boldsymbol{q}_{\mathrm{ext}} = \binom{\boldsymbol{q}}{1}$ we have

$$\max_{1\leq k\leq K} \frac{\boldsymbol{e}_k^T \boldsymbol{\Lambda}(\boldsymbol{U})\boldsymbol{q}_{\mathrm{ext}}}{\boldsymbol{e}_k^T \boldsymbol{q}_{\mathrm{ext}}} = \max_{1\leq k\leq K} \frac{\gamma_k}{\mathrm{SINR}_k^{\mathrm{UL}}(\boldsymbol{u}_k,\boldsymbol{q})}\;. \tag{P.4}$$

We also have

$$\frac{\boldsymbol{e}_{K+1}^T \boldsymbol{\Lambda}(\boldsymbol{U})\boldsymbol{q}_{\mathrm{ext}}}{\boldsymbol{e}_{K+1}^T \boldsymbol{q}_{\mathrm{ext}}} = \frac{1}{P_{\max}}\Big(\boldsymbol{1}_K^T \boldsymbol{D}\boldsymbol{\Psi}^T(\boldsymbol{U})\boldsymbol{q} + \boldsymbol{1}_K^T \boldsymbol{D}\boldsymbol{1}_K\Big)\;. \tag{P.5}$$

Using

$$\mathbf{1}_K^T \boldsymbol{D}\boldsymbol{\Psi}^T(\boldsymbol{U})\boldsymbol{q} = \sum_{i=1}^{K} q_i \frac{\gamma_i}{\mathrm{SIR}_i^{\mathrm{UL}}(\boldsymbol{u}_i, \boldsymbol{q})}$$

and

$$\mathbf{1}_K^T \boldsymbol{D}\mathbf{1}_K = \sum_{i=1}^{K} q_i \frac{\gamma_i}{\mathrm{SNR}_i^{\mathrm{UL}}(\boldsymbol{u}_i, q_i)} ,$$

where $\mathrm{SNR}_i^{\mathrm{UL}}(\boldsymbol{u}_i, q_i) \stackrel{\text{def}}{=} q_i \boldsymbol{u}_i^H \boldsymbol{R}_i \boldsymbol{u}_i / \sigma_i^2$, we can conclude that

$$\begin{aligned}\frac{\boldsymbol{e}_{K+1}^T \boldsymbol{\Lambda}(\boldsymbol{U})\boldsymbol{q}_{\mathrm{ext}}}{\boldsymbol{e}_{K+1}^T \boldsymbol{q}_{\mathrm{ext}}} &= \frac{1}{P_{\max}} \sum_{i=1}^{K} q_i \gamma_i \left(\frac{1}{\mathrm{SIR}_i^{\mathrm{UL}}(\boldsymbol{u}_i, \boldsymbol{q})} + \frac{1}{\mathrm{SNR}_i^{\mathrm{UL}}(\boldsymbol{u}_i, q_i)} \right) \\ &= \frac{1}{P_{\max}} \sum_{i=1}^{K} q_i \frac{\gamma_i}{\mathrm{SINR}_i^{\mathrm{UL}}(\boldsymbol{u}_i, \boldsymbol{q})} . \end{aligned} \tag{P.6}$$

Now we can use

$$\begin{aligned}\frac{1}{P_{\max}} \sum_{i=1}^{K} q_i \frac{\gamma_i}{\mathrm{SINR}_i^{\mathrm{UL}}(\boldsymbol{u}_i, \boldsymbol{q})} &\leq \left(\max_{1 \leq k \leq K} \frac{\gamma_k}{\mathrm{SINR}_k^{\mathrm{UL}}(\boldsymbol{u}_k, \boldsymbol{q})} \right) \frac{1}{P_{\max}} \sum_{i=1}^{K} q_i \\ &= \max_{1 \leq k \leq K} \frac{\gamma_k}{\mathrm{SINR}_k^{\mathrm{UL}}(\boldsymbol{u}_k, \boldsymbol{q})} , \end{aligned} \tag{P.7}$$

which shows that (P.5) is never greater than (P.4), i.e.,

$$\hat{\lambda}_n(\boldsymbol{U}, \boldsymbol{q}_{\mathrm{ext}}) = \max_{1 \leq k \leq K+1} \frac{\boldsymbol{e}_k^T \boldsymbol{\Lambda}(\boldsymbol{U})\boldsymbol{q}_{\mathrm{ext}}}{\boldsymbol{e}_k^T \boldsymbol{q}_{\mathrm{ext}}} = \max_{1 \leq k \leq K} \frac{\boldsymbol{e}_k^T \boldsymbol{\Lambda}(\boldsymbol{U})\boldsymbol{q}_{\mathrm{ext}}}{\boldsymbol{e}_k^T \boldsymbol{q}_{\mathrm{ext}}} .$$

P.4. Proof of Theorem 1

For any $\nu > 0$ and noise variances $\sigma_i^2 > 0$, $1 \leq i \leq K$, we have

$$\mathrm{SINR}_i^{\mathrm{UL}}(\tilde{\boldsymbol{u}}_i, \nu\tilde{\boldsymbol{q}}, \sigma_i^2) \geq \mathrm{SINR}_i^{\mathrm{UL}}\big(\tilde{\boldsymbol{u}}_i, \nu\tilde{\boldsymbol{q}}, \max_{1 \leq k \leq K} \sigma_k^2\big), \quad 1 \leq i \leq K. \tag{P.8}$$

The power allocation $\tilde{\boldsymbol{q}} > 0$ solves (2.17), i.e., $\mathrm{SINR}_i^{\mathrm{UL}}(\tilde{\boldsymbol{u}}_i, \tilde{\boldsymbol{q}}, \tilde{\sigma}_i^2) \geq \gamma_i$. This implies

$$\mathrm{SINR}_i^{\mathrm{UL}}\Big(\tilde{\boldsymbol{u}}_i, \tilde{\boldsymbol{q}}, \frac{\min_{1 \leq k \leq K} \tilde{\sigma}_k^2}{2}\Big) > \gamma_i, \quad 1 \leq i \leq K . \tag{P.9}$$

From (P.8) and (P.9) it can be concluded, that $\tilde{\boldsymbol{q}}$ can always be scaled by a factor

$$\nu_0 = 2 \cdot \frac{\max_{1 \leq k \leq K} \ \sigma_k^2}{\min_{1 \leq k \leq K} \ \tilde{\sigma}_k^2}$$

such that

$$\begin{aligned}\mathrm{SINR}_i^{\mathrm{UL}}(\tilde{\boldsymbol{u}}_i, \nu_0\tilde{\boldsymbol{q}}, \sigma_i^2) &\geq \mathrm{SINR}_i^{\mathrm{UL}}(\tilde{\boldsymbol{u}}_i, \nu_0\tilde{\boldsymbol{q}}, \max_{1\leq k\leq K} \sigma_k^2)\\ &= \mathrm{SINR}_i^{\mathrm{UL}}(\tilde{\boldsymbol{u}}_i, \tilde{\boldsymbol{q}}, \frac{\max_{1\leq k\leq K}\sigma_k^2}{\nu_0})\\ &= \mathrm{SINR}_i^{\mathrm{UL}}\Big(\tilde{\boldsymbol{u}}_i, \tilde{\boldsymbol{q}}, \frac{\min_{1\leq k\leq K}\tilde{\sigma}_k^2}{2}\Big) > \gamma_i, \quad 1 \leq i \leq K \ ,\end{aligned}$$

holds for arbitrary noise powers $\sigma_i^2 > 0$.

P.5. Proof of Theorem 2

Define $\tilde{\boldsymbol{\Psi}} \overset{\text{def}}{=} \boldsymbol{\Psi}(\tilde{\boldsymbol{U}})$. Assume that $\lambda_{\max}(\boldsymbol{D}\tilde{\boldsymbol{\Psi}}^T) < 1$ and therefore $\rho(\boldsymbol{D}\tilde{\boldsymbol{\Psi}}^T) < 1$ (see Lemma 3). This implies [46, p. 618]

$$\big(\boldsymbol{I} - \boldsymbol{D}\tilde{\boldsymbol{\Psi}}^T\big)^{-1} = \sum_{r=0}^{\infty} (\boldsymbol{D}\tilde{\boldsymbol{\Psi}}^T)^r \ . \tag{P.10}$$

All terms of the Neuman series (P.10) are non-negative, thus for any $\boldsymbol{\sigma} > 0$ the vector $\tilde{\boldsymbol{q}} = (\boldsymbol{I} - \boldsymbol{D}\tilde{\boldsymbol{\Psi}}^T)^{-1}\boldsymbol{D}\boldsymbol{\sigma}$ is component-wise positive. With the results of Section 2.2.2 it can be concluded that $\tilde{\boldsymbol{q}}$ is an optimizer of the power minimization problem (2.17), which is therefore feasible.

To prove the reverse direction, assume that (2.17) is feasible. Thus, there exists a positive solution $\tilde{\boldsymbol{q}} > 0$ for any $\boldsymbol{\sigma} > 0$. It was shown in Section 2.2.2 that this solution fulfills

$$\boldsymbol{\Phi}\tilde{\boldsymbol{q}} = \boldsymbol{z} \ , \quad \text{where } \boldsymbol{\Phi} \overset{\text{def}}{=} \big(\boldsymbol{I} - \boldsymbol{D}\tilde{\boldsymbol{\Psi}}^T\big) \text{ and } \boldsymbol{z} \overset{\text{def}}{=} \boldsymbol{D}\boldsymbol{\sigma}. \tag{P.11}$$

Now, it will be shown that $\boldsymbol{\Phi}$ is regular. Observe that each $\boldsymbol{z}$ lies in the range of $\boldsymbol{\Phi}$, i.e., $\boldsymbol{z} \in \boldsymbol{\Phi}(\mathbb{R}_+^K)$. The operator $\boldsymbol{\Phi}$ is linear and continuous, thus the range $\boldsymbol{\Phi}(\mathbb{R}_+^K)$ is a closed subspace of $\mathbb{R}_+^K$. Let $\boldsymbol{e}_k$, $1 \leq k \leq K$, be non-negative orthogonal vectors spanning $\mathbb{R}_+^K$. The Cauchy sequences

$$\boldsymbol{z}_k^{(n)} = \boldsymbol{e}_k + \frac{1}{n}\boldsymbol{1}_K, \quad 1 \leq k \leq K$$

always have strictly positive components, which follows from $[\boldsymbol{z}_k^{(n)}]_l \geq 1/n > 0$, $1 \leq l \leq K$. Thus, for each $\boldsymbol{z}_k^{(n)}$ there exists a $\tilde{\boldsymbol{q}}$ such that (P.11) is fulfilled. Consequently, each $\boldsymbol{z}_k^{(n)}$ lies in the range of $\boldsymbol{\Phi}$. With

$$\lim_{n\to\infty} \|\boldsymbol{z}_k^{(n)} - \boldsymbol{e}_k\|_2^2 = \lim_{n\to\infty} \sum_{l=1}^{K} \frac{1}{n^2} = 0, \quad 1 \leq k \leq K \ ,$$

it can be concluded that $\boldsymbol{e}_k \in \boldsymbol{\Phi}(\mathbb{R}_+^K)$. Consequently, the operator $\boldsymbol{\Phi}$ maps $\mathbb{R}_+^K$ on $\mathbb{R}_+^K$. It follows from Banach's homomorphism theorem that $\boldsymbol{\Phi}$ is regular.

It remains to show that the assumption of feasibility implies $\rho(\boldsymbol{D}\tilde{\boldsymbol{\Psi}}^T) < 1$. It is known from Theorem 1 that the power minimization problem (2.17) has a strictly positive solution for any noise vector $\boldsymbol{\sigma} \in \mathbb{R}_+^K$ with $[\boldsymbol{\sigma}]_l > 0,\ l = 1, \ldots, K$. Considering special noise vectors $\boldsymbol{\sigma}_k(\alpha)$ with

$$[\boldsymbol{\sigma}_k(\alpha)]_l = \begin{cases} 1, & l = k \\ \alpha, & l \neq k \end{cases}, \quad 1 \leq k, l \leq K \;, \quad \alpha > 0$$

it can be concluded that the power vectors $\boldsymbol{q}_k = \lim\limits_{\alpha \to 0} \boldsymbol{\Phi}^{-1}\boldsymbol{D}\boldsymbol{\sigma}_k(\alpha)$ are strictly positive, i.e., $[\boldsymbol{q}_k]_l > 0,\ l, k = 1, \ldots, K$. This implies that each component of $\boldsymbol{\Phi}^{-1}$ is non-negative.

Next, consider noise vectors $\mathbf{1}_K$ and $\boldsymbol{\sigma}$, where $\|\boldsymbol{\sigma}\|_1 \leq 1$. Since $\boldsymbol{\Phi}^{-1}$ is non-negative, we have

$$[\boldsymbol{\Phi}^{-1}\boldsymbol{D}\boldsymbol{\sigma}]_m \leq [\boldsymbol{\Phi}^{-1}\boldsymbol{D}\mathbf{1}_K]_m, \quad 1 \leq m \leq K \;. \tag{P.12}$$

Using these noise vectors we can define sequences

$$\begin{aligned} \boldsymbol{q}^{(k+1)} &= \boldsymbol{D}\boldsymbol{\sigma} + (\boldsymbol{D}\tilde{\boldsymbol{\Psi}}^T)\boldsymbol{q}^{(k)} \;, \quad \boldsymbol{q}^{(0)} = \boldsymbol{D}\boldsymbol{\sigma}, \\ \boldsymbol{q}_1^{(k+1)} &= \boldsymbol{D}\mathbf{1}_K + (\boldsymbol{D}\tilde{\boldsymbol{\Psi}}^T)\boldsymbol{q}_1^{(k)} \;, \quad \boldsymbol{q}_1^{(0)} = \boldsymbol{D}\mathbf{1}_K \;. \end{aligned}$$

Hence,

$$\begin{aligned} \boldsymbol{q}^{(k+1)} &= \sum_{r=0}^{k+1} (\boldsymbol{D}\tilde{\boldsymbol{\Psi}}^T)^r \boldsymbol{D}\boldsymbol{\sigma} \;, \\ \boldsymbol{q}_1^{(k+1)} &= \sum_{r=0}^{k+1} (\boldsymbol{D}\tilde{\boldsymbol{\Psi}}^T)^r \boldsymbol{D}\mathbf{1}_K \;. \end{aligned}$$

Since the components of $\boldsymbol{D}\tilde{\boldsymbol{\Psi}}^T$ are non-negative, we have

$$[\boldsymbol{q}^{(k+1)}]_l \geq [\boldsymbol{q}^{(k)}]_l \;, \quad 1 \leq l \leq K \;.$$

That is, the l^{th} component of $\boldsymbol{q}^{(k+1)}$ is monotonically increasing in k. The same holds for $\boldsymbol{q}_1^{(k+1)}$. Using (P.10) we have

$$\boldsymbol{q}^{(k+1)} = (\boldsymbol{I} - \boldsymbol{D}\tilde{\boldsymbol{\Psi}}^T)^{-1}\boldsymbol{b}^{(k)} \;,$$

where $\boldsymbol{b}^{(k)} \stackrel{\text{def}}{=} (\boldsymbol{I} - (\boldsymbol{D}\tilde{\boldsymbol{\Psi}}^T)^{k+2})\boldsymbol{D}\boldsymbol{\sigma}$. The components of $(\boldsymbol{D}\tilde{\boldsymbol{\Psi}}^T)^{k+1}$ are non-negative, thus $[\boldsymbol{b}^{(k)}]_l \leq [\boldsymbol{D}\boldsymbol{\sigma}]_l$ for $1 \leq l \leq K$. Since $\boldsymbol{\Phi}^{-1}$ has been shown to be non-negative, it follows

$$[\boldsymbol{q}^{(k+1)}]_l = [\boldsymbol{\Phi}^{-1}\boldsymbol{b}^{(k)}]_l \leq [\boldsymbol{\Phi}^{-1}\boldsymbol{D}\boldsymbol{\sigma}]_l \;, \quad 1 \leq l \leq K \;. \tag{P.13}$$

Combining (P.12) and (P.13), it can be concluded that for any $\boldsymbol{\sigma}$ with $\|\boldsymbol{\sigma}\|_1 \leq 1$ we have

$$[\boldsymbol{q}^{(k+1)}]_l \leq [(\boldsymbol{I} - \boldsymbol{D}\tilde{\boldsymbol{\Psi}}^T)^{-1}\boldsymbol{D}\boldsymbol{1}_K]_l \ , \quad 1 \leq l \leq K \ . \tag{P.14}$$

Now, it is known form Lemma 3 that $\boldsymbol{D}\tilde{\boldsymbol{\Psi}}^T$ can be decomposed as follows:

$$\boldsymbol{D}\tilde{\boldsymbol{\Psi}}^T\boldsymbol{q}_* = \lambda^*_{\max}\boldsymbol{q}_* = \rho(\boldsymbol{D}\tilde{\boldsymbol{\Psi}}^T)\boldsymbol{q}_* \ , \tag{P.15}$$

where $\lambda^*_{\max}$ is the maximal eigenvalue of $\boldsymbol{D}\tilde{\boldsymbol{\Psi}}^T$ equaling the spectral radius $\rho(\boldsymbol{D}\tilde{\boldsymbol{\Psi}}^T)$. The associated non-negative eigenvector $\boldsymbol{q}^*$ can be scaled such that $\boldsymbol{q}^* \leq 1$. Now consider a series

$$\boldsymbol{q}_*^{(k+1)} = \boldsymbol{q}_* + \boldsymbol{D}\tilde{\boldsymbol{\Psi}}^T\boldsymbol{q}_*^{(k)} \ , \quad \boldsymbol{q}_*^{(0)} = \boldsymbol{q}_* \ . \tag{P.16}$$

Defining $\rho \overset{\text{def}}{=} \rho(\boldsymbol{D}\tilde{\boldsymbol{\Psi}}^T)$ and using (P.15), the series (P.16) can be expressed as

$$\boldsymbol{q}_*^{(k)} = \sum_{r=0}^{k} \rho^r \boldsymbol{q}_* = \begin{cases} \frac{1-\rho^{k+1}}{1-\rho}\boldsymbol{q}_* \ , & \rho \neq 1 \\ (k+1)\boldsymbol{q}_* \ , & \rho = 1 \end{cases} \ .$$

The case $\rho = 1$ can be ruled out since $\boldsymbol{I} - \boldsymbol{D}\tilde{\boldsymbol{\Psi}}^T$ has been shown to be regular. For $\rho > 1$, the relation (P.14) implies

$$\frac{\rho^{k+1} - 1}{\rho - 1}[\boldsymbol{q}^*]_l \leq [(\boldsymbol{I} - \boldsymbol{D}\tilde{\boldsymbol{\Psi}}^T)^{-1}\boldsymbol{D}\boldsymbol{1}_K]_l \ . \tag{P.17}$$

There is at least one l for which $[\boldsymbol{q}^*]_l \neq 0$, thus relation (P.17) cannot hold for all k and $\rho > 1$ (the left side tends to infinity for $k \to \infty$ and the right side does not depend on k). This leaves $\rho < 1$. From Lemma 3 we know that this is equivalent to $\lambda_{\max}(\boldsymbol{D}\tilde{\boldsymbol{\Psi}}^T) < 1$.

P.6. Proof of Theorem 10

Assume that $\bar{\boldsymbol{U}}$ solves the eigenvalue minimization problem (3.7). This implies

$$\begin{aligned}
\max_{\boldsymbol{x}>0} \frac{\boldsymbol{x}^T\boldsymbol{D}\boldsymbol{\Psi}^T(\boldsymbol{U})\bar{\boldsymbol{q}}}{\boldsymbol{x}^T\bar{\boldsymbol{q}}} &\geq \min_{\boldsymbol{y}>0}\max_{\boldsymbol{x}>0} \frac{\boldsymbol{x}^T\boldsymbol{D}\boldsymbol{\Psi}^T(\boldsymbol{U})\boldsymbol{y}}{\boldsymbol{x}^T\boldsymbol{y}} \\
&= \lambda_{\max}\big(\boldsymbol{D}\boldsymbol{\Psi}^T(\boldsymbol{U})\big) \qquad \leftarrow \text{Eq. (3.10)} \\
&\geq \lambda_{\max}\big(\boldsymbol{D}\boldsymbol{\Psi}^T(\bar{\boldsymbol{U}})\big) \\
&= \frac{\boldsymbol{z}^T\boldsymbol{D}\boldsymbol{\Psi}^T(\bar{\boldsymbol{U}})\bar{\boldsymbol{q}}}{\boldsymbol{z}^T\bar{\boldsymbol{q}}} \qquad \leftarrow \text{Eq. (3.18)}
\end{aligned}$$

for any $\boldsymbol{U}$ and $\boldsymbol{z} > 0$. Thus,

$$\min_{\boldsymbol{U}}\max_{\boldsymbol{x}>0} \frac{\boldsymbol{x}^T\boldsymbol{D}\boldsymbol{\Psi}^T(\boldsymbol{U})\bar{\boldsymbol{q}}}{\boldsymbol{x}^T\bar{\boldsymbol{q}}} \geq \frac{\boldsymbol{z}^T\boldsymbol{D}\boldsymbol{\Psi}^T(\bar{\boldsymbol{U}})\bar{\boldsymbol{q}}}{\boldsymbol{z}^T\bar{\boldsymbol{q}}} \ .$$

There always exists an optimizer $\boldsymbol{x}_0 > 0$ such that

$$\min_{\boldsymbol{U}} \frac{\boldsymbol{x}_0^T \boldsymbol{D}\boldsymbol{\Psi}^T(\boldsymbol{U})\bar{\boldsymbol{q}}}{\boldsymbol{x}_0^T \bar{\boldsymbol{q}}} \geq \frac{\boldsymbol{x}_0^T \boldsymbol{D}\boldsymbol{\Psi}^T(\bar{\boldsymbol{U}})\bar{\boldsymbol{q}}}{\boldsymbol{x}_0^T \bar{\boldsymbol{q}}} \ .$$

This inequality can only be fulfilled with equality. Moreover, it can be observed from (3.15) that the minimization with respect to $\boldsymbol{U}$ is independent of $\boldsymbol{x}_0$. Thus, for all $\boldsymbol{x} > 0$ and $\boldsymbol{U}$ we have

$$\min_{\boldsymbol{U}} \frac{\boldsymbol{x}^T \boldsymbol{D}\boldsymbol{\Psi}^T(\boldsymbol{U})\bar{\boldsymbol{q}}}{\boldsymbol{x}_0^T \bar{\boldsymbol{q}}} = \frac{\boldsymbol{x}^T \boldsymbol{D}\boldsymbol{\Psi}^T(\bar{\boldsymbol{U}})\bar{\boldsymbol{q}}}{\boldsymbol{x}^T \bar{\boldsymbol{q}}} \ .$$

In the reverse direction assume that a certain matrix $\bar{\boldsymbol{U}}$ fulfills (3.17), thus for all $\boldsymbol{x} > 0$ we have

$$\frac{\boldsymbol{x}^T \boldsymbol{D}\boldsymbol{\Psi}^T(\boldsymbol{U})\bar{\boldsymbol{q}}}{\boldsymbol{x}^T \bar{\boldsymbol{q}}} \geq \frac{\boldsymbol{x}^T \boldsymbol{D}\boldsymbol{\Psi}^T(\bar{\boldsymbol{U}})\bar{\boldsymbol{q}}}{\boldsymbol{x}^T \bar{\boldsymbol{q}}} \ . \tag{P.18}$$

Using (3.10) we have

$$\begin{aligned} \lambda_{\max}\big(\boldsymbol{D}\boldsymbol{\Psi}^T(\boldsymbol{U})\big) &= \min_{\boldsymbol{x}>0} \max_{\boldsymbol{y}>0} \frac{\boldsymbol{x}^T \boldsymbol{D}\boldsymbol{\Psi}^T(\boldsymbol{U})\boldsymbol{y}}{\boldsymbol{x}^T \boldsymbol{y}} \\ &\geq \min_{\boldsymbol{x}>0} \frac{\boldsymbol{x}^T \boldsymbol{D}\boldsymbol{\Psi}^T(\boldsymbol{U})\bar{\boldsymbol{q}}}{\boldsymbol{x}^T \bar{\boldsymbol{q}}} \ . \end{aligned} \tag{P.19}$$

Combining (P.18) and (P.19) we can conclude that

$$\lambda_{\max}\big(\boldsymbol{D}\boldsymbol{\Psi}^T(\boldsymbol{U})\big) \geq \min_{\boldsymbol{x}>0} \frac{\boldsymbol{x}^T \boldsymbol{D}\boldsymbol{\Psi}^T(\bar{\boldsymbol{U}})\bar{\boldsymbol{q}}}{\boldsymbol{x}^T \bar{\boldsymbol{q}}} = \lambda_{\max}\big(\boldsymbol{D}\boldsymbol{\Psi}^T(\bar{\boldsymbol{U}})\big) \ . \tag{P.20}$$

Hence, $\bar{\boldsymbol{U}}$ is the global minimizer of the function $\lambda_{\max}\big(\boldsymbol{D}\boldsymbol{\Psi}^T(\boldsymbol{U})\big)$.

P.7. Proof of Theorem 11

Suppose that $\mathrm{SINR}_i^{\mathrm{UL}} \geq \gamma_i$, $1 \leq i \leq K$, is feasible. This implies that the eigenvalue optimization problem (3.7) has a solution $B_{\mathrm{Inf}}^{\mathrm{UL}} = 1/\lambda_{max}^{opt} > 1$. The optimizers $\boldsymbol{q}^{opt} > 0$ and $\boldsymbol{u}_i^{opt}$ fulfill $\mathrm{SIR}_i^{\mathrm{UL}}(\boldsymbol{u}_i^{opt}, \boldsymbol{q}^{opt}) \geq \mathrm{SIR}_i^{\mathrm{UL}}(\boldsymbol{u}_i, \boldsymbol{q}^{opt})$ for any $\boldsymbol{u}_i \in \mathbb{C}^M$. Thus,

$$\lambda_{max}^{opt} = \frac{\gamma_i}{\mathrm{SIR}_i^{\mathrm{UL}}(\boldsymbol{u}_i^{opt}, \boldsymbol{q}^{opt})} \leq \frac{\gamma_i}{\mathrm{SIR}_i^{\mathrm{UL}}(\boldsymbol{u}_i, \boldsymbol{q}^{opt})} \ , \quad 1 \leq i \leq K \ ,$$

which can be rewritten as

$$\boldsymbol{u}_i^H \boldsymbol{\Omega}_i(\lambda_{max}^{opt}, \boldsymbol{q}^{opt}) \boldsymbol{u}_i \leq 0 \ , \quad 1 \leq i \leq K \ . \tag{P.21}$$

Thus, $\boldsymbol{\Omega}_i(\lambda_{max}^{opt}, \boldsymbol{q}^{opt})$ is negative semidefinite. Inequality (P.21) can only be fulfilled with equality if $\boldsymbol{u}_i$ lies in the nullspace of $\boldsymbol{\Omega}_i(\lambda_{max}^{opt}, \boldsymbol{q}^{opt})$.

Conversely, assume that there exists a power allocation $\tilde{\boldsymbol{q}} > 0$ and $\lambda < 1$ such that the matrices $\boldsymbol{\Omega}_i(\lambda, \tilde{\boldsymbol{q}})$, $1 \leq i \leq K$, are singular. This implies that there exist non-trivial solutions $\tilde{\boldsymbol{u}}_k \neq [0, \ldots, 0]^T$ such that $0 = \tilde{\boldsymbol{u}}_i^H \boldsymbol{\Omega}_i(\lambda, \tilde{\boldsymbol{q}}) \tilde{\boldsymbol{u}}_i$, $1 \leq i \leq K$. This can be rewritten as $\gamma_i / \mathrm{SIR}_i^{\mathrm{UL}}(\tilde{\boldsymbol{u}}_i, \tilde{\boldsymbol{q}}) = \lambda$. Thus, $\mathrm{SIR}_i^{\mathrm{UL}}(\tilde{\boldsymbol{u}}_i, \tilde{\boldsymbol{q}}) > \gamma_i$, which implies feasibility and concludes the proof.

P.8. Proof of Theorem 13

Assume $\tilde{\lambda}_n(\boldsymbol{x}) = \lambda_{\max}(n)$ for any $\boldsymbol{x} > 0$. This implies

$$\begin{aligned}
\lambda_{\max}\big(\boldsymbol{D}\boldsymbol{\Psi}^T(\boldsymbol{U})\big) &\overset{\text{(a)}}{=} \max_{\boldsymbol{y}>0} \min_{\boldsymbol{x}>0} \frac{\boldsymbol{x}^T \boldsymbol{D}\boldsymbol{\Psi}^T(\boldsymbol{U})\boldsymbol{y}}{\boldsymbol{x}^T \boldsymbol{y}} \\
&\geq \min_{\boldsymbol{x}>0} \frac{\boldsymbol{x}^T \boldsymbol{D}\boldsymbol{\Psi}^T(\boldsymbol{U})\boldsymbol{q}^{(n-1)}}{\boldsymbol{x}^T \boldsymbol{q}^{(n-1)}} \\
&\geq \min_{\boldsymbol{x}>0} \min_{\boldsymbol{U}} \frac{\boldsymbol{x}^T \boldsymbol{D}\boldsymbol{\Psi}^T(\boldsymbol{U})\boldsymbol{q}^{(n-1)}}{\boldsymbol{x}^T \boldsymbol{q}^{(n-1)}} \\
&\overset{\text{(b)}}{=} \min_{\boldsymbol{x}>0} \tilde{\lambda}_n(\boldsymbol{x}) \\
&= \lambda_{\max}(n) \,,
\end{aligned} \tag{P.22}$$

where (a) follows from Lemma 6 and (b) follows from the fact that $\boldsymbol{U}^{(n)}$ minimizes $\boldsymbol{x}^T \boldsymbol{D}\boldsymbol{\Psi}^T(\boldsymbol{U})\boldsymbol{q}^{(n-1)}$ for an arbitrary $\boldsymbol{x} > 0$ (see the proof of Theorem 9). Inequality (P.22) holds for any $\boldsymbol{U}$, thus we can conclude that

$$\lambda_{\max}\big(\boldsymbol{D}\boldsymbol{\Psi}^T(\boldsymbol{U}^{(n)})\big) = \lambda_{\max}(n) \leq \min_{\boldsymbol{U}} \lambda_{\max}\big(\boldsymbol{D}\boldsymbol{\Psi}^T(\boldsymbol{U})\big) = \lambda_{max}^{opt} \,. \tag{P.23}$$

Since λ_{max}^{opt} is the global minimum, (P.23) can only be satisfied with equality. Thus, $\boldsymbol{U}^{(n)} \in \mathcal{M}^{\mathrm{DL}}$.

To prove the reverse direction assume that $\boldsymbol{U}^{(n)}$ solves the eigenvalue minimization problem (3.7), i.e., $\boldsymbol{U}^{(n)} \in \mathcal{M}^{\mathrm{DL}}$. Since $\boldsymbol{U}^{(n)}$ is computed by Algorithm 1, we have

$$\boldsymbol{U}^{(n)} = \arg\min_{\boldsymbol{U}} \frac{\boldsymbol{x}^T \boldsymbol{D}\boldsymbol{\Psi}^T(\boldsymbol{U})\boldsymbol{q}^{(n-1)}}{\boldsymbol{x}^T \boldsymbol{q}^{(n-1)}} \,.$$

Since $\boldsymbol{U}^{(n)}$ is the global optimizer of (3.7), Theorem 10 implies

$$\boldsymbol{D}\boldsymbol{\Psi}^T(\boldsymbol{U}^{(n)})\boldsymbol{q}^{(n-1)} = \lambda_{\max}(n)\boldsymbol{q}^{(n-1)} \,. \tag{P.24}$$

Combining (3.23) and (P.24) we have

$$\tilde{\lambda}_n(\boldsymbol{x}) = \frac{\boldsymbol{x}^T \boldsymbol{D}\boldsymbol{\Psi}^T(\boldsymbol{U}^{(n)})\boldsymbol{q}^{(n-1)}}{\boldsymbol{x}^T \boldsymbol{q}^{(n-1)}} = \lambda_{\max}(n) \,,$$

for any $\boldsymbol{x} > 0$, which concludes the proof.

P.9. Proof of Theorem 15

The equivalence of (3.41) and (3.42) for a given ℓ_1 solution $(\hat{\boldsymbol{U}}, \hat{\boldsymbol{p}})$ follows from (3.34). Now, assume that (3.41) holds true. This implies that the ℓ_1 solution is balanced, thus

$$\begin{aligned} B_1 = F_1(\hat{\boldsymbol{U}}, \hat{\boldsymbol{p}}) &= \frac{\gamma_i}{\mathrm{SIR}_i^{\mathrm{DL}}(\hat{\boldsymbol{U}}, \hat{\boldsymbol{p}})} , \quad 1 \le i \le K \\ &= \lambda_{\max}\big(\boldsymbol{\Gamma}\boldsymbol{\Psi}(\hat{\boldsymbol{U}})\big) \ge \lambda_{\max}^{opt} . \end{aligned} \tag{P.25}$$

From (3.40) we know that this can only be satisfied with equality, thus $\lambda_{\max}^{opt} = B_1$ must hold.

In the reverse direction, assume that $(\hat{\boldsymbol{U}}, \hat{\boldsymbol{p}})$ solves the ℓ_∞ problem (3.33). The solution is balanced, thus $\lambda_{\max}^{opt} = \gamma_i / \mathrm{SIR}_i^{\mathrm{DL}}(\hat{\boldsymbol{U}}, \hat{\boldsymbol{p}})$, $\forall i$ and $\hat{\boldsymbol{p}}$ is the dominant right-hand eigenvector of $\boldsymbol{\Gamma}\boldsymbol{\Psi}(\hat{\boldsymbol{U}})$. With Theorem 14, the optimum is characterized by

$$B_{\mathrm{Inf}}^{\mathrm{DL}} = \frac{1}{\lambda_{\max}^{opt}} = \frac{\hat{p}_i}{\gamma_i \sum\limits_{\substack{k=1 \\ k\neq i}}^{K} \hat{p}_k \hat{\boldsymbol{u}}_k^H \boldsymbol{R}_i \hat{\boldsymbol{u}}_k} , \quad 1 \le i \le K \tag{P.26}$$

$$= \frac{1}{\hat{p}_i \hat{\boldsymbol{u}}_i^H \boldsymbol{G}_i(\hat{\boldsymbol{p}}) \hat{\boldsymbol{u}}_i} , \quad 1 \le i \le K . \tag{P.27}$$

Using matrix notation, (P.26) and (P.27) can be rewritten as (3.41) and (3.42), respectively.

P.10. Proof of Theorem 16

Assume that $\hat{\boldsymbol{U}}$ solves (3.46) and $\boldsymbol{q}^g$ is the dominant left-hand eigenvector of the matrix $\boldsymbol{\Gamma}\boldsymbol{\Psi}(\hat{\boldsymbol{U}})$. With (3.30), this implies that for all $\boldsymbol{x} > 0$,

$$\begin{aligned} \hat{\boldsymbol{U}} &= \arg\min_{\boldsymbol{U}} F_1(\boldsymbol{U}, (\boldsymbol{q}^g)^{-1}), \quad \text{s.t. } \boldsymbol{u}_i^H \boldsymbol{R}_i \boldsymbol{u}_i = 1, \ 1 \le i \le K \\ &= \arg\min_{\boldsymbol{U}} \sum_{i=1}^{K} [\boldsymbol{x}]_i \boldsymbol{u}_i^H \Bigg(\sum_{\substack{k=1 \\ k\neq i}}^{K} [\boldsymbol{q}^g]_k \gamma_k \boldsymbol{R}_k \Bigg) \boldsymbol{u}_i, \quad \text{s.t. } \boldsymbol{u}_i^H \boldsymbol{R}_i \boldsymbol{u}_i = 1, \ 1 \le i \le K \\ &= \arg\min_{\boldsymbol{U}} \frac{\boldsymbol{x}^T \big(\boldsymbol{\Gamma}\boldsymbol{\Psi}(\boldsymbol{U})\big)^T \boldsymbol{q}^g}{\boldsymbol{x}^T \boldsymbol{q}^g}, \quad \text{s.t. } \ \boldsymbol{u}_i^H \boldsymbol{R}_i \boldsymbol{u}_i = 1, \ \ 1 \le i \le K . \end{aligned} \tag{P.28}$$

Hence, the following relation holds for all $\boldsymbol{U}$ and $\boldsymbol{x} > 0$:

$$\frac{\boldsymbol{x}^T \big(\boldsymbol{\Gamma}\boldsymbol{\Psi}(\boldsymbol{U})\big)^T \boldsymbol{q}^g}{\boldsymbol{x}^T \boldsymbol{q}^g} \ge \frac{\boldsymbol{x}^T \big(\boldsymbol{\Gamma}\boldsymbol{\Psi}(\hat{\boldsymbol{U}})\big)^T \boldsymbol{q}^g}{\boldsymbol{x}^T \boldsymbol{q}^g} . \tag{P.29}$$

Using (3.10) we have

$$\lambda_{\max}\Big(\big(\boldsymbol{\Gamma\Psi}(\boldsymbol{U})\big)^T\Big) = \min_{\boldsymbol{x}} \max_{\boldsymbol{y}} \frac{\boldsymbol{x}^T\big(\boldsymbol{\Gamma\Psi}(\boldsymbol{U})\big)^T\boldsymbol{y}}{\boldsymbol{x}^T\boldsymbol{y}} \geq \min_{\boldsymbol{x}} \frac{\boldsymbol{x}^T\big(\boldsymbol{\Gamma\Psi}(\boldsymbol{U})\big)^T\boldsymbol{q}^g}{\boldsymbol{x}^T\boldsymbol{q}^g} . \tag{P.30}$$

Combining (P.29) and (P.30) we can conclude that

$$\lambda_{\max}\Big(\big(\boldsymbol{\Gamma\Psi}(\boldsymbol{U})\big)^T\Big) \geq \min_{\boldsymbol{x}} \frac{\boldsymbol{x}^T\big(\boldsymbol{\Gamma\Psi}(\hat{\boldsymbol{U}})\big)^T\boldsymbol{q}^g}{\boldsymbol{x}^T\boldsymbol{q}^g} = \lambda_{\max}\Big(\big(\boldsymbol{\Gamma\Psi}(\hat{\boldsymbol{U}})\big)^T\Big) . \tag{P.31}$$

Hence, $\hat{\boldsymbol{U}}$ is the global minimizer of the function $\lambda_{\max}\big(\boldsymbol{\Gamma\Psi}(\boldsymbol{U})\big)$. From the discussion in Section 3.1.1 it is known that in this case $\hat{\boldsymbol{U}}$ and $\boldsymbol{p}^g$ solve the ℓ_∞-problem (3.33).

In the reverse direction, assume that $\hat{\boldsymbol{U}}$ is the ℓ_∞-optimizer, which implies

$$\lambda_{\max}\big(\boldsymbol{\Gamma\Psi}(\hat{\boldsymbol{U}})\big) \leq \lambda_{\max}\big(\boldsymbol{\Gamma\Psi}(\boldsymbol{U})\big) .$$

Thus, the following inequality holds for any $\boldsymbol{U}$ and $\boldsymbol{z} > 0$:

$$\begin{aligned}
\max_{\boldsymbol{x}>0} \frac{\boldsymbol{x}^T\big(\boldsymbol{\Gamma\Psi}(\boldsymbol{U})\big)^T\boldsymbol{q}^g}{\boldsymbol{x}^T\boldsymbol{q}^g} &\geq \min_{\boldsymbol{y}>0} \max_{\boldsymbol{x}>0} \frac{\boldsymbol{x}^T\big(\boldsymbol{\Gamma\Psi}(\boldsymbol{U})\big)^T\boldsymbol{y}}{\boldsymbol{x}^T\boldsymbol{y}} \\
&= \lambda_{\max}\Big(\big(\boldsymbol{\Gamma\Psi}(\boldsymbol{U})\big)^T\Big) \qquad \leftarrow \text{Eq. (3.10)} \\
&\geq \lambda_{\max}\Big(\big(\boldsymbol{\Gamma\Psi}(\hat{\boldsymbol{U}})\big)^T\Big) \\
&= \frac{\boldsymbol{z}^T\big(\boldsymbol{\Gamma\Psi}(\hat{\boldsymbol{U}})\big)^T\boldsymbol{q}^g}{\boldsymbol{z}^T\boldsymbol{q}^g} . \qquad \leftarrow \text{Eq. (3.18)}
\end{aligned}$$

The above inequality holds for any $\boldsymbol{U}$, thus

$$\min_{\boldsymbol{U}} \max_{\boldsymbol{x}>0} \frac{\boldsymbol{x}^T\big(\boldsymbol{\Gamma\Psi}(\boldsymbol{U})\big)^T\boldsymbol{q}^g}{\boldsymbol{x}^T\boldsymbol{q}^g} \geq \frac{\boldsymbol{z}^T\big(\boldsymbol{\Gamma\Psi}(\hat{\boldsymbol{U}})\big)^T\boldsymbol{q}^g}{\boldsymbol{z}^T\boldsymbol{q}^g} .$$

There exists an optimizer $\boldsymbol{x}_0 > 0$ such that

$$\min_{\boldsymbol{U}} \frac{\boldsymbol{x}_0^T\big(\boldsymbol{\Gamma\Psi}(\boldsymbol{U})\big)^T\boldsymbol{q}^g}{\boldsymbol{x}_0^T\boldsymbol{q}^g} \geq \frac{\boldsymbol{x}_0^T\big(\boldsymbol{\Gamma\Psi}(\hat{\boldsymbol{U}})\big)^T\boldsymbol{q}^g}{\boldsymbol{x}_0^T\boldsymbol{q}^g} .$$

This inequality can only be fulfilled with equality. Moreover, it can be observed from (3.15) that the minimization with respect to $\boldsymbol{U}$ is independent of $\boldsymbol{x}_0$. Thus, for all $\boldsymbol{x} > 0$ and $\boldsymbol{U}$ we have

$$\min_{\boldsymbol{U}} \frac{\boldsymbol{x}^T\boldsymbol{\Gamma\Psi}^T(\boldsymbol{U})\boldsymbol{q}^g}{\boldsymbol{x}_0^T\boldsymbol{q}^g} = \frac{\boldsymbol{x}^T\boldsymbol{\Gamma\Psi}^T(\hat{\boldsymbol{U}})\boldsymbol{q}^g}{\boldsymbol{x}^T\boldsymbol{q}^g} .$$

It can be concluded with (P.28) that $\hat{\boldsymbol{U}}$ solves (3.46).

P.11. Proof of Theorem 19

Assume that (4.28) holds. Combining (4.12) and the monotony result (4.26) we have

$$\min_{\boldsymbol{x}>0} \frac{\boldsymbol{x}^T \boldsymbol{\Lambda}(\boldsymbol{U}^{(n)}, P_{\max})\boldsymbol{q}_{\text{ext}}^{(n-1)}}{\boldsymbol{x}^T \boldsymbol{q}_{\text{ext}}^{(n-1)}} = \lambda_{\max}\big(\boldsymbol{\Lambda}(\boldsymbol{U}^{(n)}, P_{\max})\big) \ . \tag{P.32}$$

The same arguments that have led to (4.17) can be used to show that $\boldsymbol{U}^{(n)}$ fulfills

$$\min_{\boldsymbol{U}} \min_{\boldsymbol{x}>0} \frac{\boldsymbol{x}^T \boldsymbol{\Lambda}(\boldsymbol{U}, P_{\max})\boldsymbol{q}_{\text{ext}}^{(n-1)}}{\boldsymbol{x}^T \boldsymbol{q}_{\text{ext}}^{(n-1)}} = \min_{\boldsymbol{x}>0} \frac{\boldsymbol{x}^T \boldsymbol{\Lambda}(\boldsymbol{U}^{(n)}, P_{\max})\boldsymbol{q}_{\text{ext}}^{(n-1)}}{\boldsymbol{x}^T \boldsymbol{q}_{\text{ext}}^{(n-1)}} \ . \tag{P.33}$$

Combining (P.32) and (P.33) we have

$$\begin{aligned}
\min_{\boldsymbol{U}} \lambda_{\max}(\boldsymbol{\Lambda}(\boldsymbol{U}, P_{\max})) &= \min_{\boldsymbol{U}} \min_{\boldsymbol{x}>0} \max_{\boldsymbol{y}>0} \frac{\boldsymbol{x}^T \boldsymbol{\Lambda}(\boldsymbol{U}, P_{\max})\boldsymbol{y}}{\boldsymbol{x}^T \boldsymbol{y}} \\
&\geq \min_{\boldsymbol{U}} \min_{\boldsymbol{x}>0} \frac{\boldsymbol{x}^T \boldsymbol{\Lambda}(\boldsymbol{U}, P_{\max})\boldsymbol{q}_{\text{ext}}^{(n-1)}}{\boldsymbol{x}^T \boldsymbol{q}_{\text{ext}}^{(n-1)}} \\
&= \min_{\boldsymbol{x}>0} \frac{\boldsymbol{x}^T \boldsymbol{\Lambda}(\boldsymbol{U}^{(n)}, P_{\max})\boldsymbol{q}_{\text{ext}}^{(n-1)}}{\boldsymbol{x}^T \boldsymbol{q}_{\text{ext}}^{(n-1)}} \\
&= \lambda_{\max}\big(\boldsymbol{\Lambda}(\boldsymbol{U}^{(n)}, P_{\max})\big) \ .
\end{aligned}$$

This can only be satisfied with equality, thus $\boldsymbol{U}^{(n)} \in \mathcal{M}$.

To prove the reverse direction, assume that $\boldsymbol{U}^{(n)} \in \mathcal{M}$. From Theorem 17 we know that $\boldsymbol{U}^{(n)}$ is characterized by

$$\boldsymbol{\Lambda}(\boldsymbol{U}^{(n)}, P_{\max})\boldsymbol{q}_{\text{ext}}^{(n-1)} = \lambda_{\max}(n)\boldsymbol{q}_{\text{ext}}^{(n-1)} \ . \tag{P.34}$$

Left-hand multiplication on both sides of (P.34) with $\boldsymbol{x}^T/(\boldsymbol{x}^T\boldsymbol{q}_{\text{ext}}^{(n-1)})$, $\boldsymbol{x} \in \mathbb{R}_+^K$, leads to

$$\lambda_{\max}(n) = \frac{\boldsymbol{x}^T \boldsymbol{\Lambda}(\boldsymbol{U}^{(n)}, P_{\max})\boldsymbol{q}_{\text{ext}}^{(n-1)}}{\boldsymbol{x}^T \boldsymbol{q}_{\text{ext}}^{(n-1)}} \ . \tag{P.35}$$

Equation (P.35) holds for all $\boldsymbol{x} > 0$, hence

$$\min_{\boldsymbol{x}>0} \frac{\boldsymbol{x}^T \boldsymbol{\Lambda}(\boldsymbol{U}^{(n)}, P_{\max})\boldsymbol{q}_{\text{ext}}^{(n-1)}}{\boldsymbol{x}^T \boldsymbol{q}_{\text{ext}}^{(n-1)}} = \max_{\boldsymbol{x}>0} \frac{\boldsymbol{x}^T \boldsymbol{\Lambda}(\boldsymbol{U}^{(n)}, P_{\max})\boldsymbol{q}_{\text{ext}}^{(n-1)}}{\boldsymbol{x}^T \boldsymbol{q}_{\text{ext}}^{(n-1)}} \ .$$

With Lemma 13 this implies (4.28).

Notation and Symbols

$\mathcal{E}\{\cdot\}$	expectation operator	
$[\cdot]_{ij}$	component with index i, j of a matrix or a vector	
$(\boldsymbol{a})^{-1}$	if applied to a vector: component-wise inversion	
$(\cdot)^T$	transpose	
$(\cdot)^H$	Hermitian (complex conjugate) transpose	
$(\cdot)^{(n)}$	n^{th} iteration step	
$(\cdot)^{\text{UL}}$	uplink quantity	
$(\cdot)^{\text{DL}}$	downlink quantity	
B_1	optimum of the ℓ_1 cost function	p. 33
B_{Inf}	asymptotically achievable upper bound for $\min_i \text{SINR}_i$	p. 16
$C(\boldsymbol{U}, P_{\max})$	balanced SINR optimum for a given beamforming matrix $\boldsymbol{U}$	p. 13,18
$C_{\text{opt}}(P_{\max})$	balanced SINR optimum optimized over all beamformers and power allocations	p. 43,44
$\boldsymbol{D}$	normalized threshold matrix	p. 13
F_1	ℓ_1 cost function	p. 33
$\boldsymbol{G}_i(\boldsymbol{p})$	$= \sum_{k \neq i}^{K} \frac{\gamma_k \boldsymbol{R}_k}{p_k}$	p. 33
γ_i	target threshold for the i^{th} user	
$\boldsymbol{\Gamma}$	threshold matrix $\boldsymbol{\Gamma} = \text{diag}\{\gamma_1, \ldots, \gamma_K\}$	p. 34
$\boldsymbol{h}_i$	channel vector of the i^{th} user	p. 7
K	number of users (non-cooperating terminals)	
$\lambda_{\max}(\cdot)$	maximal eigenvector	
$\lambda_{\max}^{opt}$	optimum of the eigenvalue minimization problem in the absence of noise	p. 28
$\tilde{\lambda}_n$	cost function for SIR balancing	p. 30
$\check{\lambda}_n$	cost function for extended ℓ_1 balancing	p. 40
$\hat{\lambda}_n$	cost function for SINR balancing	p. 45
$\boldsymbol{\Lambda}(\boldsymbol{U}, P_{\max})$	extended uplink coupling matrix	p. 13
M	number of base station antennas (cooperating terminals)	
$\boldsymbol{\Psi}(\boldsymbol{U})$	coupling matrix	p. 10
$P_{\max}$	maximal total power	
p_i	downlink power of the i^{th} user	
$\boldsymbol{p}$	downlink power allocation	p. 8

q_i	uplink power of the i^{th} user	
$\boldsymbol{q}$	uplink power allocation	p. 10
$\boldsymbol{q}_{\text{ext}}$	extended uplink power vector $\boldsymbol{q}_{\text{ext}} = \binom{q}{1}$	p. 45
$\boldsymbol{Q}_i(\boldsymbol{q})$	interference covariance in the absence of noise	p. 27
σ_i^2	noise variance of the i^{th} user	
$\boldsymbol{\sigma}$	noise vector $\boldsymbol{\sigma} = [\sigma_1^2, \ldots, \sigma_K^2]^T$	
SIR	signal-to-interference ratio	p. 16,24
SINR	signal-to-interference-plus-noise ratio	p. 9,10
$\boldsymbol{u}_i$	beamforming vector of the i^{th} user (both uplink an downlink)	
$\boldsymbol{U}$	beamforming matrix $\boldsymbol{U} = [\boldsymbol{u}_1, \ldots, \boldsymbol{u}_K]$	p. 8
$\boldsymbol{\Upsilon}(\boldsymbol{U}, P_{\max})$	extended downlink coupling matrix	p. 19
$\boldsymbol{x}$	auxiliary variable	p. 45
$\boldsymbol{\xi}$	vector with ratios SIR_i/γ_i	p. 25
$\boldsymbol{Z}_i(\boldsymbol{q})$	interference-plus-noise spatial covariance matrix	p. 45
$\hat{\boldsymbol{Z}}_i(q_1 \ldots q_{i-1})$	interference-plus-noise spatial covariance matrix with successive decoding, order $K \ldots 1$	p. 56

Publication List

[1] H. Boche and M. Schubert, "A general duality theory for uplink and downlink beamforming," in *IEEE Vehicular Techn. Conf. (VTC) fall, Vancouver, Canada*, Sept. 2002.

[2] M. Schubert and H. Boche, "Joint 'dirty paper' pre-coding and downlink beamforming," in *Proc. ISSSTA, Prague, Czech Republic*, vol. 2, pp. 536–540, Sept. 2002.

[3] H. Boche and M. Schubert, "Comparison of infinity-norm and 1-norm optimization for multi-antenna downlink transmission," in *Proc. IEEE Int. Symp. on Inf. Theory (ISIT), Lausanne, Switzerland*, p. 452, June 2002.

[4] H. Boche and M. Schubert, "Optimum SIR balancing using extended 1-norm beamforming optimization," in *Proc. IEEE Internat. Conf. on Acoustics, Speech, and Signal Proc. (ICASSP), Orlando, USA*, May 2002.

[5] M. Schubert and H. Boche, "SIR balancing for multiuser downlink beamforming – a convergence analysis," in *Proc. Internat. Conf. Comm. (ICC), New York, USA*, Apr. 2002.

[6] H. Boche and M. Schubert, "Solution of the SINR downlink beamforming problem," in *Proc. Conf. on Information Sciences and Systems (CISS), Princeton, USA*, Mar. 2002.

[7] M. Schubert and H. Boche, "A unifying theory for uplink and downlink multiuser beamforming," in *Proc. IEEE Intern. Zurich Seminar, Zurich, Switzerland*, Feb. 2002.

[8] H. Boche and M. Schubert, "Analysis of SIR-based downlink beamforming," *IEICE Trans. Commun.*, vol. E85-B, pp. 1160–1168, June 2002.

[9] H. Boche and M. Schubert, "Theoretical and experimental comparison of optimization criteria for downlink beamfoming," *European Trans. on Telecomm. (ETT)*, vol. 12, pp. 417–426, Sept. 2001.

References

[10] D. Gerlach and A. Paulraj, "Base station transmitting antenna arrays for multipath environments," *Signal Processing (Elsevier Science)*, vol. 54, pp. 59–73, 1996.

[11] E. Telatar, "Capacity of multi-antenna Gaussian channels," Tech. Rep. BL0112170-950615-07TM, AT&T Bell Labs, June 1995.

[12] G. J. Foschini and M. J. Gans, "On limits of wireless communications in a fading environment when using multiple antennas," *Signal Processing (Elsevier Science)*, vol. 6, pp. 311–335, 1999.

[13] H. Bölcskei and A. J. Paulraj, *Multiple-input multiple-output (MIMO) wireless systems*, pp. 90.1 – 90.14. 2002.

[14] S. Kasturia, J. Aslanis, and J. Cioffi, "Vector coding for partial-response channels," *IEEE Trans. on Information Theory*, vol. 36, pp. 741–762, July 1990.

[15] V. Tarokh, N. Seshadri, and A. Calderbank, "Space-time codes for high data rates wireless communications: performance criterion and code construction," *IEEE Trans. on Information Theory*, vol. 44, pp. 744–765, Mar. 1998.

[16] S. Alamouti, "A simple transmitter diversity technique for wireless communications," *IEEE Journal on Selected Areas in Comm.*, vol. 16, no. 8, p. 14511458, 1998.

[17] V. Tarokh, H. Jafarkhani, and A. Calderbank, "Space-time block codes from orthogonal designs," *IEEE Trans. on Information Theory*, vol. 45, pp. 1456–1467, July 1999.

[18] D. Tse and S. V. Hanly, "Linear multiuser receivers: Effective interference, effective bandwidth and user capacity," *IEEE Trans. on Information Theory*, vol. 45, no. 2, pp. 641–657, 1999.

[19] R. A. Monzingo and T. W. Miller, *Introduction to Adaptive Arrays.* Wiley, New York, 1980.

[20] J. E. Hudson, *Adaptive Array Principles.* U.K.: Peregrinus, 1981.

[21] D. H. Johnson and D. E. Dudgeon, *Array Signal Processing: Concepts and Methods.* Prentice Hall, Inc., Englewood Cliffs, New Jersey, 1992.

[22] S. U. Pillai, *Array Signal Processing.* Springer, NY, 1989.

[23] B. D. Van Veen and K. M. Buckley, “Beamforming: A versatile approach to spatial filtering,” *IEEE Acoustics, Speech and Signal Processing Mag.*, pp. 4–24, Apr. 1988.

[24] G. J. Foschini and Z. Miljanic, “A simple distributed autonomous power control algorithm and its convergence,” *IEEEtvt*, vol. 42, pp. 541–646, nov 1993.

[25] J. Zander, “Distributed cochannel interference control in cellular radio systems,” *IEEE Trans. on Vehicular Technology*, vol. 41, pp. 305–311, Aug. 1992.

[26] J. Zander, “Performance of optimum transmitter power control in cellular radio systems,” *IEEE Trans. on Vehicular Technology*, vol. 41, pp. 57–62, Feb. 1992.

[27] J. Zander and M. Frodigh, “Comment on performance of optimum transmitter power control in cellular radio systems,” *IEEE Trans. on Vehicular Technology*, vol. 43, Aug. 1994.

[28] W. Yang and G. Xu, “Optimal downlink power assignment for smart antenna systems,” in *Proc. IEEE Internat. Conf. on Acoustics, Speech, and Signal Proc. (ICASSP)*, May 1998.

[29] J. Zander and S.-L. Kim, *Radio Resource Management for Wireless Networks.* Artech House, Boston, London, 2001.

[30] G. Caire and S. Shamai (Shitz), “On achievable rates in a multi-antenna broadcast downlink,” in *Proc. Annual Allerton Conf. on Commun., Control and Computing, Monticello, USA*, Oct. 2000.

[31] G. Caire and S. Shamai (Shitz), “On the multiple-antenna broadcast channel,” in *Proc. Asilomar Conf. on Signals, Systems and Computers, Monterey, CA*, Nov. 2001.

[32] W. Yu and J. M. Cioffi, “Trellis precoding for the broadcast channel,” in *Proc. IEEE Globecom, San Antonio, USA*, 2001.

[33] S. Vishwanath, N. Jindal, and A. Goldsmith, “On the capacity of multiple input multiple output broadcast channels,” in *Proc. IEEE Int. Conf. on Comm. (ICC)*, 2001.

[34] D. Tse and P. Viswanath, “Downlink-uplink duality and effective bandwidths,” in *Proc. IEEE Int. Symp. on Inf. Theory (ISIT), Lausanne, Switzerland*, July 2002.

[35] M. K. Varanasi and T. Guess, “Optimum decision feedback multiuser equalization with successive decoding achieves the total capacity of the Gaussian multiple-access channel,” in *Proc. Asilomar Conf. on Signals, Systems and Computers, Monterey, CA*, pp. 1405–1409, Nov. 1997.

[36] C. Farsakh and J. A. Nossek, “Channel allocation and downlink beamforming

in an SDMA mobile radio system," in *Proc. Int. Symp. on Personal, Indoor and Mobile Radio Comm. (PIMRC), Toronto, Canada*, pp. 687–691, 1995.

[37] C. Farsakh and J. A. Nossek, "Spatial covariance based downlink beamforming in an SDMA mobile radio system," *IEEE Trans. on Communications*, vol. 46, pp. 1497–1506, Nov. 1998.

[38] F. Rashid-Farrokhi, L. Tassiulas, and K. J. Liu, "Transmit beamforming and power control for cellular wireless systems," *IEEE Trans. on Communications*, vol. 46, pp. 1313–1323, Oct. 1998.

[39] F. Rashid-Farrokhi, K. J. Liu, and L. Tassiulas, "Transmit beamforming and power control for cellular wireless systems," *IEEE Journal on Selected Areas in Comm.*, vol. 16, pp. 1437–1449, Oct. 1998.

[40] E. Visotsky and U. Madhow, "Optimum beamforming using transmit antenna arrays," in *Proc. IEEE Vehicular Techn. Conf. (VTC) spring, Houston, Texas*, vol. 1, pp. 851–856, May 1999.

[41] M. Bengtsson and B. Ottersten, "Optimal downlink beamforming using semidefinite optimization," in *Proc. Annual Allerton Conf. on Commun., Control and Computing, Monticello, USA*, pp. 987–996, Sept. 1999.

[42] M. Bengtsson and B. Ottersten, *Handbook of Antennas in Wireless Communications*, ch. Optimal and Suboptimal Transmit Beamforming. CRC press, 2001. to be published.

[43] G. Montalbano and D. T. M. Slock, "Matched filter bound optimization for multiuser downlink transmit beamforming," in *Proc. IEEE ICUPC, Florence, Italy*, Oct. 1998.

[44] D. Gesbert, H. Bölcskei, D. A. Gore, and A. J. Paulraj, "Outdoor MIMO wireless channels: Models and performance prediction," *IEEE Trans. Communications*, 2002.

[45] P. Wolniansky, G. Foschini, G. Golden, and R. Valenzuela, "V-blast: an architecture for realizing very high data rates over the rich-scattering wireless channel," *Proc. URSI Intern. Symp. on Signals, Systems, and Electronics., New York, NY, USA*, pp. 295–300, 1998.

[46] C. D. Meyer, *Matrix Analysis and Applied Linear Algebra*. SIAM, 2000.

[47] E. Seneta, *Non-Negative Matrices and Markov Chains*. Springer, 1981.

[48] E. Telatar, "Capacity of multiple-antenna Gaussian channels," *European Trans. Telecommun.*, vol. 10, pp. 585–595, Nov. 1999.

[49] T. M. Cover and J. A. Thomas, *Elements of Information Theory*. Wiley, 1991.

[50] M. Costa, "Writing on dirty paper," *IEEE Trans. on Information Theory*, vol. 29, pp. 439–441, May 1983.

[51] U. Erez, S. Shamai (Shitz), and R. Zamir, "Capacity and lattice-strategies for cancelling known interference," in *Proc. ISITA, Honolulu, Hawaii*, Nov. 2000.

[52] M. Tomlinson, "New automatic equaliser employing modulo arithmetic," *Electronics Letters*, vol. 7, pp. 138–139, Mar. 1971.

[53] H. Harashima and H. Miyakawa, "Matched transmission technique for channles with intersymbol interference," *IEEE Trans. on Communications*, vol. COM-20, pp. 774–80, Aug. 1972.

[54] R. F. Fischer, C. Windpassinger, A. Lampe, and J. B. Huber, "MIMO precoding for decentralized receivers," in *Proc. IEEE Int. Symp. on Inf. Theory (ISIT), Lausanne, Switzerland*, p. 496, July 2002.

[55] A. Lapidoth, "Nearest neighbor decoding for additive non-Gaussian noise channels," *IEEE Trans. on Information Theory*, vol. 42, pp. 1520–1529, Sept. 1996.

[56] W. Yu and J. M. Cioffi, "Sum capacity of Gaussian vector broadcast channels," *submitted to IEEE Transactions on Information Theory*, Nov. 2001.

[57] L. Vandenberghe, S. Boyd, and S.-P. Wu, "Determinant maximization with linear matrix inequality constraints," *SIAM Journal on Matrix Analysis and Applications*, vol. 19, no. 2, pp. 499–533, 1998.

[58] G. Caire and S. Shamai (Shitz), "On the achievable throughput of a multi-antenna Gaussian broadcast channel," submitted to IEEE Trans. on Inform. Theory, July 2001.

[59] G. Ginis and J. Cioffi, "Vectored transmission for digital subscriber line system," *submitted to IEEE JSAC special issue on twisted pair transmission*, 2002.

[60] R. W. Heath Jr., H. Bölcskei, and A. J. Paulraj, "Space-time signaling and frame theory," in *Proc. IEEE Internat. Conf. on Acoustics, Speech, and Signal Proc. (ICASSP)Salt Lake City, Utah*, 2001.

[61] K. Liu and A. M. Sayeed, "Space-time multiplexing for multi-antenna channels," in *Proc. IEEE Int. Symp. on Inf. Theory (ISIT), Lausanne, Switzerland*, p. 222, July 2002.

[62] L. Zheng and D. Tse, "Diversity and freedom: A fundamental tradeoff in multiple antenna channels," in *Proc. IEEE Int. Symp. on Inf. Theory (ISIT), Lausanne, Switzerland*, July 2002.

[63] E. Jorswieck and H. Boche, "On transmit diversity with imperfect channel state information," in *Proc. IEEE Internat. Conf. on Acoustics, Speech, and Signal Proc. (ICASSP), Orlando, USA*, May 2002.

[64] S. A. Jafar and A. J. Goldsmith, "On optimality of beamforming for multiple antenna systems with imperfect feedback," in *Proc. IEEE Int. Symp. on Inf. Theory (ISIT), Washington D.C., USA*, 2001.

[65] W. Yu, W. Rhee, S. Boyd, and J. M. Cioffi, "Iterative water-filling for Gaussian vector multiple access channels," in *Proc. IEEE Int. Symp. on Inf. Theory (ISIT), Washington DC, USA*, June 2001.

[66] R. Knopp and P. A. Humblet, "Information capacity and power control in single-cell multiuser communications," in *Proc. Int. Conf. on Communications, Seattle, USA*, June 1995.

[67] D. Tse and S. Hanly, "Optimal power allocation over parallel Gaussian broadcast channels," *Proc. IEEE Int. Symp. on Inf. Theory (ISIT), Ulm, Germany*, 1997.